Norwegian University
of Life Sciences

Master's Thesis 2024 60 ECTS
Faculty of Chemistry, Biotechnology and Food Science

To investigate how TFEB affects NAD^+ regulated lifespan and healthspan of *C. elegans*

Nikolai Jensrud Skaar
Master of Biotechnology

To investigate how TFEB affects NAD^+ regulated lifespan and healthspan of *C. elegans*

Master's Thesis in Biotechnology
(60 credits)

By
Nikolai Jensrud Skaar

Supervisors

Dr. Åsmund Røhr Kjendseth (NMBU)
Dr. Queena Shu-qing Cao (UiO)
Associate Professor Evandro Fei Fang (UiO)

Department
Norwegian University of Life Sciences (NMBU)
Post Box 5003
1432 Ås

May 2024

Acknowledgments

This thesis was conducted at the Fang group at UiO, located in Ahus. The leader of this group is Professor Evandro Fei Fang, a researcher in the field of ageing with a specialization in mitophagy and NAD^+. It has been an interesting journey working with all the Fei Fang team and I am so grateful to have gotten the opportunity to work with them.

I would express my most sincere thanks to Evandro for letting me work in his team of brilliant scientists. The questions asked in the Tuesday meetings have really helped me to seek out knowledge in the field and to sharpen these tools that have been handed to me. I have gotten a great deal of help and Evandro has always showed that he has always had the desire to help me when needed.

I would also like to thank my daily supervisor Dr. Queena Shu-qing Cao for the great amount of help she has given me, from daily questions about small things to the bigger questions. She has always planed and showed me that even though I can sometime be forgetful, she has showed the best interest in helping out even if the worms have starved or if there has been a contamination.

Additionally, I would like to thank PhD student Beatriz Escobar Doncel for giving me great advice and for helping me with this thesis work. All the great advice and help I have gotten has been extremely helpful, and I couldn't have done this without you.

I would like to thank PhD student Thomás Schmauck-Medina for telling me about the proteostasis hypothesis they are currently working on. It has been a great deal of help and explains a lot of the data which I have gathered. You have also given a great positive vibe in the lab and it's always a pleasure working with you.

And lastly, but certainly not least, I would like to thank all my friends and family for supporting me through this thesis work. Benjamin Johan Madsen for sitting up late and help with a lot of errors that my thesis had, Mina Lihn Nesmoen who has been a super supportive friend and roommate and who has been someone I can turn to during this period. Charlotte Jensrud Skaar for being the best supportive sister a brother could ever ask for. And lastly, my mom and my dad, Line Jensrud Skaar and Are Skaar, who have always looked after me and made me the person I am today.

Sammendrag

Alderdom er argumentertbart den største riskfaktoren for ordinære sykdommer som kreft, diabetes, og nevrodegenerative sykdommer. Vi trer inn i et aldrende samfunn som bringer formidable sosioøkonomiske utfordringer. Det er viktig å forstå de molekylære mekanismene av alderdom siden disse gir forebyggende og terapeutiske ledetråder for slike alderdoms disponerte sykdommer. Hoved kjennetegn av alderdom inkluderer tap av proteostase, hemmet makroautofagi, og dysfunksjonell mitokondria. Demens påvirker omtrent 55 millioner mennesker der 70% av tilfellene er Alzheimers. Alzheimers er den mest vanlige nevrodegenererende sykdommen uten en kur. De to Alzheimers-definerende patologiske egenskaper er amyloid-β (Aβ) plakk og intracellulære fibrillære floker (NFT, oppbygd hovedsakelig av fosforylert tau proteiner). Tidligere studier av Evandro Fang laboratoriet og andre viser at restaurering av mitokondriell homeostase, via eliminering av skadde mitokondria gjennom mitokondriell autofagi (mitofagi), inhiberte både Aβ og tau patologier og/eller forhindret minnetap i forskjellige Alzheimers dyremodeller og i Alzheimers pasienter iPSC-avledet nerver. Makrofagi (herunder referert til som autofagi), er den prosessen av cellulær gjenkjenning, oppsluking, og lysosomalt degradering av subcellulære skadde og unødvendige organeller og komponenter, slikt som proteiner; mitofagi er en subtype av autofagi, hvor celler eliminere skadde eller overflødig mitokondrie via lysosomalt degradering. Transkripsjonsfaktoren EB (TFEB) er en hoved regulator for lysosomalt biogenese, og er en viktig transkripsjonsfaktor for autofagi. TFEB defosforylering er formidlet av proteiner som GSK3β (som også driver tau patologi i Alzheimers) og mekanistisk mål for Rapamycin Kompleks 1 (mTORC1). I alzheimers, mitofagi (inkludert initiering av lysosomal funksjon) er kompromittert, mens farmakologiske inngrep, som ved tilskudd av NAD^+ forløpere, gjenoppretter mitofagi som fører til inhibering av Alzheimers patologi i dyremodeller. I dette masteroppgave prosjektet ble det spurt om NAD^+-avhengig anti-Alzheimers potensial var igjennom TFEB (i rundormen *C. elegans* ortolog HLH-30). Vi sjekket effektene på levetilstand og helsetilstand av NAD^+-forløper Nikotinamid mononukleotid (NMN) og *hlh-30/TFEB* i ormer. Stammene brukt var villtype N2, en tau patologisk stamme med pan-nevronel uttrykning av menneskelig tau mutant hTau[P301L] (CK12), en tau stamme med allestedsnærværende mutasjon av *hlh-30/TFEB* (EFF033:*hlh30(tm1978);hTau[P301L]*), og en tau stamme med pan-nevronel overuttrykking av villtype *hlh-30/TFEB* (EFF030: *hlh30(+* neuronal); *hTau[P301L]*). Våre data viser at NMN og pan-nevronel overuttrykking av villtype *hlh-30/TFEB* øke levetilstanden og helsetilstanden i CK12 tau ormer; uforventet, *hlh30/TFEB* mutasjonen også økte helsetilstanden i CK12 tau ormer. Dette kan være på grunn av aktivering av kompensasjons vei som for eksempel ubiqvitin-proteosom system (UPS), men videre forskning er trengt. Kollektivt, våre data foreslår at TFEB kan ha en vitkig rolle i NAD^+-avhengig anti-Alzheimers potensial, noe som kan vise til mulige kliniske applikasjoner.

Abstract

Ageing is arguably the biggest risk factor for common diseases such as cancer, diabetes, and neurodegenerative diseases. We are now entering into an ageing society which brings formidable socio-economic challenges. It is important to understand the molecular mechanisms of ageing as they provide preventive and therapeutic clues on such age-predisposed diseases. Key hallmarks (drivers) of ageing include loss of proteostasis, disabled macroautophagy, and dysfunctional mitochondria. Dementia affects approximately 55 million people with 70% are Alzheimer's. Alzheimer's Disease (AD) is the most common neurodegeneration without a cure. The two AD-defining pathological features are amyloid-β (Aβ) plaques and intracellular fibrillary tangles (NFT, composed majorly of phosphorylated tau proteins). Previous studies from the Evandro Fang laboratory and other show that restoration of mitochondrial homeostasis, via eliminating damaged mitochondria though mitochondrial autophagy (mitophagy), inhibited both Aβ and tau pathologies and/or forestalled memory loss in different AD animal models and in AD patient iPSC-derived neurons. Macroautophagy (hereafter referred to as autophagy), is the process of cellular recognition, engulfment, and lysosomal degradation of subcellular damaged and unneeded organelles and components, such as proteins; mitophagy is a sub-type of autophagy, whereby cell eliminate damaged and superfluous mitochondria via lysosomal degradation. The transcription factor EB (TFEB) is a master regulator of lysosomal biogenesis, and an important transcription factor for autophagy. TFEB dephosphorylation is mediated by proteins like GSK3β (which drives tau pathology in AD) and mechanistical Target of Rapamycin Complex 1 (mTORC1). In AD, mitophagy (including initiation and lysosomal function) is compromised, while pharmacological approaches, such as the supplementation with NAD^+ precursors, restore mitophagy leading to inhibition of AD pathologies in animal models. In this master thesis project, we asked whether NAD^+-dependent anti-AD potential was through TFEB (the roundworm *C. elegans* ortholog HLH-30). We checked the effects on lifespan and healthspan by NAD^+ precursor Nicotinamide mononucleotide (NMN) and *hlh-30*/TFEB in worms. The strains used were wild type N2, a Tau pathology strain with pan-neuronal expression of the human tau mutant hTau[P301L] (CK12), a tau strain with ubiquitous mutation of *hlh-30*/TFEB (EFF033:*hlh30(tm1978);hTau[P301L]*), and a Tau strain with pan-neuronal overexpression of WT *hlh-30/TFEB* (EFF030: *hlh30(+* neuronal); *hTau[P301L]*). Our data show that NMN and pan-neuronal overexpression of WT *hlh-30/TFEB* extended lifespan and healthspan in CK12 Tau worms; unexpected, *hlh-30/TFEB* mutation also extended lifespan in the CK12 Tau worms, this couls be due to the activation of compensatory pathways such as ubiquitin-proteosome system (UPS) system, with further investigations needed. Collectively, our data suggest that TFEB may play an essential role in NAD^+-dependent anti-AD potential, shedding light on possible clinical applications.

Contents

1.0 Introduction & Theory

1.1 The global pandemic of ageing related diseases

Longevity, a global phenomenon which indicates the elongated length of people's living due to developments such as improved living environments, financial conditions, and medical technologies. However, age-related issues like cancer, diabetes, and neurodegenerative diseases are accompanied. Therefore, healthy longevity has become a hot topic worldwide. According to Carlos López-Otín (2023), there are 12 hallmarks of ageing related to the ageing process, for example disabled macroautophagy and dysfunctional mitochondria. NAD^+ is an essential molecule for cell survival and is linked to mitochondrial function and longevity [1, 2]. The transcription factor EB (TFEB) has been shown to increase mitochondrial autophagy (mitophagy) and increase mitochondrial function [3]. Therefore, one of the goals of this presenting thesis is to evaluate how NAD^+ affect healthy lifespan [4].

Ageing-related diseases contribute to the reduction of health quality and additionally reduces the average human lifespan. The most common ageing-related disease is dementia [5-7]. According to the World Health Organization (WHO), the estimated cases of patients with dementia are around 55 million people in 2023, where 60% of whom live in lower- to middle-income countries. WHO also estimated that the number of dementia cases will increase by nearly 10 million people every yearly, and, through an estimate by the European and French dementia cases, it is estimated that the cases of dementia will reach up to 1.81 million people [7, 8]. Further explained by WHO, "In 2019, dementia cost economies globally 1.3 trillion US dollars, approximately 50% of these costs are attributable to care provided by informal carers (e.g. family members and close friends), who provide on average 5 hours of care and supervision per day." There are several types of dementia such as vascular dementia, dementia with Lewy bodies (abnormal deposits of protein inside nerve cells), and a group of diseases that contribute to frontotemporal dementia (degradation of the frontal lobe of the brain) [6], and Alzheimer's disease (AD). AD is the most common form of dementia, which contributes to 60-70% of all dementia cases [7], and will be majorly discussed in the present thesis.

1.2 Alzheimer's disease, mechanics and how it occurs

1.2.1 Alzheimer's disease overview

AD is a neurodegenerative disease that can affect anyone from 45 up until later life stages, which progressively affects human brain areas like the hippocampus and the cerebral cortex. AD affects different stages of life, where different factors are involved. Three classifications of AD is usually presented: FAD, EOAD, and LOAD. Dominantly inheritable familial AD (FAD) can be caused by mutations, for example, in amyloid precursor protein (*APP*), presenilin 1 (*PSEN1*) or the *PSEN2* genes. These familial forms of AD are rare and are only occurrent for less than 1% of all AD cases [5, 9]. Early onset Alzheimer's disease (EOAD) is defined by those affected before age 65; and though they are slightly more common than FAD cases, they account for

about 4-6% of all AD cases, but is a more aggressive form of AD [9, 10]. The most common form of AD is Late Onset Alzheimer's Disease (LOAD), and occurs randomly, even though genetic risk factors have been identified. The most notable genetic risk factor of LOAD is apolipoprotein E (*APOE*). The factors that have the greatest risks of developing AD are age, family history in a first degree relative, and *APOE4* genotype. Individuals carrying a single copy of the *APOE4* polymorphism have an odds ratio for AD of 3 compared to non-carriers. Those homozygous for *APOE4* have an odds ratio of 12 [5, 9, 11]. *APOE4* allele appears to increase risk for vascular dementia, Lewy body dementia, Down's syndrome, and traumatic brain injury as well [5, 9]. Other risk factors for LOAD including TREM2, ADAM10 and PLD3 that can cause aggregated tau proteins or an accumulation of Aβ plaques. While TREM2 and PLD3 are shown to increase the amount of Amyloid-β in the brain, ADAM10 is (in of itself) reducing the amount of Aβ plaques by splicing the amyloid-β protein precursor (APP). ADAM10 will increase the amount of Aβ when it is mutated (Q170H, R181G) and cannot reduce the effect of α-secretase [5, 12-14].

The key features of Alzheimer's disease (AD) are the accumulation of extracellular Amyloid-β (Aβ) plaques and intracellular hyperphosphorylated Tau proteins (p-Tau), which subsequently aggregates into intracellular $A\beta_{1\text{-}42}$ peptides ($iA\beta_{1\text{-}42}$) and neurofibrillary tangles (NFTs), respectively. This will eventually induce synaptic toxicity and loss of neurons [5, 6, 9-11]. Despite there being a lot of research on AD for half a century, treatment to slow or halt the disease has not yet been found [9]. Understanding of the molecular mechanisms of AD might give an insight on how to treat AD.

1.2.2 Macroscopic features of AD

This thesis we will be mainly focusing on the microscopic aspects of Alzheimer's and ageing, but understanding the macroscopic features of Alzheimer's is important to understand how the disease operates. Macroscopic features, in of itself, doesn't signify AD pathology as they can indicate other neurodegenerative diseases, but conflictingly these macroscopic characteristics can indicate AD [9]. The AD brain often has at least some moderate shrinkage that is most marked in multimodal association cortices and limbic lobe structures [9, 15, 16]. The frontal and temporal cortices often have enlarged sulcal spaces (larger space between the grooves) with atrophy of the gyri (shrinkage between the ridges/folds), while primary motor and somatosensory cortices most often appear unaffected [9, 17-19]. There is increasing recognition of shrinkage in posterior cortical areas in AD, where the precuneus and posterior cingulate gyrus are the most noteworthy, partially projected by functional imaging studies. As a result of this atrophy, there is often enlargement of the frontal and temporal horns of the lateral ventricles, and decreased brain weight can be observed in most affected AD patients [9].

In a review written by Asgeir Kobro-Flatmoen (2021), it is stated that:

"None of the macroscopic features can be associated by other neurodegenerative diseases (ND) than AD, and unaffected clinically normal people may have moderate cortical shrinkage, especially affecting frontal lobes, with white matter being the most affected by loss of volume. Medial temporal shrinkage affecting amygdala and hippocampus, which is usually accompanied by temporal horn enlargement is typical of AD but can be observed in other age-related disorders such as hippocampal sclerosis or argyrophilic grain disease. Another macroscopic feature commonly observed in AD is loss of neuromelanin pigmentation in the locus coeruleus. None of these observations alone are specific to AD, but often they can be highly supportive, especially in the

absence of macroscopic changes specific to other neurodegenerative diseases." (Kobro-Flatmoen, A. *et.al.*, 2021, p. 101-307)

1.2.3 Amyloid-β plaques

Aβ is mentioned as one of the main neurotoxic compounds found in AD. Therefore, is important to understand how amyloid-β affects the neurons in AD patients. However, the main focus of this thesis is the tau pathology since this pathology has a direct link to TFEB, and therefore a brief theoretical background of this neurotoxic compound will be explained [20]. The amyloid-β (Aβ) is described as a 4 kDa fragment and is a "byproduct" of the amyloid precursor protein (APP). APP is a larger precursor molecule which is proteolytically cleaved by secretases and is considered to be a membrane-anchored receptor [21, 22]. There are to secretases that proteolytically cleaves APP, β-secretase (β-APP-cleaving enzyme-1 (BACE1)) at the ectodomain and γ-secretase at intra-membranous sites. These cleavages generate Aβ and studies have shown that inhibition of these two enzymes reduces the accumulation of Aβ aggregates [21, 23, 24]. In 2001, H. F. Dovey analyzed if inhibition of γ-secretase could reduce the amount of Aβ aggregates accumulated in HEK293 (293 cell line of Human Embryonic Kidney) cells. They discovered that there was a reduction of neuronal Aβ accumulation when a secretase inhibitor was introduced [23, 25].

According to Roychaudhuri, R., *et.al.* (2009), amyloid beta works in this following way:

"In AD, Aβ (which is expressed normally and ubiquitously throughout life as a 40-42 residue peptide) forms fibrils that deposit in the brain as "amyloid plaques". Aβ is an amphipathic peptide. The side chains of 16 of the first 28 residues are polar; 12 are charged at neutral pH. The remaining 12 ($A\beta_{40}$) or 14 ($A\beta_{42}$) side chains are apolar. Structures such as these can form micelles or interact with membranes directly. Recent work has shown that $A\beta_{40}$ inserts into membranes of hippocampal neurons from AD brains. Membrane insertion can perturb plasma membrane structure and function. Mitochondrial dysfunction has been linked directly to the aging process, a process that is the largest single risk factor for AD. Exacerbation of age-related dysfunction by toxic Aβ assemblies may explain the linkage of both age and Aβ to AD. Increasing evidence suggests that Aβ-induced mitochondrial dysfunction does in fact occur. The interaction of full-length Aβ or turnicated forms with mitochondria which causes potent inhibition of electron transport chain enzyme complexes and reductions in the activities of tricarboxylic acid cycle enzymes, leading to inhibition of ATP production, mitochondrial swelling, cytochrome *c* release, caspase activation, transition pore opening, increased mitochondrial reactive oxygen species production, and decreased mitochondrial membrane potential and respiration rates. Complexation of Aβ with Aβ-binding alcohol dehydrogenase, a mitochondrial matrix enzyme, or with endoplasmic reticulum-associated Aβ-binding protein also produces this type of damage [26]." (Roychaudhuri, R., *et.al.*, 2009, p. 4749-53)

1.2.4 Tau proteins

Tau proteins is a microtubule-associated protein (MAP), meaning that tau proteins in of themselves stabilize the microtuble by binding to the axons [9, 27, 28]. However, once tau is highly phosphorylated by multiple different proteins, like Glycogen Synthase Kinase 3 β (GSK3β), Cyclin Dependent Kinase 5 (CDK5), c-Jun N-terminal Kinases (JNK), and Mitogen-Activated Protein Kinases (MAPK), it undergoes a conformational change and can no longer bind microtubles [28-30]. This can lead to neuronal cell death in a range of neurodegenerative disorders, which is referred to as tauopathies [28-30].

1.2.4.1 Tau protein structure

Tau is normally used to stabilize the far microtubule in the distal portions of the axons, where the tau structure is important for it to function normally [28, 29]. Human tau is encoded by a single gene consisting of 16 exons present on chromosome 17q21, which is also called the Microtubule-Associated Protein Tau (*MAPT*) gene [27, 31]. Six tau isoforms can derive from alternate splicing of 11 of these exons retrieved in the central nervous system (CNS). The different splice variants can vary in size from between 352-441 amino acids, where they can include any combination of the exons E2, E3, and E10. These different combinations creates isomers of tau, which can contain either three (3R) or four (4R) C-terminal tandem repeats of 31-32 amino acid microtubule binding domains encoded by the exons E9, E10, E11 and E12 [32]. In addition, the triplets of 3R and 4R isoforms differ from one another by the presence or absence of E2 and E3 to generate tau isoforms with either 0 (form 0N), 29 (1N), or 58 (2N) amino acid inserts at the N-terminus [31, 32].

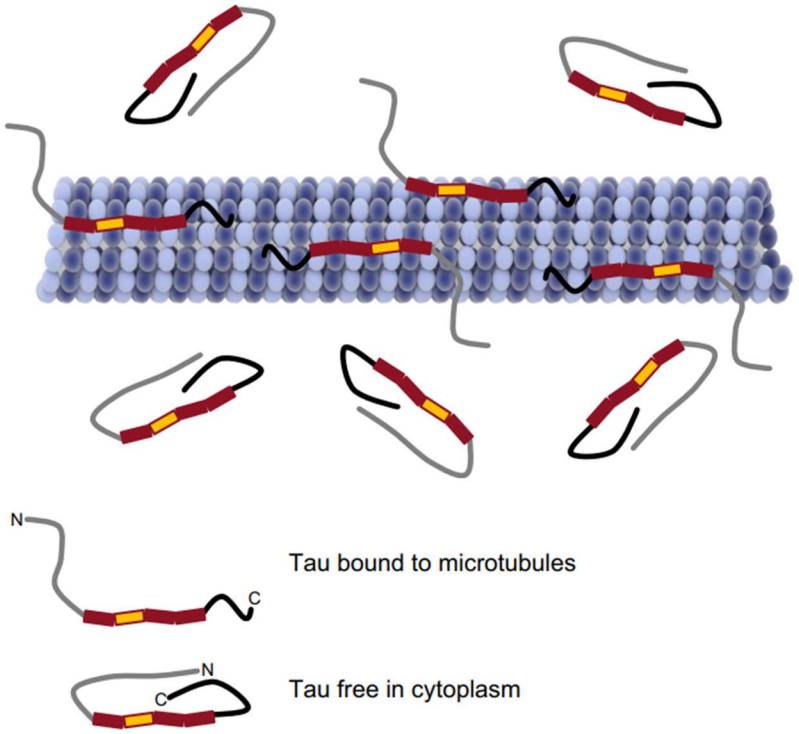

Fig. 1 Tau proteins binding to microtubules. Tau binds to microtubules mainly through the microtubule binding domain (MBD). These binding domains consists of either 3 or four microtubule binding repeats (MBR). The N- and C-terminal of tau are close together, forming a sort of "paper-clip" structure when it is free in the cytoplasm. When tau is bound to the microtubules, the terminal regions of tau separate and the N-terminal of tau points away from the microtubule surface. Image taken from (Guo, T., *et.al.*, 2017).

1.2.4.2 Phosphorylation of Tau proteins

Post-translational modifications (PTM) are changes that can occur after translation of a protein, where tau protein pathology is strongly linked with PTMs. Tau is exposed to a variety of PTMs, including phosphorylation, isomarisation, acetylation, glycation, nitration, oxidation, SUMOylation, ubiquitylation, and

more [33]. Different tau interacting molecules are exposed to post-translational modifications, and can react to the same PTMs as tau, for example, protein kinases and phosphatases [28, 33].

Tau protein contains 85 alleged phosphorylation sites, with 45 serine residues, 35 threonine residues, and 5 tyrosine residues [34, 35]. Because of the amount of amino acid residues in the tau protein that is potential phosphorylation sites, site-specific phosphorylation of tau is one of the main factors that are affected by tau aggregation [36]. When tau is phosphorylated, it also loses its ability to bind to the microtubule, leading to cytoskeleton destabilization and reduced intracellular transportation [28, 29, 33]. A study conducted by G. Farías (2011) found that tau post-translational modifications between AD individuals is heterogenous, suggesting no defined AD-associated phosphorylation pattern but rather a certain propensity for phosphorylation at certain phosphorylation sites [37].

Tau also has the ability to "self-aggregate" when it no longer can bind to the microtubule, which will lead to the formation of neuro fibrillary tangles (NFT) [38]. Phosphomimicking, or pseudophosphorylation, is the process of altering the amino sequence of the tau protein to simulate phosphorylation [39]. Replacing one of the phosphorylation sites of tau with a negatively charged amino acid, like glutamate or aspartate, showed similar effects of phosphorylation and provoked neurotoxic effects as well, like apoptosis [28, 40].

Phosphorylation of the different regions of tau have different effects, like phosphorylation of the proline-rich regions of the MBRs compared to the C-terminal region. Phosphorylation of the C-terminal region greatly promoted self-aggregation [41], whilst phosphorylation of the MBR showed less self-aggregation [37, 38].

Phosphorylation is highly controlled by protein kinases and phosphatases, where disruption has been shown to reduce the amount of tau aggregates [42]. There are several protein kinases that can affect tau, where each kinase affect tau in differently. According to a review by Guo, T. *et.al.* (2017), these kinases can be classified accordingly:

"(1) Proline-directed serine/threonine-protein kinases, including glycogen synthase kinase (GSK) 3α/β, cyclin-dependent kinase-5 (Cdk5), mitogen-activated protein kinases (MAPKs), and several other kinases including those activated by stress [28, 42, 43]. (2) Non-proline-directed serine/thronine-protein kinases, such as tau-tublin kinase 1/2 (TTBK1/2), casein kinase 1 (CK1), dual-specificity tyrosine phosphorylation regulated kinase 1A (DYRK1A), microtubule affinity-regulating kinases (MARKs), Akt/protein kinase B, cAMP-dependent protein kinase A (PKA), protein kinase C, protein kinase N, 5' adenosine monophosphate-activated protein kinase (AMPK), calcium/calmodulin-dependent protein kinase II (CaMKII), and thousand and one amino acid protein kinases (TAOKs) 1 and 2 [28, 42, 43]. (3) Protein kinases specific for tyrosine residues, such as Src, Fyn, Abl, and Syk [28, 42, 43]." (Vol. 133, p. 665-704)

Allegedly, more than 40 phosphorylation sites are targeted by GSK3, where increased activation of GSK3β greatly increased the levels of phosphorylation of tau in the AD brain, proving increased levels of GSK3 correlates with neurodegeneration [44]. The levels of NFTs in AD brain is also shown to increase with the overactivation of GSK3β where this enzyme was also shown to occupy the same space as the NFTs [45]. Furthermore, a study conducted in 2011 (Sangmook Lee, *et.al.*) proved that GSK3β increase tau phosphorylation, along another proline-directed kinase Cdk5. They concluded in the study that multiple phosphorylation enzymes enhances the phosphorylation of tau[46].

1.3 The twelve hallmarks of ageing

1.3.1 The twelve hallmarks of ageing

Ageing is characterized by progressive functional decline at all molecular, cellular, tissue, and organismal levels, and as an organism age, it becomes frail, its susceptibility to disease increases, and its probability of dying raises [47]. With these characterizations of ageing, we can gather multiple factors that decrease as we age. These factors are usually referred to as "The twelve hallmarks of ageing" which, according to Carlos López-Otín *et.al.* (2023) fulfills the following three premises: (1) their age-associated manifestation, (2) the acceleration of ageing by experimentally accentuating them, and (3) the opportunity to declare, stop, or reverse ageing by therapeutic interventions on them [4]. The twelve hallmarks of ageing are as follows:

1. Genomic instability
2. Telomere attrition
3. Epigenetic alterations
4. Loss of proteostasis
5. Disabled macroautophagy
6. Deregulated nutrient-sensing
7. Mitochondrial dysfunction
8. Cellular senescence
9. Stem cell exhaustion
10. Altered intercellular communication
11. Chronic inflammation
12. Dysbiosis

In this thesis, the focus will be on the mitochondrial dysfunction (7) and the disabled macroautophagy (5), since these hallmarks are strongly associated with AD and with tauopathy [48, 49].

1.3.2 Loss of proteostasis

Protein homeostasis, or "proteostasis", is reduced as we age. This is prevalent in ageing related diseases such as amyotrophic lateral sclerosis (ALS), AD, and Parkinson's disease [50-52]. Normally, systems involved in proteostasis will discover disturbances and repair them to keep balance. As we age, these systems, like the ubiquitin-proteosome system (UPS), are weakened and therefore struggle to keep proteostasis balance, which leads to protein aggregates [53].

Loss of proteostasis can cause missfolded proteins, which is a common feature of neurodegenerative diseases, where accumulation of these missfolded proteins can lead to stress in the cell, along with PTMs [54]. There are four major phases of translation, where a balance of all four is important to maintain a proper proteostasis. There have been multiple reports supporting that the elongation phase is the most exposed, where both protein folding and mRNA decoding are rate limited and supervision of the synthesized protein is necessary to form healthy proteins [55, 56]. Mutations in these chaperones can cause protein misfolding, which has been found in both AD and in ALS [57, 58]. This proves that the mechanisms behind protein folding, and repair are important to maintain cellular health.

1.3.3 Disabled macroautophagy

Macroautophagy (From now on referred to as "Autophagy") is a cellular recycling process that uses autophagy related proteins (ATG) to form a double membrane layer around a damaged organelle or protein. These targets of autophagy are ubiquitinated, and lysosome is attached at the end of the autophagy process to decompose these structures to smaller amino acids and proteins [59].

Autophagy not only targets proteins to create proteostasis along with other cell recycling systems, but it can also target larger organelles that have damage or is tagged, for example, mitochondria (mitophagy), lysosomes (lysophagy), the ER (reticulophagy), peroxisomes (pexophagy), or other invading pathogens (xenophagy) [60-64]. Evidence shows that as we age, autophagic activity is also decreased, meaning that one of the most important systems to remove and recycle organelles is also reduced [65].

Some genes and proteins that are involved in autophagy are also involved in alternative degradation proceeded, like the microtubule-associated protein light-chain 3 (LC3) which is involved in a process called associated phagocytosis (LAP), where LC3 is recruited to a single-membrane phagosome instead of a double-membrane phagosome as in autophagy [66]. More details on autophagy and mitophagy will be discussed in section **1.4 Autophagy**. With that being said, there are strong evidence that autophagy is related to ageing.

1.3.4 Mitochondrial dysfunction

Mitochondria is famously known as "the power house of the cell", but not only does mitochondria play a key part in energy production, but according to Keshav K. Singh (2004), it is also involved in "respiration, heme synthesis, lipid synthesis, metabolism of amino acids, nucleotides, and iron, and maintenance of intracellular homeostasis" (vol.5, p. 127-132). When mitochondria is damaged, it can trigger an inflammatory response in the cell where reactive oxygen species (ROS) or mitochondrial DNA (mtDNA) leak out of the mitochondria and in worst case cell death is lethal enzymes are leaked into the cell [67].

As we age, mitochondrial functions deteriorate and there is a decline in the respiratory function in the cell. This can affect different cell types including the neurons, where mtDNA can mutate and accumulate which can in turn cause respiratory deficiency [68].

This accumulation of mtDNA can lead to increased production of ROS in the cell and can therefore increase pathological diseases linked with these oxidative species, dysfunction of the permeability transition pore (PTP) leading to diffusion of solutes into the mitochondria creating swelling and rupture which can cause cell death [69]. Therefore, it is important to maintain the health of mitochondria by targeting the mitochondria damaging factors which is accompanied by ageing [67-69].

1.3.4.1 Tau and mitochondrial dysfunction

Tau pathology has been proven to be linked to mitochondrial dysfunction and dynamin-related protein 1 (DRP1) which can bind to tau and cause neurodegeneration [70]. A study in 2017 (Ramesh Kandimalla, *et.al.*) conducted on mice with Proline 301 Leucine (P301L) human tau mutation, they analyzed the mitochondrial structure and function and dynamics protein. They found increased levels of hydrogenperoxide (H_2O_2) as well as decreased levels of ATP level in hippocampal regions as well as increased number of mitochondria in 12-month old tau mice, suggesting that tau pathology does affect mitochondrial function and structure [71]. Another study conducted by Abtahi, S., L., *et.al.* (2020) targeted the *MFN2* ortholog *Marf* and *Drp1* genes in

tau model *Drosophila melanogaster*, which are both mitochondrial genes. What they found was that *Drp1* was upregulated in tau expressing flies, and that *Marf* was downregulated, meaning that in presence of aggregated tau, mitochondrial fission is upregulated, and mitochondrial fusion is downregulated [72].

Furthermore, Maria Manczak, *et.al.* (2012) suggests that interactions between DRP1 and tau increase mitochondrial fragmentation, leading to neuronal deficiency. It was later suggested that a partial knock down of DRP1 could seemingly normal synaptic, dendric and mitochondrial function [73]. GSK3β has also been shown to increase Drp1 and mitochondrial fragmentation in tau mice [74], and decreasing expression of DRP1 decreases amount of phosphorylated tau in P301L mice, which in turn reduces neuronal mitochondrial dysfunction [75].

N-terminal tau fragment (Tau_{26-230}) is found to be enhanced in mitochondria in AD brain, which also showed correlated with synaptic and mitochondrial dysfunction [76, 77].

Overexpression of tau can also lead to defective mitophagy in neurons, leading to mitochondrial dysfunction and accumulation of tau in the outer mitochondrial membrane leading to an increase of mitochondrial membrane potential [78].

1.4 Autophagy

As previously mentioned in section **1.3.3 disabled macroautophagy**, autophagy is the process of cellular recycling of proteins and organelles by lysosomal degradation. Autophagy starts by forming a bowl-shaped structure, which is called the phagophore, that is developed in the ER. It creates its shape, grabbing the target molecule in its center and closes with a help from membrane fission, which will form a double-membrane structure called the autophagosome [60, 79]. The autophagosome swallows a piece of the cytoplasm when fusing together [60, 79]. After the formation of the autophagosome, it will fuse with lysosomes to create a autolysosome where the proteins or organelles are degraded and recycled. [80].

Autophagy is mostly activated when needed [79], but it is also used to keep cellular homeostasis by degrading dam In addition, autophagy maintains cellular homeostasis by selectively degrading proteins, organelles and foreign entities; this process is particularly important for long-living cells such as neurons [81]. There are multiple functions in the autophagic (*ATG*) genes both in autophagy and not, where these different functions are exocytosis, secretion, and extracellular vesicle biogenesis [82]. Multiple research fields have turned their attention to *ATG* genes because of its multiple functions and applications.

There has been conducted a lot of research on the different functions of *ATG* genes, where these findings was made possible by new technologies such as cryo-electron tomography, nanostructure-based probes, and CRISPR/Cas9 technology, which hopefully in the future can lead to increased knowledge in structural and functional mechanisms behind in both non-autophagic and autophagy research [83-85].

Autophagy is also relevant in neurodegenerative diseases such as AD, where blood samples and animal models have identified downregulated *ATG* genes in AD models, and by upregulating these *ATG* genes was beneficial for neuronal protection [86-88].

1.4.1 Initiation of autophagy

Initiation of autophagy starts with the central regulator called the ULK complex, which consists of the scaffold protein FIP200, ATG13, ATG101 and the serine/threonine kinases ULK1 or ULK2 [89].

The mechanistical target of rapamycin complex 1 (mTORC1) is the main regulator of the ULK complex, where upon starvation mTORC1 will be activated and start the activation and assembly of the ULK complex near the ER membrane; this results in recruitment of downstream ATG proteins which initiate autophagosome formation [90]. Furthermore, the ULK complex is also driven by autophagy cargos, like SQSTM1 (also called p62) which forms fluid-like condensates with ubiquitinated proteins and interacts with FIP200 which in turn recruits the ULK complex [91].

The ULK complex then recruits ATG9 vesicles, which is the sole multispanning membrane protein that is essential for autophagosome formation and is proposed to have a large role in delivering lipids that is needed for autophagosome formation [92].

The recruitment is accomplished by interaction between the Hop1, Rev7, and Mad2 (HORMA) domains, which are multifunctional protein-protein interaction modules, of the ATG13-ATG101 subcomplex and the most C-terminal region of ATG9A (human ATG9) [93-95].

ATG9 vesicles are recruited in the parkin-dependent mitophagy as well, through binding the autophagy adaptor OPTN, where OPTN is present on damaged, ubiquitinated mitochondria [96].

1.4.2 Membrane formation and elongation

Another important molecule in autophagy is the molecule phosphatidylinositol 3-phosphate (PI3P). This molecule is synthesized by the type III phosphatidylinositol 3-kinase (PI3Kinase), which is composed of 5 subunits: Vps34, Vps15, BECN1, ATG14 and NRBF2; PI3P is synthesized by the hVps34 seat of this complex [97]. PI3P is used in the autophagosome formation by spatiotemporal control of autophagy initiation [98].

PI3P contains effectors that helps to bind the phosphoinositides (WIPI) family, where there are four (WIPI1-4), proteins through β-propellers which help phagophores evolve into autophagosomes; the WIPI proteins further recruits the ATG2 protein [99, 100]. ATG2 helps with the formation of autophagosomes by creating a rod-shaped structure that attaches itself to the ER membrane with its N-terminal tip and the autophagic membrane with its C-terminal tip [100], but so far there have been no reports on how the transfer occurs. There has been reported that there is a possible interaction between WIPI3 and WIPI4 to recruit ATG2 to the autophagic membranes with rich amounts of PI3P [101]. Furthermore, WIPI2 binds to the ATG16L1 which is used in the complex ATG12-ATG5-ATG16L [102]. The phagophore is enriched with phosphatifylethanolamine (PE) which are an abundant phospholipid that acts as the recruitment center for ATG8, consisting of LC3 and GABARAP [103].

ATG2 is also interacting with the LIR motif in the ATG8 complex, which is essential for the autophagosome formation. ATG2 will continue to move lipids from the ER with the help of WIPI3, these lipids will be modeled by the ATG9 which is promoted from the pre-autophagosome structure (PAS). The ATG9 will move alongside ATG2-WIPI3/4 binding complex and form the autophagic membrane as shown in **Fig. 2**; how ATG9 in mammals forms the initial inner membrane remains unclear [104].

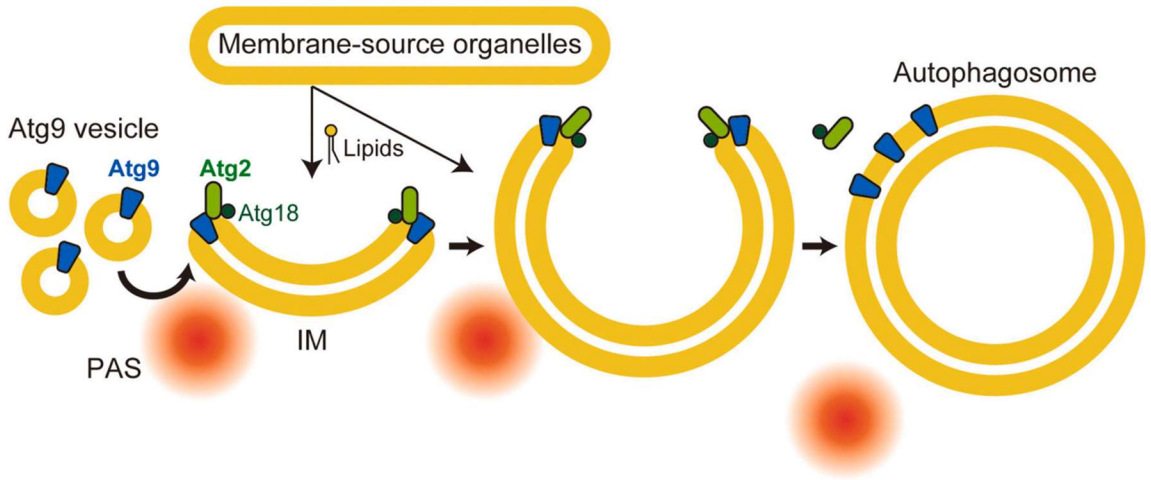

Fig. 2 Double-membrane formation of the autophagophore. A schematic illustration of how the autophagophore membrane is formed. ATG9 moves onto the IM and localizes at the expanding edge from the pre-autophagosomal structure (PAS), ATG2 and WIPI4 (ATG18 in yeast) will form the lipid shape around the outer membrane. Lipids are believed to come from the ER and other various membrane-source organelles. When the formation of the autophagosomal membrane is complete, ATG2 and WIPI3/4 leaves the phagophore membrane, but ATG9 still remains. Image taken from (Collier, J. J., *et.al.*, 2021)

An important step of the membrane formation in autophagy is the conjugation of lipids. A review done by Collier, J., J., *et.al.* (2021) explains the conjugation system as follows:

"ATG8 bound to PE (ATG8-PE, or LCII) are one of the two ubiquitin-like conjugation systems present in the formation of autophagosome. ATG7 is an E1-like enzyme, which is a ubiquitin-activating-like enzyme, which is driven by multiple steps using the ATG8, ATG4, ATG3, ATG10 and ATG12. First, ATG4 opens up the C-terminal of ATG8 (LCI), exposing it for ATG7 to interact with it. ATG8 is then adenylated by ATG7 before it is transferred to ATG3. ATG8 is then conjugated to PE to generate form 2 of ATG8 (LCII), which is localized in both the inner and outer membrane of the autophagosome, which is then degraded upon autolysosome formation. ATG7 joins the second conjugation step with ATG12 which is also adenylated by ATG7. It is from there transferred to ATG5 via ATG10, and ubiquitin-conjugating-like enzyme, which generates ATG5-ATG12 conjugates. This structure is restricted to the outer membrane of the autophagosome and the is removed when sealing the autophagosome. ATG5-ATG12 forms a complex with ATG16L which promotes LC3 lipidation." (Vol. 13, issue 12, p. e14824) [105]

What is important to note is that these systems can be disrupted in mammalian cells, but the cells can still form autophagosomes. These systems seem to be more important to the fusion of lysosomes and are still essential for the autophagic system [106].

1.4.3 Recognition of cargo by autophagosome

Autophagosomes engulf a part of the cytoplasm, it is believed that most of the soluble cargos are merged with the autophagosomes non-selectively [107], but damaged organelles, intracellular bacteria, and certain proteins do have tags that is recognized by the autophagosome [108]. ATG8 is used as a cargo recognition, as well as necessary in the formation of the autophagic membrane; ATG interacts with the LC3-interacting region (LIR) motifs attached to the cargos, which can either be ubiquitin-dependent or -independent [109]. Among the ubiquitin-independent soluble cargo adaptors are SQSTM1 and OPTN [110, 111], and for the

ubiquitin-independent category are, for instance, mitophagy related proteins (for example, BNIP3, BNIP3L/NIX, FUNDC1, FKBP8 and BCL2L13) as well as LIR-containing soluble proteins (such as CALCOCO1) [112-114]. LIR also has a function in recruitment of some important autophagy initiation proteins, like FIP200, ULK1 and ATG13 [115-117].

1.4.4 Closure of autophagosomes

Closure of the autophagosome is one of the autophagic events that is not well known. The reason being that by viewing the autophagosome, it is hard to distinguish the unclosed ones from the actual closed ones, but some discoveries have been made; it was previously thought that the autophagosome would close through fusion, but it has been lately discovered that it is using fission of the inner- and outer membrane of the autophagosome [118]. Another factor of the closure of autophagosomes is the use of the endosomal sorting complex required for transport (ESCRT) complex; how the ESCRT complex is localized to the open rim of the phagophore is still not understood in mammals [119].

1.4.5 Autolysosome formation

According to Hayashi Yamamoto, *et. al.*, (2023), he wrote in his review about autophagy about the autolysosome formation:

"Autophagosomes will fuse with lysosomes to become autolysosomes after closure. In mammals, fusion is mediated by the soluble *N*-ethylmaleimide-sensitive factor attachment protein receptor (SNARE) proteins STX17 and YKT6, which are recruited to autophagosomes when they are closed, thereby preventing premature fusion between unclosed autophagosomes and lysosomes. STX17 and YKT6 form SNARE bundles with cytosolic SNAP29 and lysosomal VAMP7/VAMP8 and STX7, respectively [120]. The relationship and functional differences between these two autophagosomal SNAREs (STX17 and YKT6) are not well understood; thus far, they seem to function redundantly. Tethering between autophagosomes and lysosomes is mediated by multiple tethering factors, including HOPS, PLEKHM1 and EPG5 [121]. PLEKHM1 and EPG5 have LIR motif and therefore interact with autophagosomal ATG8.

After fusing with lysosomes, the inner autophagosomal membrane is degraded. Most organisms, including mammals, possess multiple lysosomal phospholipases, which might be redundantly involved in inner membrane degradation. One major remaining question is how degradation is limited to only the inner membrane when both the outer and inner membranes, which are derived from the same phagophore membrane, are exposed to lysosomal enzymes [122].

After prolonged starvation, autolysosomes deform to generate protolysosomes that then mature into functional lysosomes, in a process called autophagic lysosome reformation (ALR). This process recycles lysosomal membrane proteins and is triggered by the reactivation of mTOR in response to increased amino acid levels owing to prolonged macroautophagy [123]. Upon induction of ALR, the PI(4)P 5-kinase PIP5K1B produces $PI(4,5)P_2$ on the membrane of autolysosomes, generating $PI(4,5)P_2$-rich microdomains that are further organized by clathrin and adaptor protein 2 (AP2) [124]. Lysosomal membrane proteins are captured in these microdomains, which subsequently undergo tubulation driven by the kinesin heavy chain KIF5B [125]. The mechanism by which protolysosomes mature into lysosomes remains to be elucidated [79].

An additional autolysosome recycling mechanism called autophagosomal components recycling (ACR) was recently reported. This mechanism recycles autophagosome-derived membrane-anchoring proteins such as ATG9 and STX17 via the bugging of autolysosomal membranes depending on the SNX4-SNX5-SNX17 recycler complex and the dynenin-dynactin complex [126]. Thus, autophagosomal and lysosomal membrane proteins are recycled by ACR and ALR, respectively. ACR occurs earlier than ALR [79]." (Vol. 24, p. 382-400)

1.4.6 Autophagy-lysosome pathway (ALP)

Daniel L. Kenney, *et. al.*, (2015) wrote in a review about the Autophagy-lysosome pathway (ALP) which said:

"Lysosomes are spherical vesicles containing more than 50 different hydrolytic enzymes (including proteases, lipases, glycosidases, nucleases, and phosphatases) that are optimally active at about 5.0 pH (acidic). The genes encoding lysosomal protein genes are transcribed in the nucleus, and the mRNA transcripts exit the nucleus and are translated by ribosomes. Lysosomal enzymes are released from the Golgi apparatus in small vesicles that ultimately fuse with acidic vesicles called endosomes, thus becoming full lysosomes [127, 128]. Most developed lysosomal enzymes are specifically tagged with mannose 6-phosphate and bind to mannose-6-phosphate receptors in the trans-Golgi network; the enzymes traffic to early and late endosomes, which then fuse to the lysosomes [129]. The endosomes and lysosomes maintain an acidic intravesicular pH by pumping protons from the cytosol across their membrane via the proton vacuolar adenosine triphosphatase (V-ATPase); this process is coupled with a countertransport of chloride (Cl^-) ions via the CIC-7 Cl^-/H^+ antiporter [130, 131]. Mucolipin 1 (transient receptor potential mucolipin, TRPML1) is a Ca^{2+} and H^+ permeable cation channel that regulates the maturation of late endosomes to lysosomes [132]. ATP13A2 is a lysosomal type P5B-ATPase that also regulates lysosomal function; it may act as a flippase, transporting lipids or peptides from one membrane leaflet to the other, thereby controlling local lipid dynamics during vesicle formation and membrane fusion events [133]. Lysosomes differ from endosomes in their degree of acidification, higher Ca^{2+} content, and more abundant levels of lysosomal membrane proteins (LAMPs) such as LAMP1 and LAMP2 [134, 135]. TFEB is the master regulator of lysosomal expression and regulation where it binds to the coordinated lysosomal expression and regulation (CLEAR) motif [128, 136, 137]." (Kenney, L. D., *et. al.*, 2015, p. 634-45)

1.5 Nicotinamide dinucleotide (NAD^+)

In 1906, Nicotinamide adenine dinucleotide, of NAD^+, was firstly discovered as a coenzyme in fermentation [138], and is now known to have an essential role in many cellular functions; ranging from redox homeostasis, glycolysis, the tricarboxylic acid cycle (TCA), mitochondrial oxidative phosphorylation (OXPHOS), and cell signaling pathways [1, 139]. NAD^+ has a lot of different precursors, like nicotinic acid (NA), nicotinamide (NAM), nicotinamide riboside (NR), nicotinamide mononucleotide (NMN), and dihydronicotinamide riboside (NRH) [140, 141]. Since NAD^+ have so many different functions, it is been increasingly studied as a drug in modern medicine, and has shown ageing improving effects [142]. Precursors have been long been studied for their prevention of ageing phenotypes and to promote long-term wellness as well as reducing ageing related phenotypes, like NR and NMN [143].

1.5.1 Synthesis of NAD^+

NAD^+ is reversibly converted into NADH, but it can also convert to $NADP^+$ which also reversibly converted to NADPH [141, 144]. Enzymes like SIRTs, ADP ribosyl transferases (ARTs) and poly (ADP-ribose) polymerases (PARPs) consume NAD^+ and is therefore important for synthesis of NAD^+ to maintain a healthy amount [145]. Synthesis

of NAD^+ can be achieved by multiple pathways, like the kynurenine pathway, the Preiss-Handler pathway, the salvage pathway, and the emerging NRH-salvage pathway [146-149]. Importantly, even though the salvage pathway and the NRH-salvage pathway are intertwined, they can be separated since the NRH precursor in of itself has been reported to increase the level of NAD^+ in blood by 3-10 fold in a variety of cultured mammalian cells [149]. For this thesis, we have worked with NMN which is synthesized to NAD^+ through the salvage pathway.

1.5.1.1 The salvage pathway

According to the review by Reiten, O. K., *et.al* (2021), the salvage pathway goes as follows:

"The salvge pathway is considered to be a powerful approach to boost intracellular NAD^+ in a fast and efficient manner. Within the cell, NAM is metabolized into NMN via nicotinamide phosphoribosyltransferase (NAMPT) and then by NMNAT1-3 into NAD^+. There is intracellular NAMPT (iNAMPT) and extracellular NAMPT (eNAMPT). As NAMPT is the rate-limiting enzyme of the salvage pathway, the importance of iNAMPT-induced initiation of NAM-dependent NAD^+ recycling is highlighted. Of the three NMNATs, NMNAT1 is a nuclear enzyme with expression level tissue-specific; there are higher levels in skeletal muscle, heart, kidney, liver, and pancreas, whereas the levels measured in the brain are sparse. NMNAT2 is predominantly found in cytosol and Golgi apparatus, while NMNAT3 is located in the mitochondria/cytoplasm. In addition to the endogenous NAM and NMN for the salvage pathway, exogenous molecules like NAD^+, NMN, NR, and NAM, also participate in this pathway. Extracellular NAD^+ and NMN are normally catabolized to NR or NAM by the membrane-bound NADases ADP-ribosyl cyclases (CD38/CD157), and CD73. While the relatively small NAM molecule can diffuse into cells, the larger NR molecule is transported into the cell via the equilibrative nucleoside transporter (ENT) family ENT1, ENT2, and ENT4. There are inconsistent reports as to whether extracellular NMN could be taken up by the cells. For example, some studies shows that extracellular NMN is dephosphorylated to NR for cellular uptake, while another report argued SLC12A8 was a cellular transporter of NMN whereby the data got challenges. As NAM enters the cell, it participates in the salvage pathway directly. For internalized NR, it is phosphorylated to NMN by nicotinamide riboside kinase 1 or 2 (NRK1/NRK2), then further converts to NAD^+ [141, 148]." (Reiten, O. K., *et.al.*, 2021, p. 111-567)

1.5.2 Functions of NAD^+

The NAD^+ and NADH level is necessary for maintaining metabolic homeostasis through catabolism of carbohydrates, proteins and lipids; $NADP^+$ and NADPH is necessary for the synthesis of fatty acids, nucleotides and amino acids [150]; NADPH also functions as a substrate for NADPH oxidase, which provides support in resistance against ROS [151]. NAD^+ can convert to $NADP^+$ by NAD^+ kinases (NADKs) which allows for the many functions of these redox molecules to occur [152]. This also suggests that there is an important interaction between NAD^+/NADH and $NADP^+$/NADPH to keep a cellular homeostasis, which could explain why imbalances can lead to severe side effects and how increasing the NAD^+ levels could prove beneficial [153]. Normally, NAD^+/NADH is used in oxidative reactions for processes like glycolysis, the TCA cycle, and OXPHOS, which requires a lot of cellular energy; this leads to a shift in the cellular environment which can favor oxidative reactions in the cell, like gluconeogenesis and ketone body synthesis [154]. NAD^+ is divided into the different parts of the cell: the nucleus, cytoplasm and mitochondria; there are different subcellular channels that regulate the NAD^+ homeostasis [155], for instance, the SLC25A51 transporter, which transfers NAD^+ across mitochondrial membranes [156].

1.5.2.1 Consumption of NAD^+ and metabolism

Cell signaling, regulation of transcription and calcium homeostasis are other functions in the cell that requires NAD^+ apart from the functions previously discussed. Enzymes like the sirtuins (SIRTs), poly-ADP-ribose polymerases (PARPs), require NAD^+ as a co-substrate to function; proteins like CD38, CD157, and SARM1 also require NAD^+ to be fully operational [138, 157, 158], where NAD^+ is converted into NAM in the reaction chain with these proteins. These proteins control many different cellular functions where NAD^+ is necessary [141].

SIRTs are deacetylases, converting NAD^+ to NAM and 2/3-o-acetyl-ADP-ribose in the process of removing acyl groups from lysine residues on target proteins. There are seven SIRTs in mammals, specific to different subcellular compartments. Whereas SIRT1, SIRT6 and SIRT7 are mainly located in the nucleus, SIRT2 is cytoplasmic, and SIRT3-5 are mitochondrial [159]. The nuclear sirtuins are particularly associated with deacetylating histones, transcription factors and transcription coactivators, thereby regulating the transcription of genes involved in metabolism, mitochondrial homeostasis, stem cell rejuvenation, as well as both tumor growth and inhibition [160]. Among the seven SIRTs, some of the key discoveries have related to SIRT1, SIRT6, and SIRT3. SIRT1 regulates mitochondrial homeostasis through mitochondrial biogenesis via deacetylation of the transcription coactivators α (PGC-1α) and the clearance of damaged mitochondria via mitophagy [161]. While SIRT6 acts as a longevity protein in rodents via enhancing DNA repair and other mechanisms, deficiencies in this molecule result in developmental impediment [162]. Additionally, mitochondrial SIRT3 plays an important role by regulating substances with reactive oxygen species (ROS) by deacetylation of substrates involved in both ROS production and detoxification [163].

1.5.3 NAD^+ and autophagy

ROS production is usually associated with protein and DNA damage, and with ageing, the repair mechanisms are weakened and cannot resolve this kind of damage; reduced levels of autophagy and NAD^+ have been proposed in diseases and reduced cellular function that comes with age [164]. Research has shown that increasing autophagic factors or intracellular NAD^+ pools can improve eukaryotic health and lifespan; autophagy levels have also been elevated by NAD^+ supplementation which also improved cellular function [165]. There is evidence of mitophagy being improved by NAD^+ supplementation and is shown to improve health for a while; reduction of NAD^+ has been proven to reduce autophagy which can lead to cell death [166]. In short, autophagy and NAD reciprocally depend on each other for optimal cellular function. However, the mechanisms underlying this seemingly bidirectional relationship remain poorly characterized [164].

In a review by Wilson, N., *et.al.*, (2023) it was described how the NAD^+ regulated promoters' work:

"Previous studies have shown that SIRT1 promotes autophagy through post-translational modification of autophagy initiation proteins (ATG5/7/8 and microtubule-associated protein light chain 3 (LC3)) and the deacetylation-dependent activation of autophagy related transcription factors (TFEB and FoxO) [161, 167, 168]. Numerous studies, however, have highlighted that mitochondrial quality control, executed by mitophagy, is also associated with SIRT1 activity [166]. This was first established in human cells with defective DNA repair caused by deficiency of XPA (xeroderma pigmentosum complementation group A) protein. XPA-deficient cells exhibited downregulated SIRT1 activity, paired with compromised mitophagy/mitochondrial health and PARP1 hyperactivity. This aberration was rescuable by supplementing cells with NAD^+ precursors [169].

Furthermore, there has been reports that the SIRT1/3 potentiator resveratrol was shown to enhance mitochondrial function by strengthening interactions between the key mitophagy components Parkin and p62 [170, 171]. Considering that:

1. SIRT1 promotes ATP production via stimulating PGC1α-dependent mitochondrial biogenesis,
2. ATP abundance can increase translation of PTEN-induced kinase 1 (PINK1; a mitochondrial damage sentinel and Parkin recruiter),

SIRT1 may be involved in promoting PINK1/Parkin/p62-dependent mitophagy [172].” (Wilson, N., *et.al.*, 2023, p. 788-803)

1.6 The transcription factor EB

In a review paper about the transcription factor EB by Yang, J., *et.al.*, (2023) it explains:

“In the 1990s, TFEB (Transcription factor EB) was originally identified as a protein containing helix-loop-helix (HLH) and leucine-zipped region, which recognizes E-box sequence at promoter regions of heavy-chain immunoglobulin [173]. Recently, TFEB was found to be a key regulator of lysosomal biogenesis and autophagy [174]. In normal conditions, TFEB is mainly located in the cytoplasm and exists in an inactive form. Upon translocation from the cytoplasm into the nucleus, TFEB binds to the motif of the coordinated lysosomal expression and regulation (CLEAR) element to upregulate many genes responsible for lysosomal biogenesis and autophagy [137]. The cytoplasm or the nuclear localization of TFEB is mainly regulated by its phosphorylation status at certain Ser residues. A variety of kinases or phosphatases have been reported to regulate the phosphorylation status of TFEB by various mechanisms, including ERK2 (extracellular signal-regulated kinase 2), MTORC1, GSK3β, Akt, PKC (protein kinase C), PP2A (protein phosphatase 2A), calcineurin and GCN5 (general control non-repressed protein 5) [175-177].

The lysosome is an organelle for degrading and recycling misfolded and dysfunctional proteins, and it fuses with autophagosomes as autolysosomes to degrade sequestered cargos. Activation of TFEB-mediated lysosomal biogenesis to degrade protein aggregates is beneficial to NDs that are characterized by the accumulation of protein aggregates, like AD. Notably, impairment of lysosomal biogenesis and autophagy has been reported to be associated with the progression of these NDs [178, 179]. Therefore, activation of TFEB or increasing TFEB expression is a potential therapeutic for these NDs. In recent years, numerous small-molecule TFEB activators have been identified and some of them show promising neuroprotective effects in multiple animal models of AD [180].” (Yang, J., *et.al.*, 2023, p. 652-669).

1.6.1 TFEB and autophagy

Normally, TFEB is inactive and located in the cytoplasm. When activated, TFEB translocates into the nucleus, and binds directly to the CLEAR sequence at promoter regions of multiple lysosomal and autophagy-associated genes, leading to upregulating the expression of these target genes and subsequent enhancement of lysosomal biogenesis and autophagy [137, 173]. Autophagy serves as a crucial catabolic process to degrade misfolded and toxic proteins via lysosomes [81]. As TFEB is the key regulator of lysosomal biogenesis, it will promote the expression of multiple genes involved in lysosomal biogenesis and autophagy, including *LAMP1*, *CTSD*, *UVRAG*, *SQSTM1*, *MAPLC3B*, *ATG9* and others [173].

TFEB transcriptionally regulates autophagy by targeting multiple processes in autophagy, which include lysosomal biogenesis, autophagosome formation, and the fusion of autophagosomes with lysosomes [173, 181].

TFEB-mediated autophagy-lysosomal pathway (ALP) activation is different from canonical autophagy activators that only promote autophagosomes formation since a key role of TFEB activation is to increase the lysosomal functions [182]. Since the impairment of lysosomal functions has been implicated in NDs, TFEB activators may show advantages for treating NDs compared with autophagy activators that promote the formation of autophagosomes [173].

1.6.2 TFEB activation

TFEB located either in the nucleus or the cytoplasm depends on its phosphorylation status. Normally, phosphorylated TFEB is retained in the cytoplasm as an inactive form isolated by the cytosolic chaperone 14-3-3 proteins [183]. TFEB translocates from the cytoplasm into the nucleus to promote lysosomal biogenesis and autophagy upon dephosphorylation in response to multiple stimulus, which include lysosomal stresses, nutrient starvation, glucose deprivation and cholesterol stress [184]. TFEB has several phosphorylation sites, which can be regulated by multiple kinases (e.g., mTORC1, ERK2, GSK3β) and phosphatases (e.g., calcineurin, PP2A) that are critical for its subcellular localization. mTORC1, ERK2, and GSK3β phosphorylate and inactivate TFEB, as in contrast to PP2A and calcineurin who dephosphorylate and activate TFEB [176, 185, 186]. TFEB phosphorylation by mTORC1 is mediated by Rag GTPase and this is different from other normal mTORC1 substrates such as S6K1 and 4E-BP1 [173, 187]. ERK2, one of the extracellular signal-regulated kinases (ERKs), is another major candidate for the phosphorylation of Ser142 in TFEB [188, 189]. GSK3β phosphorylates TFEB at Ser134 and Ser138, PKCα and PKCδ induce TFEB translocation into the nucleus through inhibition of GSK3β-induced phosphorylation of TFEB [190]. Akt phosphorylates TFEB at Ser467 in an mTOR-independent manner to promote its cytoplasm accumulation as well [191]. Calcineurin binds to and dephosphorylates TFEB, leading to its nuclear accumulation [192]. Activation of PP2A has been shown to dephosphorylate TFEB, facilitating its nuclear translocation and activation [186]. SetA, a *Legionella* effector, acts as a glucosyltransferase that modifies TFEB at multiple sites, including Ser138, Ser196, Thr201, Ser203, and Thr208, showing that glucosylation is another crucial regulator of TFEB [193].

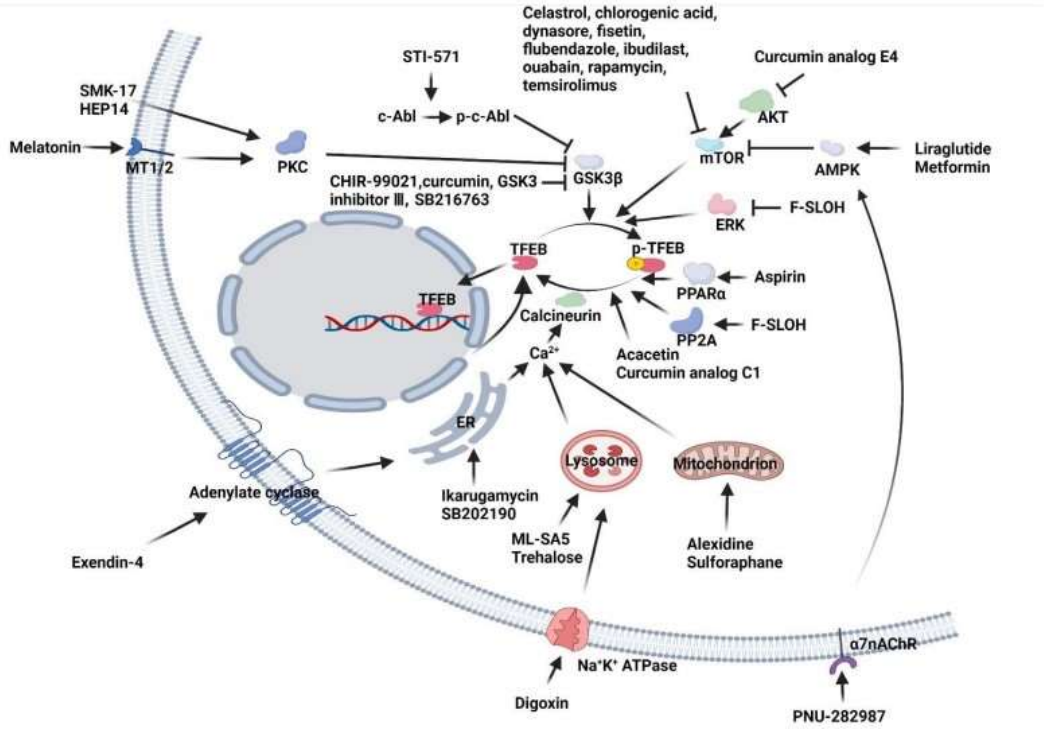

Fig. 3 TFEB nuclear translocation promoted by small molecules. TFEB can be regulated by small molecules which can be enhanced by drugs. GSK3β, which also phosphorylate tau proteins, is inhibiting the translocation into the nucleus. This is also done by mTOR and ERK, which is shown to phosphorylate TFEB at different sites. Different molecules, on the other hand, promote translocation of TFEB into the nucleus where it can bind to the CLEAR motif, for instance Calcineurin, PP2A and PPARα. Image taken from (Yang, J., *et.al.*, 2023)

There are other post-translational modifications that can regulate subcellular localization of TFEB, like acetylation. A study conducted by Jianbin Zhang (2017) showed that increased acetylation was shown in TFEB induced cells when treated with the histone deacetylase enzyme SAHA independent of mTORC1 [194]. Like SAHA, SIRT1 also seems to deacetylate TFEB to activate downstream lysosome and autophagy-related genes [195]. GCN5 is reported to be a negative regulator of autophagy, where one study reported that GCN5 inhibited the p62 transcription and inhibited the transcriptional activity of TFEB but not the intracellular distribution of TFEB [177]. These results suggest that post-translational modifications especially phosphorylation, acetylation and glucosylation are crucial for the regulation of TFEB nuclear accumulation or activities and the subsequent modulation of lysosomal biogenesis and autophagy.

1.6.3 TFEB in AD

As previously mentioned, the key characteristics of AD are Aβ plaques and neurofibrillary tangles formed by aggregated tau protein, which could lead to loss of synapses and neuron death. GSK3β is a key kinase for promoting tau phosphorylation, and thus it is critical for AD pathogenesis [44, 45]. What is important to note is that TFEB has been reported to be phosphorylated by GSK3β as mentioned previously [190]. This will lead to increased levels of TFEB in the cytosol. Inactivation of GSK3β promotes the translocation of TFEB into the nucleus, which could increase the level of lysosomal biogenesis, leading to decreased levels of hyperphosphorylated tau and alleviation of AD symptoms [20, 44]. Activated mTOR phosphorylates TFEB, and by

inactivation of mTOR will reduce the levels of phosphorylated TFEB and increase translocation of TFEB into the nucleus, activating ALP and reducing AD-like pathology [196]. Direct overexpression and knock down of TFEB has also been shown to have an effect on tau pathology in P301S mice [179].

As mentioned in section **1.2**, *APOE4* is the biggest risk factor of AD increasing the likelihood of AD 12-fold in individuals with homozygous *APOE4*. A report from Paul A. Parcon (2018) found that both the *APOE3* and *APOE4* gene did competitively bind to the CLEAR motif in *APOE* overexpressed cells, suggesting that autophagy is reduced by *APOE* genes by inhibiting expression of lysosomal genes [191]. This indicated the increased risk of *APOE4* genes not only in increased tau pathology, but also in reduced autophagic activity and lysosomal biogenesis.

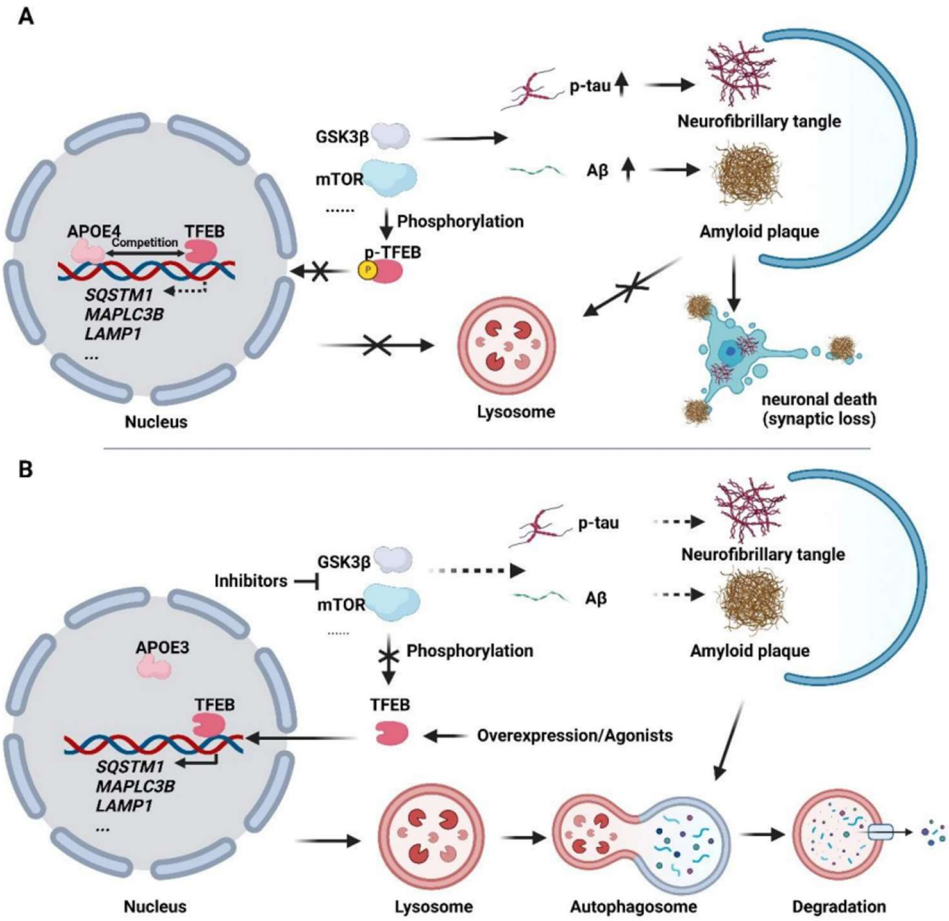

Fig. 4 TFEB mediation in Alzheimer's disease. The inactivation of TFEB decreases the levels of lysosomal biogenesis in cells. By inhibiting enzymes that is known to phosphorylate TFEB, it can increase the amount of lysosomes, ALP and autophagy. Increasing these factors has been shown to also alleviate AD-like pathology and decrease the amount of synapse loss and neuronal death. Image taken from (Yang, J., *et.al.*, 2023)

1.7 The model organism *Caenorhabditis elegans*

Caenorhabditis elegans is a nematode ringworm that is found in soil and compost heaps [197]. The animal mainly consists of self-fertilizing hermaphrodites (XX), but male *C. elegans* can occur (X0) [198]. *C. elegans* has been used as a useful model in studying a wide range of biological phenomena, and there are large amounts

of genotypic and phenotypic data available being constantly updated because of this, like WormBase [199]. The worms feeds on bacterial food, and as a standard, *Escherichia coli* OP50 is used for *in vivo* studies of these animals [200]. Phenotypes, like mobility, memory deficits, behavior, etc., can easily and noninvasively be examined and compared [201].

1.7.1 Biology of *C. elegans*

C. elegans is transparent, meaning that movements and health of organs can easily be viewed by microscopy. Fluorescent proteins can be used to study subcellular compartments and tag proteins, furthermore, they can also be used for mutant screening of cell development and function, cell development, cell isolation, and characterize *in vivo* protein interactions [198].

In a review written by Corsi, A. K., *et.al.*, (2015), there is a great explanation on the life cycle and maintenance of the *C. elegans* worms:

"As previously mentioned, *C. elegans* mainly consists for self-fertilizing hermaphrodites and has a rapid growth cycle of about 3 days in 20°C from larva to adult. These features have helped to make *C. elegans* a powerful model of choice for eukaryotic genetic studies. In addition, because the animal has an invariant number of somatic cells, researchers have been able to track the fate of every cell between fertilization and adulthood in live animals and to generate a complete cell lineage. Researchers have also reconstructed the shape of all *C. elegans* cells from electron micrographs, including each of the 302 neurons of the adult hermaphrodite and the posterior mating circuit in the adult male. Moreover, because of the invariant wild-type cell lineage and neuroanatomy of *C. elegans*, mutations that give rise to developmental and behavioral defects are readily identified in genetic screens. Finally, because *C. elegans* was the first multicellular organism with a complete genome sequence (*C. elegans* Sequencing Consortium 1998), forward and reverse genetics have led to the molecular identification of many key genes in developmental and cell biological processes.

C. elegans, although often mischaracterized as a soil nematode, can most easily be isolated from rotting vegetable matter, which contains an ample supply of their bacterial food source. In the laboratory, animals are normally grown on agar plates containing *E. coli* OP50. Once the animals deplete the bacteria, they utilize their fat supply. Without food, the development of young larval-stage animals is arrested. As a result of entering this stasis, animals can survive for at least a month (often starved plates can be usefully kept for up to 6 months at 15°C), and as stocks, they do not require constant feeding. Whenever healthy, growing animals are needed, a piece of the agar from the old plate can be transferred to a new plate with bacteria. The animals move to the new bacteria and resume their development.

Several other features greatly facilitate the maintenance of *C. elegans* stocks and their experimental use. First, because *C. elegans* is a self-fertilizing hermaphrodite, a single animal can populate a plate. Second, animal populations can be frozen for years and revived when needed. Third, the animal's small size means that many can be grown in a small space. Fourth, animals can be grown at temperatures ranging from 12°C to 25°C; their Q_{10} for growth is ~2 (that is, an increase of 10°C speeds up growth twofold). Growth at different temperatures makes it possible to control the rate of animal development and assists in the isolation and use of temperature-sensitive mutants. Continual growth above 25°C is not possible because the animals become sterile. The upper temperature limit can be a problem if animals are kept on bench tops (instead of

temperatures are possible for heat shock experiments and to increase production of males. Fifth, animals can be synchronized by isolating newly hatched larvae or by treating gravid adults with bleach (which decontaminates by killing everything but embryos) and isolating eggs, which are resistant to bleach treatment. Sixth, to facilitate biochemical studies, animals can be grown in bulk in liquid medium. "Worm storers" such as the COPAS Biosorter are also available to quickly select large quantities of individual worms with desired characteristics. Finally, one does not need especially expensive equipment beyond a good dissecting microscope and a compound microscope to work with this animal. Overall, the animals are inexpensive and convenient to maintain.

C. elegans embryogenesis takes ~16hr at 20°C (all of the subsequent times are also for development at 20°C) A virtually impermeable eggshell is made after fertilization, allowing the embryo to develop completely independent of the mother. However, embryos are usually retained within the hermaphrodite until about the 24-cell stage at which time they are laid. The hermaphrodite embryo hatches with 558 nuclei (some nuclei are in multinuclear syncytia, so the cell count is lower) and becomes a first stage (L1) larva. The animals begin to eat and develop through four larval stages (L1-L4). The L1 stage is ~16hr long; the other stages are ~12hr long. Each stage ends with a sleep-like period of inactivity called lethargus in which a new cuticle (outer collagenous layer) is made. Lethargus ends with the molting of the old cuticle. Approximately 12 hr after the L4 molt, adult hermaphrodites begin producing progeny for a period of 2-3 days until they have utilized all of their self-produced sperm; additional progeny can be generated if the sperm-depleted hermaphrodite mates with a male. After the reproductive period, hermaphrodites can live several more weeks before dying of senescence.

When bacteria are depleted and the animals are crowded, L2 larvae activate an alternative life cycle and molt into an alternative L3 larval stage called the "dauer" larva. The dauer larva cuticle completely surrounds the animal and plugs the mouth preventing the animal from eating and thereby arresting development. The dauer cuticle has enhanced resistance to chemicals, so it provides the dauer with greater protection against environmental stresses and caustic agents. Dauer larvae can survive for many months and are the dispersal from most commonly encountered in the wild. When the dauer larvae are transferred onto plates with bacteria, they shed their mouth plugs, molt, and continue their development as slightly different L4 larvae." (Corsi, A. K., *et.al.*, 2015, p. 387-407)

Table 1. Description of the worms used in the lifespan. The table gives a description of the different worms that are used in this master thesis project. The strain is the worm variant, and the column Description is a quick description and worm nomenclature.

Strain	Description
N2	N2 is known as the standard wild-type strain of *C. elegans* used for genetic and developmental studies.
CK12	CK12 is a variant of *C. elegans* with a mutated human tau (FTDP-17/P301L) pan-neuronal mutation in its genome (*Is[aex-3::tau4R1N(P301L)+myo-2p::gfp]*).
EFF033	CK12 derived worms with ubiquitous *hlh-30/TFEB* KO mutation (*hlh30(tm1978);hTau[P301L]*).

EFF030	CK12 derived worms with pan-neruonal *hlh-30/TFEB* OV mutation (*hlh30(+* neuronal); *hTau[P301L]*).

2.0 Objective

The objective of this project is to analyze how TFEB works the lifespan and healthspan of *C. elegans*. To investigate that, mutant TFEB ortholog *hlh-30* KO worms have any negative effect compared to overexpressed *hlh30* worms when both variants are affected by the Proline 301 Leucine (P301L) human tau mutation. The control groups will be the wild type (WT) strain N2, and the P301L mutated worms without any alteration of the *hlh30* gene (CK12).

The second goal of this project is to view if NMN has any effect on the lifespan and healthspan. This was done by creating two conditional groups, one vehicle group (no additional lifespan/healthspan mediated drugs) and one group with added NMN to plates.

3.0 Materials & Methods

In this section, we will look at all the materials and methods that were used in the Fang lab. The materials and methods are written in protocol and is written down in this section word for word by Nikolai Jensrud Skaar. For this project, different forms of drugs and materials were used. For details of the used drugs and materials, see **Table 2** below:

Table 2. Description of the different chemicals. A description of the different chemicals used for this experiment.

Drug	Description
FUdR	5-fluoro-2'-deoxyuridine (FUdR) is a drug that is added to lifespan assay plates to prevent larva to form by induce parental sterility to the nematode culture. FUdR is reported to inhibit reproduction without interfering with the organism's post-maturational development and ageing. Notably, FUdR has been reported to lengthen the lifespan, most prominently on different mutations of worms like *tub-1* and *gas-1* [202, 203].
Isoamyl Alcohol	"Isoamyl alcohol (IA), or 3-methyl-butan-1-ol, is a fragrant, colorless liquid used in cosmetics, fine fragrances, shampoos, toilet soaps, and other toiletries as well as in non-cosmetic products such as household cleaners and detergents. At high dosage, the odor of the alcohol becomes pleasant fruity-winey, but a study on mice showed that at high dosage caused spontaneous activity, eyelid

	closure, and ruffled fur. No mortality was observed at the highest dose. [204].“ (McGinty, D., *et. al.*, 2010, vol. 48, p. S102-9). Isoamyl alcohol is used in this project as a chemotaxis molecule for *C. elegans* to associate this smell with “no food”, where they will move away from this chemical in pursuit of other food sources if they remember the scent.

3.1 Preparation of NGM plates

3.1.1 Preparation of OP50

The *E. coli* biofilm OP50 is prepared days in advance. Colonies of *E. coli* is extracted and added to a new LB-plate for further use. This plate is then placed in an incubator with temperature roughly 37°C for 24 hours for bacterial growth. After 24 hours, the LB-plate is then wrapped in parafilm and put in a fridge which holds around 4°C. This is to prevent further growth and prolong the expiration of the plate.

When preparing the OP50, the *E. coli* plate is taken out of the fridge and placed into a fume hood to keep the plate sterile. 30µL of liquid LB-medium is then added to a 50 ml Falcon tube, and a single colony of *E. coli* is extracted with a loop and added to the medium. The 50 ml tubes with *E. coli*-LB medium are then moved to a shaker incubator where it will stir in about 37°C with at 180 rpm for 18 hours for growth in the liquid medium. The *E. coli*-LB medium should be foggy if the growth was successful. After the newly made OP50 is done, it is then placed into the fridge for further use.

3.1.2 Preparation of plates

The NGM medium used was obtained and made in the kitchen at Ahus by the staff there. The NGM medium is received from the kitchen as a solid gel, and therefore needs to be melted before use. The NGM medium is melted in a microwave at around 900W until it starts boiling. When all the NGM medium has melted and placed in a water bath at around 58°C until it has cooled to roughly the same degree. When the NGM medium has cooled, the bottle is moved to a fume hood and added 500µL Cholesterol (dissolved in alcohol), 500µL MgO4, 500µL SO4, and 12.5 mL K-buffer was added to the medium. After mixing the solvents to the medium, 8-10 mL is distributed to medium plates (), and 25 mL is distributed to large plates (). The prepared plates are then set to room temperature to solidify in about 24 hours.

3.1.3 Seeding the NGM plates with OP50

Once the plates have been cooled, the plates are moved back to the fume hood to be “seeded” with OP50. One of the prepared bottles of OP50 is taken out of the fridge, and since the *E. coli* colony will be precipitated, gently shaken to spread all the *E. coli* in the liquid. The newly prepared NGM plates will then be moved to the fume hood and added 200µl of OP50 to the medium plates and 1 ml to the large plates. The plates are then placed into room temperature to dry and for the *E. coli* to grow onto the plates in about 24 hours before use.

3.2 Preparation and addition of drugs

3.2.1 NMN

To make a solution of NMN, the concentration is calculated by using the standard concentration formula, where the known factors are concentration, volume, and the molecular weight. The formula should therefore be rewritten in favor of mass calculations:

$$m_{NMN} = c_{NMN\ stock} * V_{solution} * Mm_{NMN}$$

The β-nicotinamid mononucleotide powder is stored in a freezer which holds -20°C. The powder is then taken out and weighed as calculated by the formula. The weighted mass was then placed in a 50mL tube and taken to a fume hood. The solution is then added autoclaved water as calculated by the formula and mixed carefully until the powder has completely dissolved. The solution is then sucked up by a syringe and then added a 0.45µm filter to distribute the liquid into different Eppendorf tubes until it is roughly 500µL in each bottle.

The NMN solution is then diluted by using the formula. It is then, as with FuDR, dispersed onto the plates, but only on the number of plates that is used for drug analysis. The plates are then left to dry for about 24 hours. The plates that are not in use are stored in the cold room.

3.2.2 FuDR

FuDR is stored at solid state, the same as NMN and therefore can be prepared the same way as with NMN. Calculate the mass to create the stock concentration and distribute it to multiple Eppendorf tubes, which is then stored in the freezer.

After FuDR is prepared, the concentration is then diluted to 0.75mM. This is done by using the dilution formula, where the first concentration (c_1) is the concentration of the premade solution, and the second concentration (c_2) is the concentration of the desired solution of FuDR. The known volume of this formula is the end formula, where it will end up being 200µL, so by changing the formula, we get the volume required to make a solution with the desired concentration as seen below.

$$V = \frac{c_{End} V_{End}}{c_{FuDR}}$$

The solution is diluted with autoclaved water. After diluting the solution, 200µL is then dispersed onto one of the prepared plates in droplets to spread the drug evenly onto the plate, as shown in figure 3-?. This step is repeated on every plate that is used for the experiment. After the drug has been dispersed, the plates are left to dry for about 24 hours before use. If the plates were not used, they are placed in a cooling room which holds about 4°C for preservation.

3.3 *C. elegans*

3.3.1 Maintenance of *C. elegans*

For general maintenance, the worms that are going to be used for maintenance are taken out of the incubator and placed under the microscope, along with a large/medium plate which is seeded with OP50 and with no additional drugs added allowing for reproduction. With a worm picker made from platinum and a glass pipet, OP50 is taken onto the tip of the tool. Then, the worms from the old plate are picked up by attaching them to the OP50 on the picker and placed onto the new plate. For general maintenance, 2 worms are taken and left there until maintenance is required. For egg laying, 15-20 worms are placed onto the new plate and left for 3-4 hours before being removed. The age of the worms picked for general maintenance should be around D1, but earlier ages could be used for prolonged maintenance time.

3.3.2 Synchronizing *C. elegans*

To synchronize the *C. elegans* strands, the worms form the plate with mixed population (population with different age) is bleached. This bleaching solution is prepared beforehand, where the solution is mixed with 5M sodium hydroxide and a bleaching solution (Klorin, which contains sodium hypochlorite and sodium hydroxide [205]). This solution is prepared in a 50 ml bottle and stored inn room temperature.

The plate with mixed population is then added miliQ H_2O to wash out the worms, and then the water containing the worms is extracted from the plate and added to an Eppendorf tube. The adult worms will fall to the bottom of the tube due to gravity, and the water laying on the top is then available to be extracted and discarded. After the water has been discarded, 1 ml of bleaching solution is then added into the tube and vortexed for about 30-60 seconds. The worms are then shaken until 80% of the worms are dissolved and the only things remaining are the eggs. The eggs are then centrifuged at 12000 rpm for one minute and left at the bottom as a pellet. The bleaching solution is then extracted and discarded from the Eppendorf tube and 1 ml milliQ water is then added to the tube to wash the eggs. The eggs are then centrifuged and washed 3 more times (or until the smell of bleach has disappeared). After the final wash, the water is then taken out of the tube and milliQ H_2O is then added to the tube and the eggs are dispersed onto a new seeded large plate. The amount added to the eggs and dispersed is dependent on how many eggs you have retrieved from the bleaching process, where the standard is 200 µl milliQ H_2O is added to the Eppendorf tube and 100 µl of the egg solution is dispersed onto the plate. The plate is then left to dry for about 30 minutes, wrapped with parafilm and stored in an incubator which holds 20°C.

3.3.3 Experimental usage of *C. elegans*

When using the worms for experimental uses, the worms are taken out of the incubator after desired days, which is dependent on the age you want the worms to be. The plates with added FuDR with and without drug are then taken out of the cool room and placed at the side of the microscope next to the worms being used for the experiment. The plate with the drug is then placed under the microscope and a picker is used for picking the OP50 from the new plate without worms to create a sticky surface to attach the worms. Two and two worms are then picked up from the plate containing worms and placed onto the new plate until you

have the required number of worms on the new plate. Both plates are then wrapped with parafilm and placed into the incubator which holds around 20°C.

3.4 Lifespan and Healthspan assays

3.4.1 Lifespan

After preparing *C. elegans* for experimental usage, the plates are then labeled after the number of technical repeats one strain has. For each day, the worms are then counted, and the dead worms are taken out and discarded by flame. The number of dead worms for that day is then registered and the data is plotted into a spreadsheet with the events that has occurred and if some worms have died by any other means than old age, where these data are registered as censored data. The events that may occur are that the worm is climbing on the walls of the plates and dries up, accidentally picking up a worm that is still alive, and the worm finds a crevice and starts digging below the top layer of the agar. If the worm digs through the agar, a new plate needs to be prepared and the worms needs to be transferred as soon as possible to reduce the number of worms digging into the agar.

New plates need to be prepared for transfer of the worms to a new plate. After five days, the worms need to be transferred to a new plate to make sure they have enough food throughout the lifespan. This is done the same way as initiation of the lifespan: Two and two worms are transferred from the old plate to a new plate. The old plate which now does not contain any worms are then discarded, and any missing worms is registered as censored data.

3.4.2 Pumping assay

The pumping assay is done simultaneously as the lifespan since the pumping assay does not require the worms to be picked up or die for this assay. For preparation for the pumping rate, the microscope needs to be changed into a microscope lens with a greater zoom to get a better visual of the worm's pharynx. The plate with worms used for the pumping assay is then put under the microscope and the movement of the pharynx is then counted for 30 seconds. The counting is repeated for the number of worms required for the pumping assay. The counting is done on separate days for different ages, to analyze the rate at these ages and compare them in-between each other.

3.4.3 Thrashing assay

The thrashing assay is initiated outside of the lifespan, by preparing a NGM plate with FuDR. The worms are then placed on the new plate as done in lifespan, with the number of worms required for that day of thrashing. The worms are then stored in an incubator at 20°C until the required day. On those thrashing days, the plates are brought from the incubator and to the microscope. A glass slide is then placed under the microscope. A single droplet of milliQ water is then placed on the glass slide under the microscope and one single worm is picked up from the plate and gently placed on top of the water droplet. As with pumping, a counter and a timer are required to count for each thrashing of the tail the worm accomplishes. After counting each thrashing at the given amount of time, the worms are then discarded and the plates with the remaining worms are then wrapped and placed back into the incubator until the next day for thrashing. When the plates do not contain any more worms left, discard the plates as well.

3.4.4 Memory assay

The short memory assay is prepared days in advance. These days are listed as L4, D1, D2, and so forth for each step. D0 is the start where the mixed population of worms will be synchronized by bleaching. The worms are then added into medium plates with or without drugs. Preparation of the plates can be done either on D1 or D2. The plates that need to be prepared should not be seeded with OP50, as these plates are going to be used for the conditioning stage later in the assay, and as the memory assay plate in of itself. The conditioning plates are medium sized plates, and the memory assay plates are large sized plates. For each strain, which will be referenced as groups in the memory assay, 2 plates of both conditioning plates and memory assay plates needs to be made. One plate for the naïve group without isoamyl alcohol and one plate with isoamyl alcohol which is referred to as IA [206].

On D3, the process for the memory assay will begin. The worms are collected from the incubator and the plates will be prepared for the assay. In the conditioning plates, 10 µl of pure isoamyl alcohol is placed on top of the IA plates lid and spread around evenly. The worms will then be gathered up by washing the plates with milliQ water and added to an Eppendorf tube. The worms in the tube will, as mentioned in **3.3.2 Synchronizing *C. elegans***, fall to the bottom of the tube since all the worms will be adults. The top layer of water will then be removed, and fresh water will be added to the Eppendorf tube to remove the OP50 gathered in the washing process. This process is repeated 3 times, and the worms are then placed into the newly prepared conditioning plate, the naïve group on to the naïve plate without isoamyl alcohol and the IA group on the plates with isoamyl alcohol, and the plates are then conditioned for 90 minutes in 20°C – 22°C.

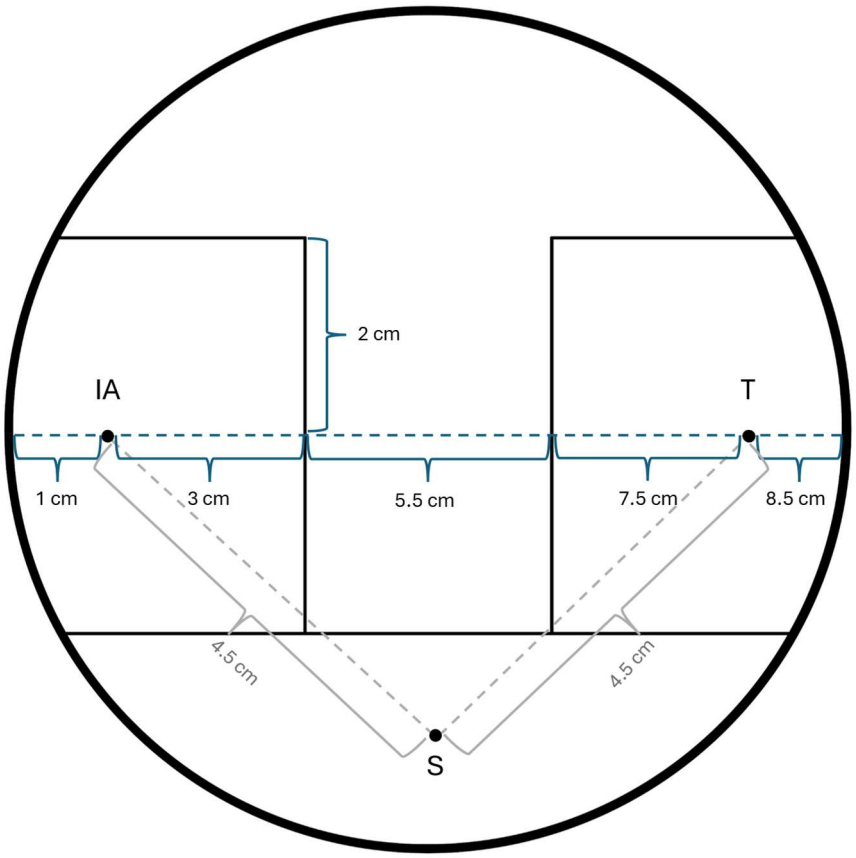

Fig. 5 a schematic overview of a memory assay plate. The memory assay plate is lined up precisely so that the worms have an equal distance between the starting point (S) and the t/IA point. The first line up starts from the left side of the large plate, where a ruler is used to measure the distance between the plate and line it up so it measures 8.5 cm. Points are then made after 1 cm, 3 cm, 5.5 cm and 7.5 cm. From the 3 cm and 5.5 cm point, draw a vertical line 2 cm up and 2 cm down. From the top point of the new vertical line, draw a horizontal line going from the top point and all the way to the other edge of the plate as shown in the figure. At the bottom point of the vertical line, draw a horizontal line from the other point and across both edges of the plate as shown in the figure. Above the 1 cm point, write down "IA" over the point, and above the 7.5 cm point, write down "T" over the point. The S point should be 4.5 cm from both the IA and the T point. Above the newly created schematics, write down the strain and the condition of the strain. Under the strain and condition, write down the treatment (either Naïve, or IA) for that particular conditioned worm.

While conditioning, the memory assay plates are drawn on to distinguish between the worms who remember the smell of isoamyl alcohol and the ones who don't. The length and distances of the markings are shown in **Fig. MM 1**. 15 minutes before the worms are put into the memory assay plate, 15 µl of 20mM NaN_3 is added on both the T and the IA spot of the assay plate, which works as a form of tranquilizer to keep the worms on the designated spots. When the NaN_3 has dried up, a small piece of parafilm is cut and placed gently on top of the IA mark on the plate. After the worms have been conditioned, the IA plate is then washed from the conditioning plates and placed into an Eppendorf tube. The worms are then placed onto the S point of the plate, where the excess water is then dried up by using a Kimtech® delicate task wipe and a 4 µl drop of diluted IA (1:50) is placed on top of the parafilm on the IA spot. The plates are then wrapped in parafilm carefully, so the drop of IA does not spill, and the worms are left in the memory assay plates for about 2 hours. After the 2 hours needed for memory assay, the number of worms that have traversed to the IA box

and the T box are then counted and the plates are discarded. The optimal amount of worms to count in total of a memory assay is between 100-200 worms. Anything below 50 is considered as a bad result.

3.5 Statistical analysis

The statistical analysis for the data was analyzed through both manual calculations and Graphpad Prism 8. Calculation for the lifespan was done by adding all the data into an excel sheet. The raw data is then calculated by analyzing how many worms have survived throughout the days:

$$N_{Survive} = \left(\sum Death\right) - Death$$

The number of survivors was then calculated by dividing on the total amount of worms used in the experiment, in other words the sum of death. By doing this form of calculation, the outcome will be the "survival rate" between the different days of events and the total amount of worms:

$$Survival\ rate\ (\%) = \frac{N_{survive}}{\sum Death} * 100\%$$

The survival rate was then analyzed individually and compared between each other by calculating the difference of percentage through the median. The data from lifespan was put into prism, and a survival assay was conducted, which gave the median of the lifespan. The difference of percentage was calculated by using this formula where group is the new group being compared with the control group:

$$\%_{diff} = -\left(100\% - \frac{Median_{group} * 100}{Median_{conrtol}}\right)$$

The *p*-value of the lifespan was gathered through a log-rank (Mantel-Cox) test in Prism. The test was conducted between each group and the control, which in turn will show the significance of the data.

For the thrashing (swimming) and the pumping assay, an unpaired t-test was conducted to compare between the conditional groups. For the comparison between different strains, one cannot assume that they will have the same standard deviation (SD), so a Welch's t test was conducted between strains.

For memory, the data collected was divided into three groups: T, IA, and S. The data from each column was used to calculate the chemotaxis index, which represents how many of the total of each group moved to each spot, this was done by calculating manually:

$$Chemotaxis\ index\ (\%) = \left(\frac{IA - T}{IA + T + S}\right) * 100\%$$

The analysis between each group was done by a two-way ANOVA analysis is conducted to compare the groups and a Tukey's multiple comparisons test is conducted to compare between each of these groups by using the chemotaxis index [206].

4.0 Results

4.1 lifespan assay

The lifespan assay was conducted using *C. elegans* strains N2 (wildtype/control), CK12 (tau pathology), EFF033, *hlh30* Knock-out (KO) strain with CK12 background, and EFF030, *hlh30* Overexpression (OV) strain with CK12 background. Each strain had 3 plates containing 30 worms each, where there was one vehicle group and one NMN group. The NMN groups were added 2mM of NMN on each plate, in addition to 2mM of FuDR added for all plates (both Veh. And NMN groups). The worms were transferred to new plates around day 5, except for the third biological repeat which was transferred on day 6. During the third biological repeat, the N2 plate number 1 showed signs of contamination and had to be redone with the same conditions as the rest of the repeat. The data was then pooled together and displayed onto a graph using excel. The results are as shown below.

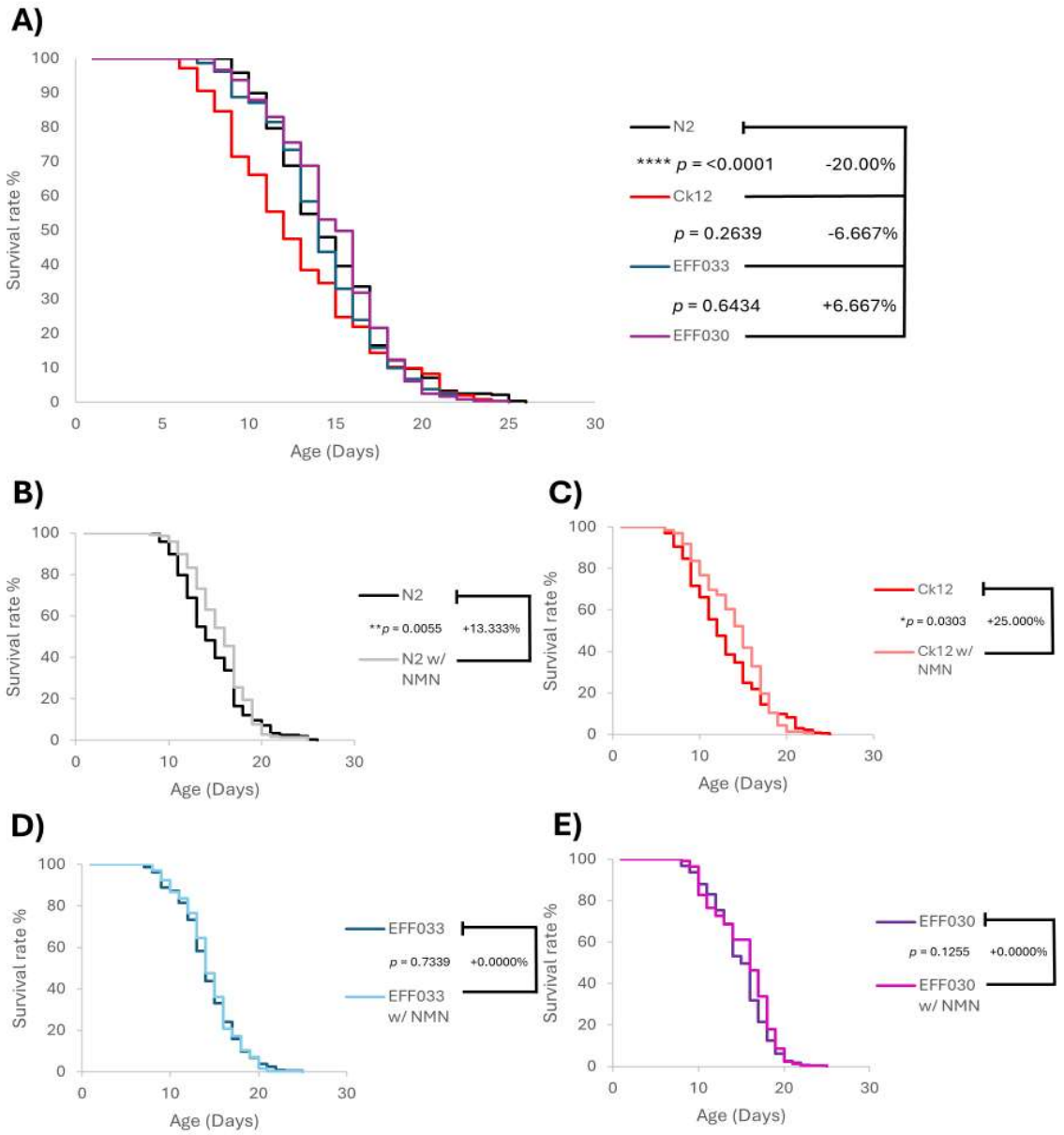

Fig. 6 NAD⁺ precursor NMN improves lifespan in *C. elegans*. (A) Survival graph of all strains without treatment. N2 strain serves as the control. **(B)** Survival graph of WT worms (N2) with and without NMN treatment. **(C)** Survival graph of CK12 worms with and without NMN treatment. **(D)** Survival graph of *hlh30* knockout worms with and without NMN treatment. **(E)** Survival graph of *hlh30* overexpressed worms with and without NMN treatment. **(B-E)** The Veh. group serves as a control for each individual strains. **(A-E)** Log-rank test was used for the statistics between each group and N2 as the control with a confidence interval of 95%. The difference of lifespan was calculated by the median between each group and the respective control. Color coding: N2 (Black), N2 w/ NMN (Grey), Ck12 (Red), Ck12 w/ NMN (Light red), EFF033 (Blue), EFF033 w/ NMN (Light blue), EFF030 (Purple), EFF030 w/ NMN (Pink). * p = <0.05, **p = <0.005, *** p = <0.0005, **** p = <0.0001.

As shown in **Fig. R1**, the N2 Veh. and CK12 Veh. lifespan had a different percentage compared to the median, where the difference is at around -20.00% with CK12 as the group compared to N2 as control. This shows

that tau pathology does influence lifespan, and section **C)** of the same figure shows that the addition of NMN had such an impact on the worms that the lifespan median had jumped up 25% compared to CK12 Veh., which gives a lifespan comparable to N2 Veh. The vehicle groups of EFF033 and EFF030 do not show to deviate that far from the N2 control group, meaning that the tau pathology and lysosomal biogenesis does not show any correlation between each other. It does not seem like NMN does have any effect on these strains as well, but it is important to note that the EFF030 strain with NMN does show signs of improved lifespan at the middle section of the **E)** graph. This could indicate that NMN does have an effect on lifespan if TFEB is present in the cell.

4.2 Analysis of the healthspan assay

4.2.1 Pumping assay

The pumping assay, as mentioned in **section 3.4.2**, is done simultaneously as the lifespan assay. The worms were transferred on day 5 except for the last biological repeat which was done on day 6. The pumping rate was measured at 30s intervals, and 5 worms per plate (in total 15 worms per condition) was measured. Measurement was done on Day 2 of adulthood, Day 4, Day 8, and Day 10. The data gathered for all biological repeats was pooled together and added into prism for analysis. The data was put into a column graph with an error bar and each individual datapoints added for each strain and condition. The result is as shown below.

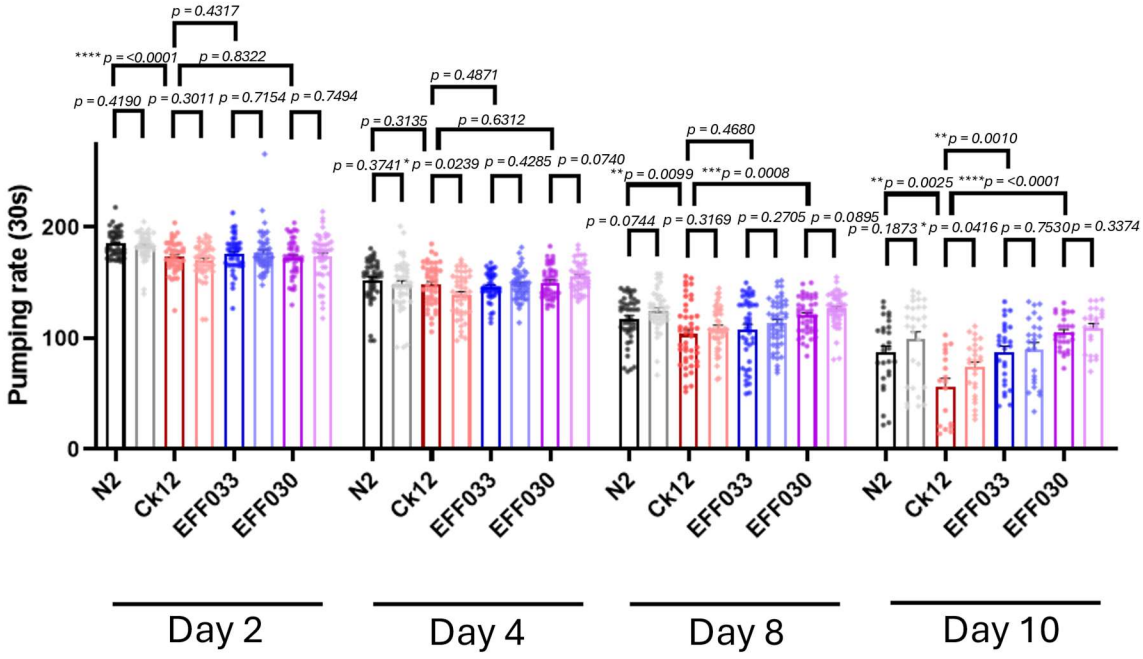

Fig. 7 Pumping rate altered from tau pathology and NAD⁺ precursor NMN. A column graph showing the contraction of the pharynx in *C. elegans*. The pumping rate was measured on day 2, 4, 8, and 10 of adulthood. The pumping rate was measured at 30 seconds, and 5 worms were measured for each plate pr. condition. There are in total 2 conditions pr. strain, and the strains measured was N2, CK12, EFF033 and EFF030. The two conditions are one vehicle group, and one group with added 2 mM NMN. Both conditions were added 2 mM of FuDR. This graph shows 3 biological repeats pooled together and analyzed in total. The *p*-value was calculated in Prism using an unpaired t-test between each condition in each individual strain with a confidence interval of 95%. An unpaired t-test was also conducted between N2-CK12, CK12-EFF030, and CK12-EFF033. Color coding: N2 (Black), N2 w/ NMN

(Grey), Ck12 (Red), Ck12 w/ NMN (Light red), EFF033 (Blue), EFF033 w/ NMN (Light blue), EFF030 (Purple), EFF030 w/ NMN (Pink). * p = <0.05, ** p = <0.005, *** p = <0.0005, **** p = <0.0001.

Throughout the days of analysis, there is a clear trend that the pumping rate overall is decreasing. As shown in the data pulled from appendix **Table 4**, it's clear to see the trend from the average between the days on Veh. control group N2, where on Day 2, Day 4, Day 8, and Day 10, the average was at 185, 152, 118, and 87 respectively. This indicates that there is a correlation between pumping rate and ageing, giving an indication on the condition of the internal health for the worms.

The pumping rate during day 2 did not show any particular significance between each group except between N2 and CK12 which had a high significance on **** p = <0.0001. This value shows that there are significant changes between Veh. N2 and CK12, and by looking at the graph, CK12 has a lower pumping rate than N2. This could be since the worms are sick and some worms might pump slower than the average N2 type. On day 4 there are no significant changes in any condition/strains, meaning on day 4 there are no effect on any treatment of the worms.

On day 8, the comparison between Veh. N2-CK12 shows a significant decrease in pumping rate, as was found on day 2, but less significant with a p-value of 0.0099. This does show that tau pathology does influence health in worms as they age. The other interesting thing is that the significance between CK12-EFF030 is also significant with a p-value of 0.0008, which indicates that having overexpression of TFEB does increase the pumping rate when it comes to tau pathology. This is further confirmed when the TFEB KO group (EFF033) is incredibly similar with no significance (p = 0.4680). It's also important to note that between EFF033 and EFF030 are a difference which is significant (* p = 0.0156), which shows that having OV of TFEB rather than KO does influence the pumping rate. All additional analysis of the pumping data is shown in appendix **Table 5**. The NMN groups show no significance on any strain, indicating at this age stage, NMN does not influence the worms.

The NMN groups on day 10 have a significance in the CK12 strain (* p = 0.0416), which indicates that NMN does influence the worms pumping rate when tau pathology is present. The pumping rate between WT and CK12 does show a higher significance (** p = 0.0025) compared to day 8 (** p = 0.0099), which indicates that tau does become more prevalent as the worms age. Comparing the TFEB groups with CK12 shows a significance between both these groups with **** p = <0.0001 and ** p = 0.0010 for EFF030 and EFF033 respectively. What is important to note is that the level of pumping between EFF030 and EFF033 is more prevalent on day 10 (** p = 0.0070) compared to day 8.

4.2.2 Thrashing assay

For each strain, 40 worms were placed onto a plate with added 2mM FuDR. For each strain, one plate was added 2mM NMN and nothing in another. 10 worms were picked up on day 4, 8, and 10 of adulthood and the thrashing rate was counted for 30 seconds. There were done 3 full biological repeats, a fourth to fill in some of the missing data, and another few plates to fill in the remaining after the fourth biological repeat. All the data was pooled together, and a column graph was made from the data. The results are as shown below.

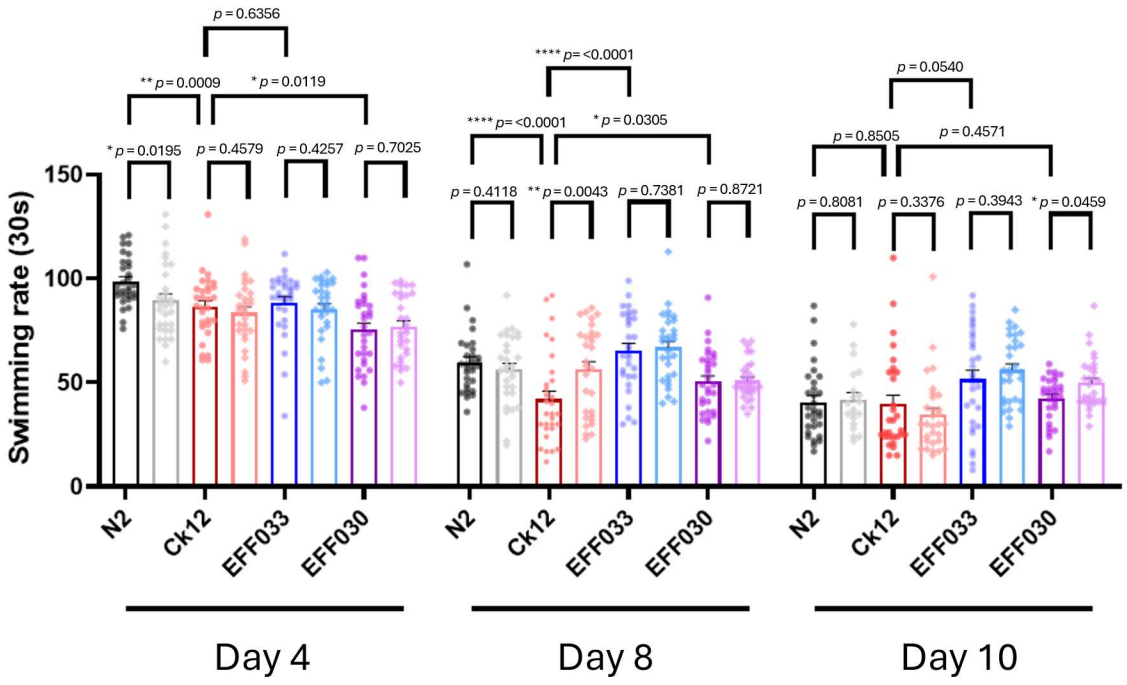

Fig. 8 swimming/thrashing rate altered by TFEB and NAD⁺ precursors in tau pathology. A column graph showing the swimming/thrashing rate of *C.* elegans. The thrashing rate was measured on day 4, 8, and 10 of adulthood. The thrashing rate was measured at 30 seconds, and 10 worms was measured for each condition on each strain. there are in total 2 conditions for each strain, where the strains measured are N2, CK12, EFF033, and EFF030. The two conditions are one vehicle group, and one group with added 2 mM NMN. Both conditions were added 2 mM of FuDR. This graph shows 3 biological repeats pooled together and analyzed in total. The p-value was calculated in Prism using an unpaired t-test between each condition in each individual strain with a confidence interval of 95%. An unpaired t-test was also conducted between N2-CK12, CK12-EFF030, and CK12-EFF033. Color coding: N2 (Black), N2 w/ NMN (Grey), Ck12 (Red), Ck12 w/ NMN (Light red), EFF033 (Blue), EFF033 w/ NMN (Light blue), EFF030 (Purple), EFF030 w/ NMN (Pink). * p = <0.05, **p = <0.005, *** p = <0.0005, **** p = <0.0001.

Day 4 data shows that the NMN groups, as with pumping, have no significance and does not affect the thrashing ability of the worms at this age. N2 Veh. thrashing rate is higher than the CK12 Veh. with ***p* = 0.0009, indicating that the thrashing rate of the worms with tau pathology is slower than the WT worms. Interestingly, the *hlh30* OV Veh. group has a lot slower thrashing rate than the CK12 Veh. group, but the *hlh30* KO Veh. group is similar to the CK12 group. This could indicate that TFEB overexpression does reduce the thrashing rate of the worms in some way.

CK12 also showed a positive response on the thrashing rate with NMN treatment, with a significance of ***p* = 0.0043 on day 8 of adulthood. This does corelate with the pumping assay that on day 8 NMN does seem to positively influence the worms. There was also a decrease in thrashing rate with CK12 compared to N2 (*****p* = <0.0001), meaning that thrashing rate is decreased by tau pathology. CK12 also shows a significance between the TFEB groups, where the *hlh30* KO and OV had a *p*-value of <0.0001 and 0.0305 respectively. This shows that the thrashing rate will slow down if lysosomal biogenesis is overexpressed. What is also interesting to note is that the *hlh30* KO strain swims faster than the *hlh30* OV worms, with a significance on ***p* = 0.0013, which further indicates that the overexpression of lysosomal biogenesis decreases the swimming rate of the worms.

On day 10 of adulthood, the EFF030 group with NMN treatment does show signs of improvement on the thrashing rate with a significance of *p = 0.0459. What is interesting to note is that the CK12 Veh. group, compared to the N2 Veh. group, is not significant with datapoints reaching higher than any other strains. The reason behind this could be that the worms picked from the CK12 strain at day 10 could be a lot healthier which would make the thrashing rate higher. This could explain why the highest data points for CK12 are at the biological repeat 4, as shown in **Table 6** in the appendix list. The EFF-groups visually show a difference between each other, but these values are not significant with a p-value of 0.0828.

4.2.3 Memory assay

The memory assay was done with 8 groups in total (4 strains + 2 conditions), leading up to a total of 16 conditional groups in total, one naïve and one IA for each group. The groups were conditioned for 90 minutes with 10 µl pure IA in room temperature (20-25°C). The worms were after 90 minutes transferred to a memory assay plate, sealed, and left in room temperature for roughly 2 hours. There were only done 2 biological repeats, and one of the repeats was not viable since the IA conditioned Veh. groups moved towards the IA point of the memory assay, which is a sign of fault in the experiment. The data and the graph from the data pooled from this particular biological repeat can be found in **Table 8** and **Fig. 12** in the appendix list. Only one biological repeat was done, and a column graph was made after putting the data into Prism. The results are as shown below.

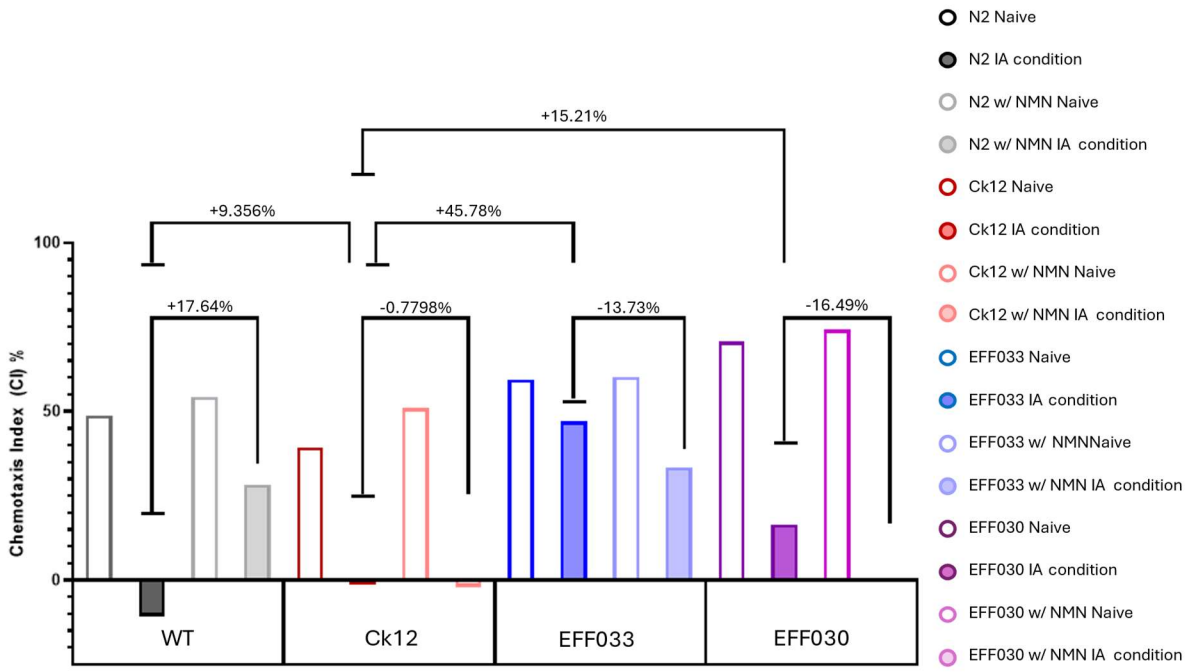

Fig. 9 *hlh30* overexpression shows signs of improved short-term memory. A column graph showing the short-term memory assay of *C. elegans*. The worms were either conditioned in an empty NGM plate (Naïve) or in a NGM plate with pure IA on top of the lid (IA) for 90 minutes. In total there are 8 groups: N2, CK12, EFF033, EFF030, where there were 2 conditions (Veh., 2mM NMN). After the 90 min conditioning, the worms were then transferred to their assigned memory assay plate where they would be left in room temperature (20-25°C) for 2 hours. This graph shows only one biological repeat. The percentage value is calculated as the difference between the different IA groups, as the IA group is the one that is being tested for memory.

The results of the short-term memory assay shows that the N2 and CK12 does have a difference between each other, with a +9.356% difference. This goes to show that the tau pathology is decreasing the level of memory in the worms, but it is not as prominent as with the EFF groups which has a much higher difference compared to CK12 (EFF033: +45.78%, EFF030: 15.21%). This could indicate a fault in this biological repeat (another strong scent that altered the association of "no food") with the EFF groups. One thing that is also important to note is that the amount of EFF033 worms moving to the IA spot compared to the EFF030 is much higher, meaning that the number of lysosomes does play a role in memory. The other thing to note is also that the NMN groups do seem to have an effect on memory as well, where the difference is always decreasing except between the N2 group where the difference is +17.64%. The increased number of worms that moved to IA in N2 could be again explained by a fault in the experiment. This fault is better represented in Fig. This should be accounted for, and more biological repeats should be conducted.

5.0 Discussion

In this study, we found that lysosomal biogenesis does not affect the worms significantly when tau pathology is present. However, we did se internal changes that show that lysosomes do play a role in the worms' healthspan and that lysosomal biogenesis does have an effect for the benefit of the worms. We also confirmed, as many other studies have shown, that tau pathology does have a role to play in both lifespan and in healthspan in these worms.

5.1 Tau pathology in worms

As the results clearly show, tau pathology does affect both the lifespan and the healthspan in these worms. This confirms with the other studies done on worms and mice on tau pathology, that tau in of itself does affect development and health of these animals. One thing that is important to note is that the CK12 worms do not target any specific neuron, but rather that the P301L mutation is ubiquitous, which means that aggregated tau does affect the whole organism. Tau aggregation does affect cells in the way that it inhibits stabilization of microtubules and as a result intracellular transport, especially in the neurons. This leads to apoptosis of nerve cells, and eventually, death of the organism.

Since the CK12 strain is already affected with the P301L mutation early on, it is shown that the pathology is affecting early healthspan and progresses to decrease healthspan later onward in life. What is also important to note is that the lifespan does decrease early, with the median lifespan being decreased substantially, but the end lifespan ends similarly with the WT worms. This shows that there might be some worms that can live as long as WT, but the general population would not survive as long. The reason of why some of these worms live longer than others can have some explanation, like for instance some form of alleviation of phosphorylation of tau by increased lysosomal activity or a reduction, or inhibition, of phosphorylating enzymes like GSK3β.

Another thing to note is that the memory of the CK12 strain is also less than the N2, which indicates that the tau aggregation is affecting the neurons of the worms and their ability of chemotaxis. This does correlate with other studies done on the subject, like the 2008 study by Ann C. McKee, et.al which found that

Ibuprofen did diminish the accumulation of hyperphosphorylated tau in mice and increased memory on 3xTg-AD mice [207]. But, as mentioned in **results 4.2.3**, more biological repeats need to be done to strengthen the hypothesis that the memory of these worms has been affected.

5.2 Lysosomal biogenesis

The *hlh-30* gene in worms is the orthologue of TFEB and translocates into the nucleus in response to nutrient deprivation, at least in part, via a TOR-dependent mechanism to ensure the transcriptional induction of many autophagy-related and lysosomal genes [208]. In a study conducted by Louis R. Lapierre (2013), they analyzed if *hlh-30* mutated worms derived from N2 do alter lifespan. What they found was that *hlh-30* OV in WT prolonged the lifespan significantly, but the *hlh-30* KO did shorten the lifespan significantly. What they also discovered is that the *hlh-30* inhibited worms prevented dauer formation in these worms, where autophagy is important. Another study done on Proline 301 Serine (P301S) htau mutated mice showed that TFEB does alleviate tau pathology. By overexpressing TFEB, they found that it decreased *MAPT*/tau by -31 ± 3% [136]. These findings can explain how the Veh. *hlh-30* OV with the CK12 background did increase lifespan compared to the CK12 Veh. group, where the Veh. *hlh-30* OV did increase lifespan.

These findings show that TFEB/hlh-30 should alleviate htau in these worms, however, this is not what our results suggests. The Veh. groups with altered *hlh-30* expression did follow the N2 line in Veh. lifespan, and shows that the healthspan of these groups are also kind of similar with different trends between each other. The healthspan between the *hlh-30* groups does show that there is a beneficial trend to have overexpression of lysosomal biogenesis, but there is no increase of lifespan median which suggests that there is no extended lifespan. A possible explanation for the EFF033 group being equal to the N2 Veh. line is that since there is downregulation of TFEB, it also downregulates autophagy expression. Studies have shown that downregulation of TFEB does also downregulate autophagy activity [174]. The ubiquitin-proteasome system (UPS) is responsible for the degradation of short-lived proteins and soluble misfolded proteins, which recognizes their targets through ubiquitin tags (the same as with autophagy). Studies have shown a crosstalk between these two interdependent systems where autophagy is downregulated, UPS is upregulated and therefore stabilizes proteostasis which is shown in **Fig. 10** below [209].

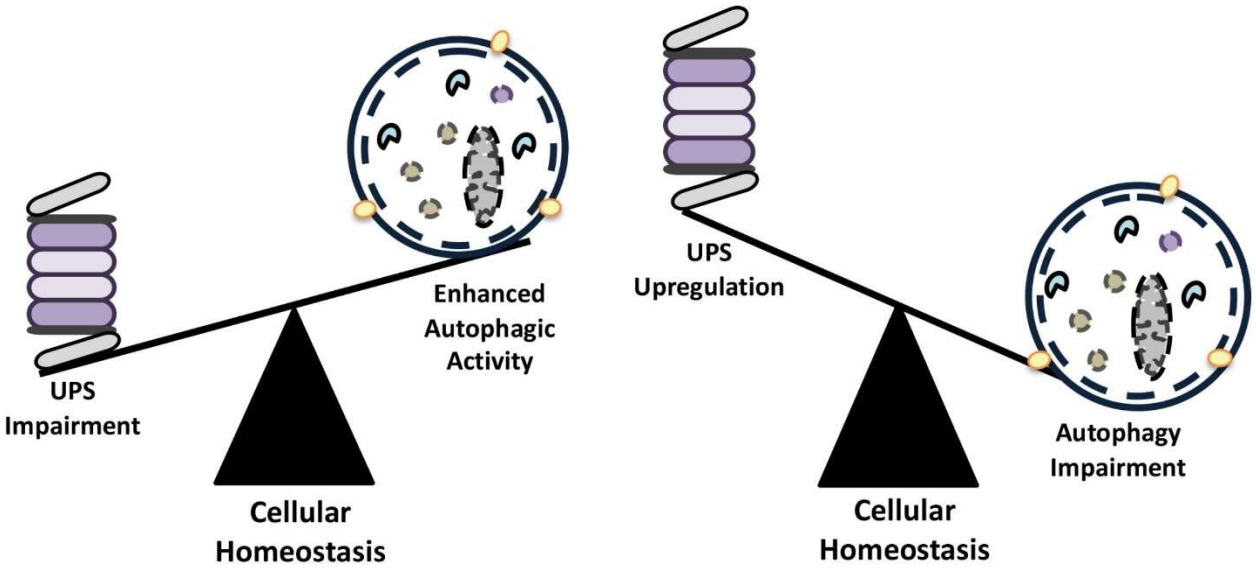

Fig. 10 Schematic illustration of the regulation between autophagy and the ubiquitine-proteosome system. This schematic figure shows the difference regulation between different proteostasis systems in cellular homeostasis. When the ubiquitin-proteosome system (UPS) is downregulates, autophagy is increases; when autophagy is downregulated, UPS regulation is upregulated.

This theory could explain how the Veh. EFF033 group doesn't have a short lifespan as with Veh. CK12, but lifespan is equal to N2. This also explains the healthspan since UPS does not increase mitophagy by targeting large organelles, but rather only targets small proteins and reduces the amount of tau that is present in the organism [209]. This could also explain how the healthspan is increased in the *hlh-30* OV groups, but not in the *hlh-30* KO worms. Another thing to point out is that the UPS system cannot usually degrade aggregated proteins [210], it has been shown that UPS does decrease tau levels in both HEK293 cells and P301S htau mice [211]. Further research is recommended to study the effects of UPS and htau in both *C. elegans* and mice and if TFEB does have a correlation between these systems.

By looking at the thrashing data, we can see that the EFF033 group has a higher thrashing rate than the EFF030 group. Interestingly, the pumping assay showed the opposite; EFF030 had a higher pumping rate than EFF033. This could indicate that the other mechanism that alleviated the tau pathology of these groups salvaged different forms of neurons. This has been shown in different worms with neurodegenerative diseases where one strain had a tau variant that affected the presynaptic synaptic transmission, and the other affected the postsynaptic transmission [212]. Tau proteins are reducing both pre- and postsynaptic neurons, and TFEB is shown to be rescuing both synaptic neurons in cells [136]. This could mean, with the data gathered from this project, that the UPS system is better at salvaging the motor neurons than TFEB, but TFEB can salvage the pharyngeal motor neurons.

5.3 NAD^+ and its effect on worm health

As clearly shown from the data collected, the worms do have a slight benefit from NMN as a drug treatment. This is really prominent in the CK12 and N2 groups, where the CK12 group does increase its lifespan significantly with supplementation of NAD^+, which indicates that the tau pathological worms do have a great

benefit from NAD^+ supplement. This is further confirmed by the healthspan assays where the NMN groups at later stages of life do show an increase in performance compared to the veh. groups, where this is also more prominent with the CK12 worms. These results can be confirmed by other studies done on the subject showing that NAD^+ does increase mitophagy and improved DNA repair, mitochondrial respiratory function, [166, 213]. The memory assay also shows that with NMN supplementation increases the ability to remember, which could be explained by decreased levels of neuronal apoptosis and heighten cognitive function compared to the non-conditioned group [213].

NAD^+ has been shown to also increase the SIRT1 enzyme, which is linked to deacetylation of TFEB and increased TFEB activity [214]. This will increase autophagic activity and increase both healthspan and lifespan as our results suggest. This can also explain how EFF030 has a slight increase in the middle of lifespan, that when the demand for TFEB, incused by stress or any other factor, increases TFEB activation and lysosomal biogenesis [190].

When looking at the *hlh-30* KO and OV data, we do not see any significant change in lifespan when added NMN as shown with CK12 or N2. This could indicate that NAD^+ is not necessary for TFEB, as NAD^+ does work in the same pathway as TFEB. This could also be the same issue as with UPS, since it is regulated by enzymes like SIRT7 which is NAD^+ dependent [215]. This could indicate that since there is more upregulation of these systems, there is no necessary need for NAD^+ supplementation.

5.4 Conclusion and future perspectives

The results from this project indicate that tau pathology does have a negative effect on both lifespan and healthspan compared to wild type *C. elegans*. Tau pathology is shown to affect neurons which is indicated by memory assay, and through neuronal loss affects both pharyngeal and motor activity. Transcription factor EB does seem to have an effect on the lifespan of the worms but could also be competitive with other mechanisms such as hormesis or UPS. NAD^+ supplementation through NMN does seem to have a significant impact on the CK12 worms, where increased levels of NAD^+ increase lifespan equal to the Veh. N2. What is interesting is that neither of the EFF groups doesn't seem to be affected by NAD^+ supplementation, which could be explained in which NAD^+ is not necessary when NAD^+ mechanisms are upregulated. One explanation for these effects is when autophagy is downregulated, the ubiquitin-protesome system is increased. Further research for studying the effects between autophagy induced compared to the proteostasis induced mechanisms in tau pathology is highly recommended to analyze if these systems are in fact linked together.

References

1. Verdin, E. (2015). NAD(+) in aging, metabolism, and neurodegeneration. *Science*, 350 (6265): 1208-13. doi: 10.1126/science.aac4854.
2. Li, W. & Sauve, A. A. (2015). NAD(+) content and its role in mitochondria. *Methods Mol Biol*, 1241: 39-48. doi: 10.1007/978-1-4939-1875-1_4.
3. Park, K., Lim, H., Kim, J., Hwang, Y., Lee, Y. S., Bae, S. H., Kim, H., Kim, H., Kang, S. W., Kim, J. Y., et al. (2022). Lysosomal Ca(2+)-mediated TFEB activation modulates mitophagy and functional

adaptation of pancreatic beta-cells to metabolic stress. *Nat Commun*, 13 (1): 1300. doi: 10.1038/s41467-022-28874-9.
4. Lopez-Otin, C., Blasco, M. A., Partridge, L., Serrano, M. & Kroemer, G. (2023). Hallmarks of aging: An expanding universe. *Cell*, 186 (2): 243-278. doi: 10.1016/j.cell.2022.11.001.
5. Masters, C. L., Bateman, R., Blennow, K., Rowe, C. C., Sperling, R. A. & Cummings, J. L. (2015). Alzheimer's disease. *Nat Rev Dis Primers*, 1: 15056. doi: 10.1038/nrdp.2015.56.
6. Arvanitakis, Z., Shah, R. C. & Bennett, D. A. (2019). Diagnosis and Management of Dementia: Review. *JAMA*, 322 (16): 1589-1599. doi: 10.1001/jama.2019.4782.
7. Organization, W. H. (2023). *Dementia*. Available at: www.who.int/news-room/fact-sheets/detail/dementia.
8. Mura, T., Dartigues, J. F. & Berr, C. (2010). How many dementia cases in France and Europe? Alternative projections and scenarios 2010-2050. *Eur J Neurol*, 17 (2): 252-9. doi: 10.1111/j.1468-1331.2009.02783.x.
9. Kobro-Flatmoen, A., Lagartos-Donate, M. J., Aman, Y., Edison, P., Witter, M. P. & Fang, E. F. (2021). Re-emphasizing early Alzheimer's disease pathology starting in select entorhinal neurons, with a special focus on mitophagy. *Ageing Res Rev*, 67: 101307. doi: 10.1016/j.arr.2021.101307.
10. Mendez, M. F. (2017). Early-Onset Alzheimer Disease. *Neurol Clin*, 35 (2): 263-281. doi: 10.1016/j.ncl.2017.01.005.
11. Uddin, M. S., Kabir, M. T., Al Mamun, A., Abdel-Daim, M. M., Barreto, G. E. & Ashraf, G. M. (2019). APOE and Alzheimer's Disease: Evidence Mounts that Targeting APOE4 may Combat Alzheimer's Pathogenesis. *Mol Neurobiol*, 56 (4): 2450-2465. doi: 10.1007/s12035-018-1237-z.
12. Jay, T. R., von Saucken, V. E. & Landreth, G. E. (2017). TREM2 in Neurodegenerative Diseases. *Mol Neurodegener*, 12 (1): 56. doi: 10.1186/s13024-017-0197-5.
13. Wang, J., Yu, J. T. & Tan, L. (2015). PLD3 in Alzheimer's disease. *Mol Neurobiol*, 51 (2): 480-6. doi: 10.1007/s12035-014-8779-5.
14. Yuan, X. Z., Sun, S., Tan, C. C., Yu, J. T. & Tan, L. (2017). The Role of ADAM10 in Alzheimer's Disease. *J Alzheimers Dis*, 58 (2): 303-322. doi: 10.3233/JAD-170061.
15. Arnold, S. E., Hyman, B. T., Flory, J., Damasio, A. R. & Van Hoesen, G. W. (1991). The topographical and neuroanatomical distribution of neurofibrillary tangles and neuritic plaques in the cerebral cortex of patients with Alzheimer's disease. *Cereb Cortex*, 1 (1): 103-16. doi: 10.1093/cercor/1.1.103.
16. Li, X., Wang, H., Tian, Y., Zhou, S., Li, X., Wang, K. & Yu, Y. (2016). Impaired White Matter Connections of the Limbic System Networks Associated with Impaired Emotional Memory in Alzheimer's Disease. *Front Aging Neurosci*, 8: 250. doi: 10.3389/fnagi.2016.00250.
17. Davies, C. A., Mann, D. M., Sumpter, P. Q. & Yates, P. O. (1987). A quantitative morphometric analysis of the neuronal and synaptic content of the frontal and temporal cortex in patients with Alzheimer's disease. *J Neurol Sci*, 78 (2): 151-64. doi: 10.1016/0022-510x(87)90057-8.
18. Salat, D. H., Kaye, J. A. & Janowsky, J. S. (2001). Selective preservation and degeneration within the prefrontal cortex in aging and Alzheimer disease. *Arch Neurol*, 58 (9): 1403-8. doi: 10.1001/archneur.58.9.1403.
19. Wiesman, A. I., Mundorf, V. M., Casagrande, C. C., Wolfson, S. L., Johnson, C. M., May, P. E., Murman, D. L. & Wilson, T. W. (2021). Somatosensory dysfunction is masked by variable cognitive deficits across patients on the Alzheimer's disease spectrum. *EBioMedicine*, 73: 103638. doi: 10.1016/j.ebiom.2021.103638.
20. Zhang, Y., Wu, Z., Huang, Z., Liu, Y., Chen, X., Zhao, X., He, H. & Deng, Y. (2022). GSK-3beta inhibition elicits a neuroprotection by restoring lysosomal dysfunction in neurons via facilitation

of TFEB nuclear translocation after ischemic stroke. *Brain Res*, 1778: 147768. doi: 10.1016/j.brainres.2021.147768.
21. Hampel, H., Hardy, J., Blennow, K., Chen, C., Perry, G., Kim, S. H., Villemagne, V. L., Aisen, P., Vendruscolo, M., Iwatsubo, T., et al. (2021). The Amyloid-beta Pathway in Alzheimer's Disease. *Mol Psychiatry*, 26 (10): 5481-5503. doi: 10.1038/s41380-021-01249-0.
22. Wilquet, V. & De Strooper, B. (2004). Amyloid-beta precursor protein processing in neurodegeneration. *Curr Opin Neurobiol*, 14 (5): 582-8. doi: 10.1016/j.conb.2004.08.001.
23. Cole, S. L. & Vassar, R. (2007). The Alzheimer's disease beta-secretase enzyme, BACE1. *Mol Neurodegener*, 2: 22. doi: 10.1186/1750-1326-2-22.
24. Dovey, H. F., John, V., Anderson, J. P., Chen, L. Z., de Saint Andrieu, P., Fang, L. Y., Freedman, S. B., Folmer, B., Goldbach, E., Holsztynska, E. J., et al. (2001). Functional gamma-secretase inhibitors reduce beta-amyloid peptide levels in brain. *J Neurochem*, 76 (1): 173-81. doi: 10.1046/j.1471-4159.2001.00012.x.
25. Shaw, G., Morse, S., Ararat, M. & Graham, F. L. (2002). Preferential transformation of human neuronal cells by human adenoviruses and the origin of HEK 293 cells. *FASEB J*, 16 (8): 869-71. doi: 10.1096/fj.01-0995fje.
26. Roychaudhuri, R., Yang, M., Hoshi, M. M. & Teplow, D. B. (2009). Amyloid beta-protein assembly and Alzheimer disease. *J Biol Chem*, 284 (8): 4749-53. doi: 10.1074/jbc.R800036200.
27. Caillet-Boudin, M. L., Buee, L., Sergeant, N. & Lefebvre, B. (2015). Regulation of human MAPT gene expression. *Mol Neurodegener*, 10: 28. doi: 10.1186/s13024-015-0025-8.
28. Guo, T., Noble, W. & Hanger, D. P. (2017). Roles of tau protein in health and disease. *Acta Neuropathol*, 133 (5): 665-704. doi: 10.1007/s00401-017-1707-9.
29. Orr, M. E., Sullivan, A. C. & Frost, B. (2017). A Brief Overview of Tauopathy: Causes, Consequences, and Therapeutic Strategies. *Trends Pharmacol Sci*, 38 (7): 637-648. doi: 10.1016/j.tips.2017.03.011.
30. Jouanne, M., Rault, S. & Voisin-Chiret, A. S. (2017). Tau protein aggregation in Alzheimer's disease: An attractive target for the development of novel therapeutic agents. *Eur J Med Chem*, 139: 153-167. doi: 10.1016/j.ejmech.2017.07.070.
31. Deshpande, A., Win, K. M. & Busciglio, J. (2008). Tau isoform expression and regulation in human cortical neurons. *FASEB J*, 22 (7): 2357-67. doi: 10.1096/fj.07-096909.
32. Castellani, R. J. & Perry, G. (2019). Tau Biology, Tauopathy, Traumatic Brain Injury, and Diagnostic Challenges. *J Alzheimers Dis*, 67 (2): 447-467. doi: 10.3233/JAD-180721.
33. Alquezar, C., Arya, S. & Kao, A. W. (2020). Tau Post-translational Modifications: Dynamic Transformers of Tau Function, Degradation, and Aggregation. *Front Neurol*, 11: 595532. doi: 10.3389/fneur.2020.595532.
34. Lebouvier, T., Scales, T. M., Williamson, R., Noble, W., Duyckaerts, C., Hanger, D. P., Reynolds, C. H., Anderton, B. H. & Derkinderen, P. (2009). The microtubule-associated protein tau is also phosphorylated on tyrosine. *J Alzheimers Dis*, 18 (1): 1-9. doi: 10.3233/JAD-2009-1116.
35. Stoothoff, W. H. & Johnson, G. V. (2005). Tau phosphorylation: physiological and pathological consequences. *Biochim Biophys Acta*, 1739 (2-3): 280-97. doi: 10.1016/j.bbadis.2004.06.017.
36. Johnson, G. V. & Stoothoff, W. H. (2004). Tau phosphorylation in neuronal cell function and dysfunction. *J Cell Sci*, 117 (Pt 24): 5721-9. doi: 10.1242/jcs.01558.
37. Wegmann, S., Biernat, J. & Mandelkow, E. (2021). A current view on Tau protein phosphorylation in Alzheimer's disease. *Curr Opin Neurobiol*, 69: 131-138. doi: 10.1016/j.conb.2021.03.003.
38. Farias, G., Cornejo, A., Jimenez, J., Guzman, L. & Maccioni, R. B. (2011). Mechanisms of tau self-aggregation and neurotoxicity. *Curr Alzheimer Res*, 8 (6): 608-14. doi: 10.2174/156720511796717258.

39. Rankin, C. A., Sun, Q. & Gamblin, T. C. (2005). Pseudo-phosphorylation of tau at Ser202 and Thr205 affects tau filament formation. *Brain Res Mol Brain Res*, 138 (1): 84-93. doi: 10.1016/j.molbrainres.2005.04.012.
40. EidenmÜLler, J., Fath, T., Maas, T., Pool, M., Sontag, E. & Brandt, R. (2001). Phosphorylation-mimicking glutamate clusters in the proline-rich region are sufficient to simulate the functional deficiencies of hyperphosphorylated tau protein. *Biochemical Journal*, 357 (3): 759-767. doi: 10.1042/bj3570759.
41. Liu, F., Li, B., Tung, E. J., Grundke-Iqbal, I., Iqbal, K. & Gong, C. X. (2007). Site-specific effects of tau phosphorylation on its microtubule assembly activity and self-aggregation. *Eur J Neurosci*, 26 (12): 3429-36. doi: 10.1111/j.1460-9568.2007.05955.x.
42. Martin, L., Latypova, X., Wilson, C. M., Magnaudeix, A., Perrin, M. L., Yardin, C. & Terro, F. (2013). Tau protein kinases: involvement in Alzheimer's disease. *Ageing Res Rev*, 12 (1): 289-309. doi: 10.1016/j.arr.2012.06.003.
43. Wang, J. Z., Grundke-Iqbal, I. & Iqbal, K. (2007). Kinases and phosphatases and tau sites involved in Alzheimer neurofibrillary degeneration. *Eur J Neurosci*, 25 (1): 59-68. doi: 10.1111/j.1460-9568.2006.05226.x.
44. Hernandez, F., Gomez de Barreda, E., Fuster-Matanzo, A., Lucas, J. J. & Avila, J. (2010). GSK3: a possible link between beta amyloid peptide and tau protein. *Exp Neurol*, 223 (2): 322-5. doi: 10.1016/j.expneurol.2009.09.011.
45. Sayas, C. L. & Avila, J. (2021). GSK-3 and Tau: A Key Duet in Alzheimer's Disease. *Cells*, 10 (4). doi: 10.3390/cells10040721.
46. Lee, S., Hall, G. F. & Shea, T. B. (2011). Potentiation of tau aggregation by cdk5 and GSK3beta. *J Alzheimers Dis*, 26 (2): 355-64. doi: 10.3233/JAD-2011-102016.
47. Booth, L. N. & Brunet, A. (2016). The Aging Epigenome. *Mol Cell*, 62 (5): 728-44. doi: 10.1016/j.molcel.2016.05.013.
48. Moreira, P. I., Carvalho, C., Zhu, X., Smith, M. A. & Perry, G. (2010). Mitochondrial dysfunction is a trigger of Alzheimer's disease pathophysiology. *Biochim Biophys Acta*, 1802 (1): 2-10. doi: 10.1016/j.bbadis.2009.10.006.
49. Nixon, R. A., Wegiel, J., Kumar, A., Yu, W. H., Peterhoff, C., Cataldo, A. & Cuervo, A. M. (2005). Extensive involvement of autophagy in Alzheimer disease: an immuno-electron microscopy study. *J Neuropathol Exp Neurol*, 64 (2): 113-22. doi: 10.1093/jnen/64.2.113.
50. Lehtonen, S., Sonninen, T. M., Wojciechowski, S., Goldsteins, G. & Koistinaho, J. (2019). Dysfunction of Cellular Proteostasis in Parkinson's Disease. *Front Neurosci*, 13: 457. doi: 10.3389/fnins.2019.00457.
51. Ruegsegger, C. & Saxena, S. (2016). Proteostasis impairment in ALS. *Brain Res*, 1648 (Pt B): 571-579. doi: 10.1016/j.brainres.2016.03.032.
52. Weidling, I. W. & Swerdlow, R. H. (2020). Mitochondria in Alzheimer's disease and their potential role in Alzheimer's proteostasis. *Exp Neurol*, 330: 113321. doi: 10.1016/j.expneurol.2020.113321.
53. Kaushik, S. & Cuervo, A. M. (2015). Proteostasis and aging. *Nat Med*, 21 (12): 1406-15. doi: 10.1038/nm.4001.
54. Kurtishi, A., Rosen, B., Patil, K. S., Alves, G. W. & Moller, S. G. (2019). Cellular Proteostasis in Neurodegeneration. *Mol Neurobiol*, 56 (5): 3676-3689. doi: 10.1007/s12035-018-1334-z.
55. Stein, K. C. & Frydman, J. (2019). The stop-and-go traffic regulating protein biogenesis: How translation kinetics controls proteostasis. *J Biol Chem*, 294 (6): 2076-2084. doi: 10.1074/jbc.REV118.002814.
56. Korovila, I., Hugo, M., Castro, J. P., Weber, D., Hohn, A., Grune, T. & Jung, T. (2017). Proteostasis, oxidative stress and aging. *Redox Biol*, 13: 550-567. doi: 10.1016/j.redox.2017.07.008.

57. Uddin, M. S., Al Mamun, A., Rahman, M. A., Behl, T., Perveen, A., Hafeez, A., Bin-Jumah, M. N., Abdel-Daim, M. M. & Ashraf, G. M. (2020). Emerging Proof of Protein Misfolding and Interactions in Multifactorial Alzheimer's Disease. *Curr Top Med Chem*, 20 (26): 2380-2390. doi: 10.2174/1568026620666200601161703.
58. Mulligan, V. K. & Chakrabartty, A. (2013). Protein misfolding in the late-onset neurodegenerative diseases: common themes and the unique case of amyotrophic lateral sclerosis. *Proteins*, 81 (8): 1285-303. doi: 10.1002/prot.24285.
59. Feng, Y., He, D., Yao, Z. & Klionsky, D. J. (2014). The machinery of macroautophagy. *Cell Res*, 24 (1): 24-41. doi: 10.1038/cr.2013.168.
60. Rubinsztein, D. C., Marino, G. & Kroemer, G. (2011). Autophagy and aging. *Cell*, 146 (5): 682-95. doi: 10.1016/j.cell.2011.07.030.
61. Papadopoulos, C., Kravic, B. & Meyer, H. (2020). Repair or Lysophagy: Dealing with Damaged Lysosomes. *J Mol Biol*, 432 (1): 231-239. doi: 10.1016/j.jmb.2019.08.010.
62. Youle, R. J. & Narendra, D. P. (2011). Mechanisms of mitophagy. *Nat Rev Mol Cell Biol*, 12 (1): 9-14. doi: 10.1038/nrm3028.
63. Cebollero, E., Reggiori, F. & Kraft, C. (2012). Reticulophagy and ribophagy: regulated degradation of protein production factories. *Int J Cell Biol*, 2012: 182834. doi: 10.1155/2012/182834.
64. Dunn, W. A., Jr., Cregg, J. M., Kiel, J. A., van der Klei, I. J., Oku, M., Sakai, Y., Sibirny, A. A., Stasyk, O. V. & Veenhuis, M. (2005). Pexophagy: the selective autophagy of peroxisomes. *Autophagy*, 1 (2): 75-83. doi: 10.4161/auto.1.2.1737.
65. Mizushima, N. (2011). Autophagy in protein and organelle turnover. *Cold Spring Harb Symp Quant Biol*, 76: 397-402. doi: 10.1101/sqb.2011.76.011023.
66. Lai, S. C. & Devenish, R. J. (2012). LC3-Associated Phagocytosis (LAP): Connections with Host Autophagy. *Cells*, 1 (3): 396-408. doi: 10.3390/cells1030396.
67. Singh, K. K. (2004). Mitochondria damage checkpoint in apoptosis and genome stability. *FEMS Yeast Res*, 5 (2): 127-32. doi: 10.1016/j.femsyr.2004.04.008.
68. Trifunovic, A. & Larsson, N. G. (2008). Mitochondrial dysfunction as a cause of ageing. *J Intern Med*, 263 (2): 167-78. doi: 10.1111/j.1365-2796.2007.01905.x.
69. James, A. M. & Murphy, M. P. (2002). How mitochondrial damage affects cell function. *J Biomed Sci*, 9 (6 Pt 1): 475-87. doi: 10.1159/000064721.
70. Shafiei, S. S., Guerrero-Munoz, M. J. & Castillo-Carranza, D. L. (2017). Tau Oligomers: Cytotoxicity, Propagation, and Mitochondrial Damage. *Front Aging Neurosci*, 9: 83. doi: 10.3389/fnagi.2017.00083.
71. Kandimalla, R., Manczak, M., Yin, X., Wang, R. & Reddy, P. H. (2018). Hippocampal phosphorylated tau induced cognitive decline, dendritic spine loss and mitochondrial abnormalities in a mouse model of Alzheimer's disease. *Hum Mol Genet*, 27 (1): 30-40. doi: 10.1093/hmg/ddx381.
72. Abtahi, S. L., Masoudi, R. & Haddadi, M. (2020). The distinctive role of tau and amyloid beta in mitochondrial dysfunction through alteration in Mfn2 and Drp1 mRNA Levels: A comparative study in Drosophila melanogaster. *Gene*, 754: 144854. doi: 10.1016/j.gene.2020.144854.
73. Manczak, M. & Reddy, P. H. (2012). Abnormal interaction between the mitochondrial fission protein Drp1 and hyperphosphorylated tau in Alzheimer's disease neurons: implications for mitochondrial dysfunction and neuronal damage. *Hum Mol Genet*, 21 (11): 2538-47. doi: 10.1093/hmg/dds072.
74. Yan, J., Liu, X. H., Han, M. Z., Wang, Y. M., Sun, X. L., Yu, N., Li, T., Su, B. & Chen, Z. Y. (2015). Blockage of GSK3beta-mediated Drp1 phosphorylation provides neuroprotection in neuronal and mouse models of Alzheimer's disease. *Neurobiol Aging*, 36 (1): 211-27. doi: 10.1016/j.neurobiolaging.2014.08.005.

75. Kandimalla, R., Manczak, M., Pradeepkiran, J. A., Morton, H. & Reddy, P. H. (2023). A partial reduction of Drp1 improves cognitive behavior and enhances mitophagy, autophagy and dendritic spines in a transgenic Tau mouse model of Alzheimer disease. *Hum Mol Genet*, 32 (12): 2119-2120. doi: 10.1093/hmg/ddad040.
76. Corsetti, V., Amadoro, G., Gentile, A., Capsoni, S., Ciotti, M. T., Cencioni, M. T., Atlante, A., Canu, N., Rohn, T. T., Cattaneo, A., et al. (2008). Identification of a caspase-derived N-terminal tau fragment in cellular and animal Alzheimer's disease models. *Mol Cell Neurosci*, 38 (3): 381-92. doi: 10.1016/j.mcn.2008.03.011.
77. Dai, C. L., Chen, X., Kazim, S. F., Liu, F., Gong, C. X., Grundke-Iqbal, I. & Iqbal, K. (2015). Passive immunization targeting the N-terminal projection domain of tau decreases tau pathology and improves cognition in a transgenic mouse model of Alzheimer disease and tauopathies. *J Neural Transm (Vienna)*, 122 (4): 607-17. doi: 10.1007/s00702-014-1315-y.
78. Cummins, N., Tweedie, A., Zuryn, S., Bertran-Gonzalez, J. & Gotz, J. (2019). Disease-associated tau impairs mitophagy by inhibiting Parkin translocation to mitochondria. *EMBO J*, 38 (3). doi: 10.15252/embj.201899360.
79. Yamamoto, H., Zhang, S. & Mizushima, N. (2023). Autophagy genes in biology and disease. *Nat Rev Genet*, 24 (6): 382-400. doi: 10.1038/s41576-022-00562-w.
80. Lorincz, P. & Juhasz, G. (2020). Autophagosome-Lysosome Fusion. *J Mol Biol*, 432 (8): 2462-2482. doi: 10.1016/j.jmb.2019.10.028.
81. Ryter, S. W., Cloonan, S. M. & Choi, A. M. (2013). Autophagy: a critical regulator of cellular metabolism and homeostasis. *Mol Cells*, 36 (1): 7-16. doi: 10.1007/s10059-013-0140-8.
82. Subramani, S. & Malhotra, V. (2013). Non-autophagic roles of autophagy-related proteins. *EMBO Rep*, 14 (2): 143-51. doi: 10.1038/embor.2012.220.
83. Popelka, H. & Klionsky, D. J. (2023). Autophagic structures revealed by cryo-electron tomography: new clues about autophagosome biogenesis. *Autophagy*, 19 (5): 1375-1377. doi: 10.1080/15548627.2023.2175305.
84. Lin, Y. X., Wang, Y. & Wang, H. (2017). Recent Advances in Nanotechnology for Autophagy Detection. *Small*, 13 (33). doi: 10.1002/smll.201700996.
85. O'Prey, J., Sakamaki, J., Baudot, A. D., New, M., Van Acker, T., Tooze, S. A., Long, J. S. & Ryan, K. M. (2017). Application of CRISPR/Cas9 to Autophagy Research. *Methods Enzymol*, 588: 79-108. doi: 10.1016/bs.mie.2016.09.076.
86. Qin, Q., Gu, Z., Li, F., Pan, Y., Zhang, T., Fang, Y. & Zhang, L. (2022). A Diagnostic Model for Alzheimer's Disease Based on Blood Levels of Autophagy-Related Genes. *Front Aging Neurosci*, 14: 881890. doi: 10.3389/fnagi.2022.881890.
87. Nafchi, A. R., Esmaeili, M., Myers, O., Oprea, T. & Bearer, E. L. (2022). Autophagy and Herpesvirus: A collaboration Contributing to Alzheimer's Disease. *FASEB J*, 36 Suppl 1. doi: 10.1096/fasebj.2022.36.S1.R2731.
88. Bordi, M., Berg, M. J., Mohan, P. S., Peterhoff, C. M., Alldred, M. J., Che, S., Ginsberg, S. D. & Nixon, R. A. (2016). Autophagy flux in CA1 neurons of Alzheimer hippocampus: Increased induction overburdens failing lysosomes to propel neuritic dystrophy. *Autophagy*, 12 (12): 2467-2483. doi: 10.1080/15548627.2016.1239003.
89. Alemu, E. A., Lamark, T., Torgersen, K. M., Birgisdottir, A. B., Larsen, K. B., Jain, A., Olsvik, H., Overvatn, A., Kirkin, V. & Johansen, T. (2012). ATG8 family proteins act as scaffolds for assembly of the ULK complex: sequence requirements for LC3-interacting region (LIR) motifs. *J Biol Chem*, 287 (47): 39275-90. doi: 10.1074/jbc.M112.378109.
90. Park, J. M., Jung, C. H., Seo, M., Otto, N. M., Grunwald, D., Kim, K. H., Moriarity, B., Kim, Y. M., Starker, C., Nho, R. S., et al. (2016). The ULK1 complex mediates MTORC1 signaling to the

autophagy initiation machinery via binding and phosphorylating ATG14. *Autophagy*, 12 (3): 547-64. doi: 10.1080/15548627.2016.1140293.
91. Lamark, T., Svenning, S. & Johansen, T. (2017). Regulation of selective autophagy: the p62/SQSTM1 paradigm. *Essays Biochem*, 61 (6): 609-624. doi: 10.1042/EBC20170035.
92. Yamamoto, H., Kakuta, S., Watanabe, T. M., Kitamura, A., Sekito, T., Kondo-Kakuta, C., Ichikawa, R., Kinjo, M. & Ohsumi, Y. (2012). Atg9 vesicles are an important membrane source during early steps of autophagosome formation. *J Cell Biol*, 198 (2): 219-33. doi: 10.1083/jcb.201202061.
93. Suzuki, S. W., Yamamoto, H., Oikawa, Y., Kondo-Kakuta, C., Kimura, Y., Hirano, H. & Ohsumi, Y. (2015). Atg13 HORMA domain recruits Atg9 vesicles during autophagosome formation. *Proc Natl Acad Sci U S A*, 112 (11): 3350-5. doi: 10.1073/pnas.1421092112.
94. Rosenberg, S. C. & Corbett, K. D. (2015). The multifaceted roles of the HORMA domain in cellular signaling. *J Cell Biol*, 211 (4): 745-55. doi: 10.1083/jcb.201509076.
95. Guardia, C. M., Tan, X. F., Lian, T., Rana, M. S., Zhou, W., Christenson, E. T., Lowry, A. J., Faraldo-Gomez, J. D., Bonifacino, J. S., Jiang, J., et al. (2020). Structure of Human ATG9A, the Only Transmembrane Protein of the Core Autophagy Machinery. *Cell Rep*, 31 (13): 107837. doi: 10.1016/j.celrep.2020.107837.
96. Yamano, K., Kikuchi, R., Kojima, W., Hayashida, R., Koyano, F., Kawawaki, J., Shoda, T., Demizu, Y., Naito, M., Tanaka, K., et al. (2020). Critical role of mitochondrial ubiquitination and the OPTN-ATG9A axis in mitophagy. *J Cell Biol*, 219 (9). doi: 10.1083/jcb.201912144.
97. Ohashi, Y. (2021). Class III phosphatidylinositol 3-kinase complex I subunit NRBF2/Atg38 - from cell and structural biology to health and disease. *Autophagy*, 17 (12): 3897-3907. doi: 10.1080/15548627.2021.1872240.
98. Vergne, I. & Deretic, V. (2010). The role of PI3P phosphatases in the regulation of autophagy. *FEBS Lett*, 584 (7): 1313-8. doi: 10.1016/j.febslet.2010.02.054.
99. Gopaldass, N., Fauvet, B., Lashuel, H., Roux, A. & Mayer, A. (2017). Membrane scission driven by the PROPPIN Atg18. *EMBO J*, 36 (22): 3274-3291. doi: 10.15252/embj.201796859.
100. Graef, M. (2018). Membrane tethering by the autophagy ATG2A-WIPI4 complex. *Proc Natl Acad Sci U S A*, 115 (42): 10540-10541. doi: 10.1073/pnas.1814759115.
101. Proikas-Cezanne, T., Takacs, Z., Donnes, P. & Kohlbacher, O. (2015). WIPI proteins: essential PtdIns3P effectors at the nascent autophagosome. *J Cell Sci*, 128 (2): 207-17. doi: 10.1242/jcs.146258.
102. Geng, J. & Klionsky, D. J. (2008). The Atg8 and Atg12 ubiquitin-like conjugation systems in macroautophagy. 'Protein modifications: beyond the usual suspects' review series. *EMBO Rep*, 9 (9): 859-64. doi: 10.1038/embor.2008.163.
103. Shpilka, T., Weidberg, H., Pietrokovski, S. & Elazar, Z. (2011). Atg8: an autophagy-related ubiquitin-like protein family. *Genome Biol*, 12 (7): 226. doi: 10.1186/gb-2011-12-7-226.
104. Noda, N. N. (2021). Atg2 and Atg9: Intermembrane and interleaflet lipid transporters driving autophagy. *Biochim Biophys Acta Mol Cell Biol Lipids*, 1866 (8): 158956. doi: 10.1016/j.bbalip.2021.158956.
105. Collier, J. J., Suomi, F., Olahova, M., McWilliams, T. G. & Taylor, R. W. (2021). Emerging roles of ATG7 in human health and disease. *EMBO Mol Med*, 13 (12): e14824. doi: 10.15252/emmm.202114824.
106. Ambrosio. (1998). LC3-I conversion to LC3-II does not necessarily result in complete autophagy. *International Journal of Molecular Medicine*. doi: 10.3892/ijmm_00000085.
107. Gatica, D., Lahiri, V. & Klionsky, D. J. (2018). Cargo recognition and degradation by selective autophagy. *Nat Cell Biol*, 20 (3): 233-242. doi: 10.1038/s41556-018-0037-z.

108. Schreiber, A. & Peter, M. (2014). Substrate recognition in selective autophagy and the ubiquitin-proteasome system. *Biochim Biophys Acta*, 1843 (1): 163-81. doi: 10.1016/j.bbamcr.2013.03.019.
109. Fracchiolla, D., Sawa-Makarska, J. & Martens, S. (2017). Beyond Atg8 binding: The role of AIM/LIR motifs in autophagy. *Autophagy*, 13 (5): 978-979. doi: 10.1080/15548627.2016.1277311.
110. Zhou, J., Wang, J., Cheng, Y., Chi, Y.-J., Fan, B., Yu, J.-Q. & Chen, Z. (2014). Correction: NBR1-Mediated Selective Autophagy Targets Insoluble Ubiquitinated Protein Aggregates in Plant Stress Responses. *PLoS Genetics*, 10 (6). doi: 10.1371/journal.pgen.1004477.
111. Zellner, S. & Behrends, C. (2021). Autophagosome content profiling reveals receptor-specific cargo candidates. *Autophagy*, 17 (5): 1281-1283. doi: 10.1080/15548627.2021.1909410.
112. Loi, M., Marazza, A. & Molinari, M. (2021). Endoplasmic Reticulum (ER) and ER-Phagy. *Prog Mol Subcell Biol*, 59: 99-114. doi: 10.1007/978-3-030-67696-4_5.
113. Marinkovic, M., Sprung, M. & Novak, I. (2021). Dimerization of mitophagy receptor BNIP3L/NIX is essential for recruitment of autophagic machinery. *Autophagy*, 17 (5): 1232-1243. doi: 10.1080/15548627.2020.1755120.
114. Nthiga, T. M., Shrestha, B. K., Lamark, T. & Johansen, T. (2020). CALCOCO1 is a soluble reticulophagy receptor. *Autophagy*, 16 (9): 1729-1731. doi: 10.1080/15548627.2020.1797289.
115. Zhou, Z., Liu, J., Fu, T., Wu, P., Peng, C., Gong, X., Wang, Y., Zhang, M., Li, Y., Wang, Y., et al. (2021). Phosphorylation regulates the binding of autophagy receptors to FIP200 Claw domain for selective autophagy initiation. *Nat Commun*, 12 (1): 1570. doi: 10.1038/s41467-021-21874-1.
116. Grunwald, D. S., Otto, N. M., Park, J. M., Song, D. & Kim, D. H. (2020). GABARAPs and LC3s have opposite roles in regulating ULK1 for autophagy induction. *Autophagy*, 16 (4): 600-614. doi: 10.1080/15548627.2019.1632620.
117. Suzuki, H., Tabata, K., Morita, E., Kawasaki, M., Kato, R., Dobson, R. C., Yoshimori, T. & Wakatsuki, S. (2014). Structural basis of the autophagy-related LC3/Atg13 LIR complex: recognition and interaction mechanism. *Structure*, 22 (1): 47-58. doi: 10.1016/j.str.2013.09.023.
118. Jiang, W., Chen, X., Ji, C., Zhang, W., Song, J., Li, J. & Wang, J. (2021). Key Regulators of Autophagosome Closure. *Cells*, 10 (11). doi: 10.3390/cells10112814.
119. Henne, W. M., Buchkovich, N. J. & Emr, S. D. (2011). The ESCRT pathway. *Dev Cell*, 21 (1): 77-91. doi: 10.1016/j.devcel.2011.05.015.
120. Wang, Y., Li, L., Hou, C., Lai, Y., Long, J., Liu, J., Zhong, Q. & Diao, J. (2016). SNARE-mediated membrane fusion in autophagy. *Semin Cell Dev Biol*, 60: 97-104. doi: 10.1016/j.semcdb.2016.07.009.
121. Ballabio, A. & Bonifacino, J. S. (2020). Lysosomes as dynamic regulators of cell and organismal homeostasis. *Nat Rev Mol Cell Biol*, 21 (2): 101-118. doi: 10.1038/s41580-019-0185-4.
122. Yim, W. W. & Mizushima, N. (2020). Lysosome biology in autophagy. *Cell Discov*, 6: 6. doi: 10.1038/s41421-020-0141-7.
123. Chen, Y. & Yu, L. (2017). Recent progress in autophagic lysosome reformation. *Traffic*, 18 (6): 358-361. doi: 10.1111/tra.12484.
124. Rong, Y., Liu, M., Ma, L., Du, W., Zhang, H., Tian, Y., Cao, Z., Li, Y., Ren, H., Zhang, C., et al. (2012). Clathrin and phosphatidylinositol-4,5-bisphosphate regulate autophagic lysosome reformation. *Nat Cell Biol*, 14 (9): 924-34. doi: 10.1038/ncb2557.
125. Liu, X. & Klionsky, D. J. (2018). Regulation of autophagic lysosome reformation by kinesin 1, clathrin and phosphatidylinositol-4,5-bisphosphate. *Autophagy*, 14 (1): 1-2. doi: 10.1080/15548627.2017.1386821.

126. Zhou, C., Wu, Z., Du, W., Que, H., Wang, Y., Ouyang, Q., Jian, F., Yuan, W., Zhao, Y., Tian, R., et al. (2022). Recycling of autophagosomal components from autolysosomes by the recycler complex. *Nat Cell Biol*, 24 (4): 497-512. doi: 10.1038/s41556-022-00861-8.
127. Zhang, Z., Yue, P., Lu, T., Wang, Y., Wei, Y. & Wei, X. (2021). Role of lysosomes in physiological activities, diseases, and therapy. *J Hematol Oncol*, 14 (1): 79. doi: 10.1186/s13045-021-01087-1.
128. Kenney, D. L. & Benarroch, E. E. (2015). The autophagy-lysosomal pathway: General concepts and clinical implications. *Neurology*, 85 (7): 634-45. doi: 10.1212/WNL.0000000000001860.
129. Zhang, W., Yang, X., Li, Y., Yu, L., Zhang, B., Zhang, J., Cho, W. J., Venkatarangan, V., Chen, L., Burugula, B. B., et al. (2022). GCAF(TMEM251) regulates lysosome biogenesis by activating the mannose-6-phosphate pathway. *Nat Commun*, 13 (1): 5351. doi: 10.1038/s41467-022-33025-1.
130. Kissing, S., Hermsen, C., Repnik, U., Nesset, C. K., von Bargen, K., Griffiths, G., Ichihara, A., Lee, B. S., Schwake, M., De Brabander, J., et al. (2015). Vacuolar ATPase in phagosome-lysosome fusion. *J Biol Chem*, 290 (22): 14166-80. doi: 10.1074/jbc.M114.628891.
131. Wartosch, L., Fuhrmann, J. C., Schweizer, M., Stauber, T. & Jentsch, T. J. (2009). Lysosomal degradation of endocytosed proteins depends on the chloride transport protein ClC-7. *FASEB J*, 23 (12): 4056-68. doi: 10.1096/fj.09-130880.
132. Cuajungco, M. P. & Kiselyov, K. (2017). The mucolipin-1 (TRPML1) ion channel, transmembrane-163 (TMEM163) protein, and lysosomal zinc handling. *Front Biosci (Landmark Ed)*, 22 (8): 1330-1343. doi: 10.2741/4546.
133. van Veen, S., Martin, S., Van den Haute, C., Benoy, V., Lyons, J., Vanhoutte, R., Kahler, J. P., Decuypere, J. P., Gelders, G., Lambie, E., et al. (2020). ATP13A2 deficiency disrupts lysosomal polyamine export. *Nature*, 578 (7795): 419-424. doi: 10.1038/s41586-020-1968-7.
134. Zimmerli, S., Majeed, M., Gustavsson, M., Stendahl, O., Sanan, D. A. & Ernst, J. D. (1996). Phagosome-lysosome fusion is a calcium-independent event in macrophages. *J Cell Biol*, 132 (1-2): 49-61. doi: 10.1083/jcb.132.1.49.
135. Huynh, K. K., Eskelinen, E. L., Scott, C. C., Malevanets, A., Saftig, P. & Grinstein, S. (2007). LAMP proteins are required for fusion of lysosomes with phagosomes. *EMBO J*, 26 (2): 313-24. doi: 10.1038/sj.emboj.7601511.
136. Akwa, Y., Di Malta, C., Zallo, F., Gondard, E., Lunati, A., Diaz-de-Grenu, L. Z., Zampelli, A., Boiret, A., Santamaria, S., Martinez-Preciado, M., et al. (2023). Stimulation of synaptic activity promotes TFEB-mediated clearance of pathological MAPT/Tau in cellular and mouse models of tauopathies. *Autophagy*, 19 (2): 660-677. doi: 10.1080/15548627.2022.2095791.
137. Settembre, C. & Medina, D. L. (2015). TFEB and the CLEAR network. *Methods Cell Biol*, 126: 45-62. doi: 10.1016/bs.mcb.2014.11.011.
138. Yang, Y. & Sauve, A. A. (2016). NAD(+) metabolism: Bioenergetics, signaling and manipulation for therapy. *Biochim Biophys Acta*, 1864 (12): 1787-1800. doi: 10.1016/j.bbapap.2016.06.014.
139. Akie, T. E., Liu, L., Nam, M., Lei, S. & Cooper, M. P. (2015). OXPHOS-Mediated Induction of NAD+ Promotes Complete Oxidation of Fatty Acids and Interdicts Non-Alcoholic Fatty Liver Disease. *PLoS One*, 10 (5): e0125617. doi: 10.1371/journal.pone.0125617.
140. Canto, C. (2022). NAD(+) Precursors: A Questionable Redundancy. *Metabolites*, 12 (7). doi: 10.3390/metabo12070630.
141. Reiten, O. K., Wilvang, M. A., Mitchell, S. J., Hu, Z. & Fang, E. F. (2021). Preclinical and clinical evidence of NAD(+) precursors in health, disease, and ageing. *Mech Ageing Dev*, 199: 111567. doi: 10.1016/j.mad.2021.111567.
142. Zhong, O., Wang, J., Tan, Y., Lei, X. & Tang, Z. (2022). Effects of NAD+ precursor supplementation on glucose and lipid metabolism in humans: a meta-analysis. *Nutr Metab (Lond)*, 19 (1): 20. doi: 10.1186/s12986-022-00653-9.

143. Covarrubias, A. J., Perrone, R., Grozio, A. & Verdin, E. (2021). NAD(+) metabolism and its roles in cellular processes during ageing. *Nat Rev Mol Cell Biol*, 22 (2): 119-141. doi: 10.1038/s41580-020-00313-x.
144. Pollak, N., Niere, M. & Ziegler, M. (2007). NAD kinase levels control the NADPH concentration in human cells. *J Biol Chem*, 282 (46): 33562-33571. doi: 10.1074/jbc.M704442200.
145. Amjad, S., Nisar, S., Bhat, A. A., Shah, A. R., Frenneaux, M. P., Fakhro, K., Haris, M., Reddy, R., Patay, Z., Baur, J., et al. (2021). Role of NAD(+) in regulating cellular and metabolic signaling pathways. *Mol Metab*, 49: 101195. doi: 10.1016/j.molmet.2021.101195.
146. Savitz, J. (2020). The kynurenine pathway: a finger in every pie. *Mol Psychiatry*, 25 (1): 131-147. doi: 10.1038/s41380-019-0414-4.
147. Bieganowski, P. & Brenner, C. (2004). Discoveries of nicotinamide riboside as a nutrient and conserved NRK genes establish a Preiss-Handler independent route to NAD+ in fungi and humans. *Cell*, 117 (4): 495-502. doi: 10.1016/s0092-8674(04)00416-7.
148. Kennedy, B. E., Sharif, T., Martell, E., Dai, C., Kim, Y., Lee, P. W. & Gujar, S. A. (2016). NAD(+) salvage pathway in cancer metabolism and therapy. *Pharmacol Res*, 114: 274-283. doi: 10.1016/j.phrs.2016.10.027.
149. Yang, Y., Zhang, N., Zhang, G. & Sauve, A. A. (2020). NRH salvage and conversion to NAD(+) requires NRH kinase activity by adenosine kinase. *Nat Metab*, 2 (4): 364-379. doi: 10.1038/s42255-020-0194-9.
150. Stromland, O., Diab, J., Ferrario, E., Sverkeli, L. J. & Ziegler, M. (2021). The balance between NAD(+) biosynthesis and consumption in ageing. *Mech Ageing Dev*, 199: 111569. doi: 10.1016/j.mad.2021.111569.
151. Marty, L., Siala, W., Schwarzlander, M., Fricker, M. D., Wirtz, M., Sweetlove, L. J., Meyer, Y., Meyer, A. J., Reichheld, J. P. & Hell, R. (2009). The NADPH-dependent thioredoxin system constitutes a functional backup for cytosolic glutathione reductase in Arabidopsis. *Proc Natl Acad Sci U S A*, 106 (22): 9109-14. doi: 10.1073/pnas.0900206106.
152. Agledal, L., Niere, M. & Ziegler, M. (2010). The phosphate makes a difference: cellular functions of NADP. *Redox Rep*, 15 (1): 2-10. doi: 10.1179/174329210X12650506623122.
153. Kawai, S. & Murata, K. (2008). Structure and function of NAD kinase and NADP phosphatase: key enzymes that regulate the intracellular balance of NAD(H) and NADP(H). *Biosci Biotechnol Biochem*, 72 (4): 919-30. doi: 10.1271/bbb.70738.
154. Nocito, L., Kleckner, A. S., Yoo, E. J., Jones Iv, A. R., Liesa, M. & Corkey, B. E. (2015). The extracellular redox state modulates mitochondrial function, gluconeogenesis, and glycogen synthesis in murine hepatocytes. *PLoS One*, 10 (3): e0122818. doi: 10.1371/journal.pone.0122818.
155. Katsyuba, E., Romani, M., Hofer, D. & Auwerx, J. (2020). NAD(+) homeostasis in health and disease. *Nat Metab*, 2 (1): 9-31. doi: 10.1038/s42255-019-0161-5.
156. Luongo, T. S., Eller, J. M., Lu, M. J., Niere, M., Raith, F., Perry, C., Bornstein, M. R., Oliphint, P., Wang, L., McReynolds, M. R., et al. (2020). SLC25A51 is a mammalian mitochondrial NAD(+) transporter. *Nature*, 588 (7836): 174-179. doi: 10.1038/s41586-020-2741-7.
157. Salmina, A. B., Komleva, Y. K., Lopatina, O. L., Gorina, Y. V., Malinovskaya, N. A., Pozhilenkova, E. A., Panina, Y. A., Zhukov, E. L. & Medvedeva, N. N. (2014). CD38 and CD157 Expression: Glial Control of Neurodegeneration and Neuroinflammation. *Messenger*, 3 (1): 78-85. doi: 10.1166/msr.2014.1037.
158. Jiang, Y., Liu, T., Lee, C. H., Chang, Q., Yang, J. & Zhang, Z. (2020). The NAD(+)-mediated self-inhibition mechanism of pro-neurodegenerative SARM1. *Nature*, 588 (7839): 658-663. doi: 10.1038/s41586-020-2862-z.

159. Carafa, V., Rotili, D., Forgione, M., Cuomo, F., Serretiello, E., Hailu, G. S., Jarho, E., Lahtela-Kakkonen, M., Mai, A. & Altucci, L. (2016). Sirtuin functions and modulation: from chemistry to the clinic. *Clin Epigenetics*, 8: 61. doi: 10.1186/s13148-016-0224-3.
160. Sauve, A. A. (2010). Sirtuin chemical mechanisms. *Biochim Biophys Acta*, 1804 (8): 1591-603. doi: 10.1016/j.bbapap.2010.01.021.
161. Li, X. (2013). SIRT1 and energy metabolism. *Acta Biochim Biophys Sin (Shanghai)*, 45 (1): 51-60. doi: 10.1093/abbs/gms108.
162. Tasselli, L., Zheng, W. & Chua, K. F. (2017). SIRT6: Novel Mechanisms and Links to Aging and Disease. *Trends Endocrinol Metab*, 28 (3): 168-185. doi: 10.1016/j.tem.2016.10.002.
163. Bause, A. S. & Haigis, M. C. (2013). SIRT3 regulation of mitochondrial oxidative stress. *Exp Gerontol*, 48 (7): 634-9. doi: 10.1016/j.exger.2012.08.007.
164. Wilson, N., Kataura, T., Korsgen, M. E., Sun, C., Sarkar, S. & Korolchuk, V. I. (2023). The autophagy-NAD axis in longevity and disease. *Trends Cell Biol*, 33 (9): 788-802. doi: 10.1016/j.tcb.2023.02.004.
165. Zhang, D. X., Zhang, J. P., Hu, J. Y. & Huang, Y. S. (2016). The potential regulatory roles of NAD(+) and its metabolism in autophagy. *Metabolism*, 65 (4): 454-62. doi: 10.1016/j.metabol.2015.11.010.
166. Aman, Y., Frank, J., Lautrup, S. H., Matysek, A., Niu, Z., Yang, G., Shi, L., Bergersen, L. H., Storm-Mathisen, J., Rasmussen, L. J., et al. (2020). The NAD(+)-mitophagy axis in healthy longevity and in artificial intelligence-based clinical applications. *Mech Ageing Dev*, 185: 111194. doi: 10.1016/j.mad.2019.111194.
167. Huang, J., Wang, X., Zhu, Y., Li, Z., Zhu, Y. T., Wu, J. C., Qin, Z. H., Xiang, M. & Lin, F. (2019). Exercise activates lysosomal function in the brain through AMPK-SIRT1-TFEB pathway. *CNS Neurosci Ther*, 25 (6): 796-807. doi: 10.1111/cns.13114.
168. Wang, L., Xu, C., Johansen, T., Berger, S. L. & Dou, Z. (2021). SIRT1 - a new mammalian substrate of nuclear autophagy. *Autophagy*, 17 (2): 593-595. doi: 10.1080/15548627.2020.1860541.
169. Fang, E. F., Scheibye-Knudsen, M., Brace, L. E., Kassahun, H., SenGupta, T., Nilsen, H., Mitchell, J. R., Croteau, D. L. & Bohr, V. A. (2014). Defective mitophagy in XPA via PARP-1 hyperactivation and NAD(+)/SIRT1 reduction. *Cell*, 157 (4): 882-896. doi: 10.1016/j.cell.2014.03.026.
170. Cao, W., Dou, Y. & Li, A. (2018). Resveratrol Boosts Cognitive Function by Targeting SIRT1. *Neurochem Res*, 43 (9): 1705-1713. doi: 10.1007/s11064-018-2586-8.
171. Feng, L., Chen, M., Li, Y., Li, M., Hu, S., Zhou, B., Zhu, L., Yu, L., Zhou, Q., Tan, L., et al. (2021). Sirt1 deacetylates and stabilizes p62 to promote hepato-carcinogenesis. *Cell Death Dis*, 12 (4): 405. doi: 10.1038/s41419-021-03666-z.
172. Guan, S., Xin, Y., Ding, Y., Zhang, Q. & Han, W. (2023). Ginsenoside Rg1 Protects against Cardiac Remodeling in Heart Failure via SIRT1/PINK1/Parkin-Mediated Mitophagy. *Chem Biodivers*, 20 (2): e202200730. doi: 10.1002/cbdv.202200730.
173. Yang, J., Zhang, W., Zhang, S., Iyaswamy, A., Sun, J., Wang, J. & Yang, C. (2023). Novel Insight into Functions of Transcription Factor EB (TFEB) in Alzheimer's Disease and Parkinson's Disease. *Aging Dis*, 14 (3): 652-669. doi: 10.14336/AD.2022.0927.
174. Nah, J., Sung, E. A., Zhai, P., Zablocki, D. & Sadoshima, J. (2022). Tfeb-Mediated Transcriptional Regulation of Autophagy Induces Autosis during Ischemia/Reperfusion in the Heart. *Cells*, 11 (2). doi: 10.3390/cells11020258.
175. Napolitano, G., Esposito, A., Choi, H., Matarese, M., Benedetti, V., Di Malta, C., Monfregola, J., Medina, D. L., Lippincott-Schwartz, J. & Ballabio, A. (2018). mTOR-dependent phosphorylation controls TFEB nuclear export. *Nat Commun*, 9 (1): 3312. doi: 10.1038/s41467-018-05862-6.

176. Hou, B., Li, Y., Li, X., Zhang, C., Zhao, Z., Chen, Q., Zhang, N. & Li, H. (2020). HGF protected against diabetic nephropathy via autophagy-lysosome pathway in podocyte by modulating PI3K/Akt-GSK3beta-TFEB axis. *Cell Signal*, 75: 109744. doi: 10.1016/j.cellsig.2020.109744.
177. Wang, Y., Huang, Y., Liu, J., Zhang, J., Xu, M., You, Z., Peng, C., Gong, Z. & Liu, W. (2020). Acetyltransferase GCN5 regulates autophagy and lysosome biogenesis by targeting TFEB. *EMBO Rep*, 21 (1): e48335. doi: 10.15252/embr.201948335.
178. Li, Q., Liu, Y. & Sun, M. (2017). Autophagy and Alzheimer's Disease. *Cell Mol Neurobiol*, 37 (3): 377-388. doi: 10.1007/s10571-016-0386-8.
179. Xu, Y., Du, S., Marsh, J. A., Horie, K., Sato, C., Ballabio, A., Karch, C. M., Holtzman, D. M. & Zheng, H. (2021). TFEB regulates lysosomal exocytosis of tau and its loss of function exacerbates tau pathology and spreading. *Mol Psychiatry*, 26 (10): 5925-5939. doi: 10.1038/s41380-020-0738-0.
180. Wang, C., Niederstrasser, H., Douglas, P. M., Lin, R., Jaramillo, J., Li, Y., Oswald, N. W., Zhou, A., McMillan, E. A., Mendiratta, S., et al. (2017). Small-molecule TFEB pathway agonists that ameliorate metabolic syndrome in mice and extend C. elegans lifespan. *Nat Commun*, 8 (1): 2270. doi: 10.1038/s41467-017-02332-3.
181. Nnah, I. C., Wang, B., Saqcena, C., Weber, G. F., Bonder, E. M., Bagley, D., De Cegli, R., Napolitano, G., Medina, D. L., Ballabio, A., et al. (2019). TFEB-driven endocytosis coordinates MTORC1 signaling and autophagy. *Autophagy*, 15 (1): 151-164. doi: 10.1080/15548627.2018.1511504.
182. Liu, Y., Xue, X., Zhang, H., Che, X., Luo, J., Wang, P., Xu, J., Xing, Z., Yuan, L., Liu, Y., et al. (2019). Neuronal-targeted TFEB rescues dysfunction of the autophagy-lysosomal pathway and alleviates ischemic injury in permanent cerebral ischemia. *Autophagy*, 15 (3): 493-509. doi: 10.1080/15548627.2018.1531196.
183. Dang, T. T. & Back, S. H. (2021). Translation Inhibitors Activate Autophagy Master Regulators TFEB and TFE3. *Int J Mol Sci*, 22 (21). doi: 10.3390/ijms222112083.
184. Li, C., Wang, X., Li, X., Qiu, K., Jiao, F., Liu, Y., Kong, Q., Liu, Y. & Wu, Y. (2019). Proteasome Inhibition Activates Autophagy-Lysosome Pathway Associated With TFEB Dephosphorylation and Nuclear Translocation. *Front Cell Dev Biol*, 7: 170. doi: 10.3389/fcell.2019.00170.
185. Napolitano, G. & Ballabio, A. (2016). TFEB at a glance. *J Cell Sci*, 129 (13): 2475-81. doi: 10.1242/jcs.146365.
186. Hasegawa, J., Tokuda, E., Yao, Y., Sasaki, T., Inoki, K. & Weisman, L. S. (2022). PP2A-dependent TFEB activation is blocked by PIKfyve-induced mTORC1 activity. *Mol Biol Cell*, 33 (3): ar26. doi: 10.1091/mbc.E21-06-0309.
187. Vega-Rubin-de-Celis, S., Pena-Llopis, S., Konda, M. & Brugarolas, J. (2017). Multistep regulation of TFEB by MTORC1. *Autophagy*, 13 (3): 464-472. doi: 10.1080/15548627.2016.1271514.
188. Hikita, T., Uehara, R., Itoh, R. E., Mitani, F., Miyata, M., Yoshida, T., Yamaguchi, R. & Oneyama, C. (2022). MEK/ERK-mediated oncogenic signals promote secretion of extracellular vesicles by controlling lysosome function. *Cancer Sci*, 113 (4): 1264-1276. doi: 10.1111/cas.15288.
189. Yang, C., Zhu, Z., Tong, B. C., Iyaswamy, A., Xie, W. J., Zhu, Y., Sreenivasmurthy, S. G., Senthilkumar, K., Cheung, K. H., Song, J. X., et al. (2020). A stress response p38 MAP kinase inhibitor SB202190 promoted TFEB/TFE3-dependent autophagy and lysosomal biogenesis independent of p38. *Redox Biol*, 32: 101445. doi: 10.1016/j.redox.2020.101445.
190. Song, H. C., Chen, Y., Chen, Y., Park, J., Zheng, M., Surh, Y. J., Kim, U. H., Park, J. W., Yu, R., Chung, H. T., et al. (2020). GSK-3beta inhibition by curcumin mitigates amyloidogenesis via TFEB activation and anti-oxidative activity in human neuroblastoma cells. *Free Radic Res*, 54 (11-12): 918-930. doi: 10.1080/10715762.2020.1791843.
191. Palmieri, M., Pal, R. & Sardiello, M. (2017). AKT modulates the autophagy-lysosome pathway via TFEB. *Cell Cycle*, 16 (13): 1237-1238. doi: 10.1080/15384101.2017.1337968.

192. Medina, D. L., Di Paola, S., Peluso, I., Armani, A., De Stefani, D., Venditti, R., Montefusco, S., Scotto-Rosato, A., Prezioso, C., Forrester, A., et al. (2015). Lysosomal calcium signalling regulates autophagy through calcineurin and TFEB. *Nat Cell Biol*, 17 (3): 288-99. doi: 10.1038/ncb3114.
193. Beck, W. H. J., Kim, D., Das, J., Yu, H., Smolka, M. B. & Mao, Y. (2020). Glucosylation by the Legionella Effector SetA Promotes the Nuclear Localization of the Transcription Factor TFEB. *iScience*, 23 (7): 101300. doi: 10.1016/j.isci.2020.101300.
194. Zhang, J., Wang, J., Zhou, Z., Park, J. E., Wang, L., Wu, S., Sun, X., Lu, L., Wang, T., Lin, Q., et al. (2018). Importance of TFEB acetylation in control of its transcriptional activity and lysosomal function in response to histone deacetylase inhibitors. *Autophagy*, 14 (6): 1043-1059. doi: 10.1080/15548627.2018.1447290.
195. Zheng, Y., Kou, J., Wang, P., Ye, T., Wang, Z., Gao, Z., Cong, L., Li, M., Dong, B., Yang, W., et al. (2021). Berberine-induced TFEB deacetylation by SIRT1 promotes autophagy in peritoneal macrophages. *Aging (Albany NY)*, 13 (5): 7096-7119. doi: 10.18632/aging.202566.
196. Cheng, L., Chen, Y., Guo, D., Zhong, Y., Li, W., Lin, Y. & Miao, Y. (2023). mTOR-dependent TFEB activation and TFEB overexpression enhance autophagy-lysosome pathway and ameliorate Alzheimer's disease-like pathology in diabetic encephalopathy. *Cell Commun Signal*, 21 (1): 91. doi: 10.1186/s12964-023-01097-1.
197. Marsh, E. K. & May, R. C. (2012). Caenorhabditis elegans, a model organism for investigating immunity. *Appl Environ Microbiol*, 78 (7): 2075-81. doi: 10.1128/AEM.07486-11.
198. Corsi, A. K., Wightman, B. & Chalfie, M. (2015). A Transparent Window into Biology: A Primer on Caenorhabditis elegans. *Genetics*, 200 (2): 387-407. doi: 10.1534/genetics.115.176099.
199. Chen, N., Harris, T. W., Antoshechkin, I., Bastiani, C., Bieri, T., Blasiar, D., Bradnam, K., Canaran, P., Chan, J., Chen, C. K., et al. (2005). WormBase: a comprehensive data resource for Caenorhabditis biology and genomics. *Nucleic Acids Res*, 33 (Database issue): D383-9. doi: 10.1093/nar/gki066.
200. Shtonda, B. B. & Avery, L. (2006). Dietary choice behavior in Caenorhabditis elegans. *J Exp Biol*, 209 (Pt 1): 89-102. doi: 10.1242/jeb.01955.
201. Yemini, E., Jucikas, T., Grundy, L. J., Brown, A. E. & Schafer, W. R. (2013). A database of Caenorhabditis elegans behavioral phenotypes. *Nat Methods*, 10 (9): 877-9. doi: 10.1038/nmeth.2560.
202. Van Raamsdonk, J. M. & Hekimi, S. (2011). FUdR causes a twofold increase in the lifespan of the mitochondrial mutant gas-1. *Mech Ageing Dev*, 132 (10): 519-21. doi: 10.1016/j.mad.2011.08.006.
203. Aitlhadj, L. & Sturzenbaum, S. R. (2010). The use of FUdR can cause prolonged longevity in mutant nematodes. *Mech Ageing Dev*, 131 (5): 364-5. doi: 10.1016/j.mad.2010.03.002.
204. McGinty, D., Lapczynski, A., Scognamiglio, J., Letizia, C. S. & Api, A. M. (2010). Fragrance materials review on isoamyl alcohol. *Food Chem Toxicol*, 48 Suppl 4: S102-9. doi: 10.1016/j.fct.2010.05.040.
205. Helsenorge. (2021). *Uhell Med Klorin - Rådene Fra Giftinformasjonen. [Accident with Klorin – Advice from the poison center of information]*. Available at: http://www.helsenorge.no/giftinformasjon/produkter-og-kjemikalier/vaskemidler/klorin/#:~:text=Klorin%20er%20et%20rengj%C3%B8ringsprodukt%20som.
206. Cao, S. Q., Wang, H. L., Palikaras, K., Tavernarakis, N. & Fang, E. F. (2023). Chemotaxis assay for evaluation of memory-like behavior in wild-type and Alzheimer's-disease-like C. elegans models. *STAR Protoc*, 4 (2): 102250. doi: 10.1016/j.xpro.2023.102250.
207. McKee, A. C., Carreras, I., Hossain, L., Ryu, H., Klein, W. L., Oddo, S., LaFerla, F. M., Jenkins, B. G., Kowall, N. W. & Dedeoglu, A. (2008). Ibuprofen reduces Abeta, hyperphosphorylated tau and

memory deficits in Alzheimer mice. *Brain Res*, 1207: 225-36. doi: 10.1016/j.brainres.2008.01.095.
208. Lapierre, L. R., De Magalhaes Filho, C. D., McQuary, P. R., Chu, C. C., Visvikis, O., Chang, J. T., Gelino, S., Ong, B., Davis, A. E., Irazoqui, J. E., et al. (2013). The TFEB orthologue HLH-30 regulates autophagy and modulates longevity in Caenorhabditis elegans. *Nat Commun*, 4: 2267. doi: 10.1038/ncomms3267.
209. Kocaturk, N. M. & Gozuacik, D. (2018). Crosstalk Between Mammalian Autophagy and the Ubiquitin-Proteasome System. *Front Cell Dev Biol*, 6: 128. doi: 10.3389/fcell.2018.00128.
210. Bence, N. F., Sampat, R. M. & Kopito, R. R. (2001). Impairment of the ubiquitin-proteasome system by protein aggregation. *Science*, 292 (5521): 1552-5. doi: 10.1126/science.292.5521.1552.
211. Xia, Y. (2022). Role of Ubiquilin-2 in Proteostasis and Tau Aggregation in Tauopathies. *J Neurosci*, 42 (32): 6168-6170. doi: 10.1523/JNEUROSCI.0839-22.2022.
212. Natale, C., Barzago, M. M. & Diomede, L. (2020). Caenorhabditis elegans Models to Investigate the Mechanisms Underlying Tau Toxicity in Tauopathies. *Brain Sci*, 10 (11). doi: 10.3390/brainsci10110838.
213. van der Velpen, V., Rosenberg, N., Maillard, V., Teav, T., Chatton, J. Y., Gallart-Ayala, H. & Ivanisevic, J. (2021). Sex-specific alterations in NAD+ metabolism in 3xTg Alzheimer's disease mouse brain assessed by quantitative targeted LC-MS. *J Neurochem*, 159 (2): 378-388. doi: 10.1111/jnc.15362.
214. Hou, Y., Lautrup, S., Cordonnier, S., Wang, Y., Croteau, D. L., Zavala, E., Zhang, Y., Moritoh, K., O'Connell, J. F., Baptiste, B. A., et al. (2018). NAD(+) supplementation normalizes key Alzheimer's features and DNA damage responses in a new AD mouse model with introduced DNA repair deficiency. *Proc Natl Acad Sci U S A*, 115 (8): E1876-E1885. doi: 10.1073/pnas.1718819115.
215. Yoshizawa, T., Karim, M. F., Sato, Y., Senokuchi, T., Miyata, K., Fukuda, T., Go, C., Tasaki, M., Uchimura, K., Kadomatsu, T., et al. (2014). SIRT7 controls hepatic lipid metabolism by regulating the ubiquitin-proteasome pathway. *Cell Metab*, 19 (4): 712-21. doi: 10.1016/j.cmet.2014.03.006.

7.0 Appendix list

7.1 Result Figures and tables

Table 3 Lifepan raw data. Table of all the data gathered for lifespan assay. The death column represents all the worms that died at their designated day of adulthood. Survive are the total amount of worms that was still alive. Sens. is the amount of worms that have died of non-ageing related causes. Total alive are the amount of worms that was used for the calculation of the survival index. Each biological repeats (BR) are represented under each strain, in total there was 3 biological repeats.

N2												
	BR1				BR2				BR3			
	Death	Survive	Sens.	Tot. alive	Death	Survive	Sens.	Tot. alive	Death	Survive	Sens.	Tot. alive
D1	0	85	0	85	0	77	0	77	0	75	0	75
D2	0	85	0		0	77	0		0	75	0	
D3	0	85	0		0	77	0		0	75	0	
D4	0	85	0		0	77	0		0	75	0	
D5	0	85	4		0	77	4		0	75	0	
D6	0	85	0		0	77	0		0	75	7	
D7	0	85	0		0	77	0		0	75	0	
D8	0	85	0		0	77	1		0	75	1	
D9	6	79	0		4	73	0		0	75	0	
D10	2	77	0		10	63	0		2	73	0	
D11	10	67	0		8	55	0		6	67	0	
D12	4	63	0		15	40	0		7	60	0	
D13	19	44	0		6	34	0		8	52	0	
D14	4	40	0		7	27	2		5	47	3	
D15	11	29	1		9	18	6		0	47	0	
D16	1	28	0		0	18	0		13	34	4	
D17	24	4	1		11	7	0		6	28	0	
D18	4	0	0		4	3	0		2	26	0	
D19	0	0	0		3	0	0		3	23	0	
D20	0	0	0		0	0	0		6	17	0	
D21	0	0	0		0	0	0		9	8	0	
D22	0	0	0		0	0	0		2	6	0	
D23	0	0	0		0	0	0		0	6	0	
D24	0	0	0		0	0	0		1	5	0	
D25	0	0	0		0	0	0		4	1	0	
D26	0	0	0		0	0	0		1	0	0	
D27	0	0	0		0	0	0		0	0	0	
D28	0	0	0		0	0	0		0	0	0	

Table 3 Continued.

N2 w/ NMN												
	BR1				BR2				BR3			
	Death	Survive	Sens.	Tot. alive	Death	Survive	Sens.	Tot. alive	Death	Survive	Sens.	Tot. alive
D1	0	65	0	65	0	73	0	73	0	78	0	78
D2	0	65	0		0	73	0		0	78	0	
D3	0	65	0		0	73	1		0	78	0	
D4	0	65	0		0	73	0		0	78	0	
D5	0	65	9		0	73	11		0	78	0	
D6	0	65	0		0	73	0		0	78	9	
D7	0	65	0		0	73	0		0	78	0	
D8	0	65	0		0	73	0		2	76	0	
D9	1	64	0		0	73	0		0	76	0	
D10	0	64	0		6	67	0		0	76	0	
D11	9	55	0		2	65	0		2	74	0	
D12	4	51	0		10	55	0		0	74	0	
D13	13	38	0		1	54	0		8	66	0	
D14	5	33	0		7	47	3		10	56	0	
D15	7	26	3		9	38	2		3	53	0	
D16	2	24	1		4	34	0		13	40	0	
D17	16	8	12		14	20	0		13	27	0	
D18	5	3	0		7	13	0		1	26	1	
D19	2	1	0		11	2	0		12	14	1	
D20	1	0	0		2	0	0		8	6	1	
D21	0	0	0		0	0	0		2	4	0	
D22	0	0	0		0	0	0		1	3	0	
D23	0	0	0		0	0	0		0	3	0	
D24	0	0	0		0	0	0		0	3	0	
D25	0	0	0		0	0	0		3	0	0	
D26	0	0	0		0	0	0		0	0	0	
D27	0	0	0		0	0	0		0	0	0	
D28	0	0	0		0	0	0		0	0	0	

Table 3 Continued.

CK12												
	BR1				BR2				BR3			
	Death	Survive	Sens.	Tot. alive	Death	Survive	Sens.	Tot. alive	Death	Survive	Sens.	Tot. alive
D1	0	81	0	81	0	78	0	78	0	83	0	83
D2	0	81	0		0	78	0		0	83	0	
D3	0	81	0		0	78	0		0	83	0	
D4	0	81	0		0	78	0		0	83	0	
D5	0	81	8		0	78	6		0	83	0	
D6	4	77	0		3	75	0		0	83	7	
D7	1	76	0		13	62	0		2	81	0	
D8	0	76	0		8	54	0		6	75	0	
D9	17	59	0		11	43	0		4	71	0	
D10	2	57	0		7	36	0		4	67	0	
D11	16	41	0		4	32	0		6	61	0	
D12	4	37	0		8	24	3		7	54	0	
D13	12	25	0		4	20	0		6	48	0	
D14	4	21	0		3	17	3		2	46	0	
D15	7	14	1		10	7	0		7	39	0	
D16	0	14	0		2	5	0		5	34	0	
D17	10	4	0		1	4	0		7	27	0	
D18	2	2	0		3	1	0		5	22	0	
D19	0	2	0		0	1	0		1	21	0	
D20	1	1	0		0	1	0		3	18	0	
D21	1	0	0		1	0	0		11	7	0	
D22	0	0	0		0	0	0		2	5	0	
D23	0	0	0		0	0	0		3	2	0	
D24	0	0	0		0	0	0		1	1	0	
D25	0	0	0		0	0	0		1	0	0	
D26	0	0	0		0	0	0		0	0	0	
D27	0	0	0		0	0	0		0	0	0	
D28	0	0	0		0	0	0		0	0	0	

Table 3 Continued.

CK12 w/ NMN												
	BR1				BR2				BR3			
	Death	Survive	Sens.	Tot. alive	Death	Survive	Sens.	Tot. alive	Death	Survive	Sens.	Tot. alive
D1	0	82	0	82	0	76	0	76	0	76	0	76
D2	0	82	0		0	76	0		0	76	0	
D3	0	82	0		0	76	0		0	76	0	
D4	0	82	0		0	76	0		0	76	0	
D5	0	82	5		0	76	12		0	76	0	
D6	0	82	0		4	72	0		0	76	9	
D7	0	82	0		3	69	0		0	76	0	
D8	0	82	0		1	68	0		11	65	0	
D9	2	80	0		5	63	0		12	53	0	
D10	3	77	0		6	57	0		7	46	0	
D11	8	69	0		3	54	0		6	40	0	
D12	1	68	0		5	49	0		0	40	0	
D13	13	55	0		3	46	0		0	40	0	
D14	9	46	0		5	41	2		5	35	0	
D15	12	34	0		7	34	0		5	30	0	
D16	4	30	2		14	20	0		3	27	4	
D17	22	8	1		5	15	0		4	23	1	
D18	2	6	0		7	8	0		13	10	0	
D19	5	1	0		5	3	0		4	6	0	
D20	1	0	0		2	1	0		4	2	0	
D21	0	0	0		0	1	0		0	2	0	
D22	0	0	0		1	0	0		0	2	0	
D23	0	0	0		0	0	0		2	0	0	
D24	0	0	0		0	0	0		0	0	0	
D25	0	0	0		0	0	0		0	0	0	
D26	0	0	0		0	0	0		0	0	0	
D27	0	0	0		0	0	0		0	0	0	
D28	0	0	0		0	0	0		0	0	0	

Table 3 Continued.

EFF033												
	BR1				BR2				BR3			
	Death	Survive	Sens.	Tot. alive	Death	Survive	Sens.	Tot. alive	Death	Survive	Sens.	Tot. alive
D1	0	80	0	80	0	73	0	73	0	80	0	80
D2	0	80	0		0	73	0		0	80	0	
D3	0	80	0		0	73	0		0	80	0	
D4	0	80	0		0	73	0		0	80	0	
D5	0	80	2		0	73	7		0	80	0	
D6	0	80	0		0	73	0		0	80	3	
D7	0	80	0		3	70	0		0	80	0	
D8	0	80	0		6	64	0		0	80	0	
D9	0	80	0		16	48	0		1	79	0	
D10	1	79	0		2	46	0		1	78	0	
D11	6	73	3		7	39	2		0	78	0	
D12	8	65	0		4	35	8		7	71	0	
D13	13	52	0		10	25	0		12	59	0	
D14	20	32	0		6	19	0		8	51	0	
D15	15	17	5		3	16	0		7	44	2	
D16	7	10	0		6	10	0		8	36	0	
D17	6	4	0		5	5	0		8	28	0	
D18	4	0	0		2	3	0		8	20	0	
D19	0	0	0		1	2	0		6	14	5	
D20	0	0	0		1	1	0		6	8	0	
D21	0	0	0		1	0	0		2	6	0	
D22	0	0	0		0	0	0		4	2	0	
D23	0	0	0		0	0	0		1	1	0	
D24	0	0	0		0	0	0		0	1	0	
D25	0	0	0		0	0	0		1	0	0	
D26	0	0	0		0	0	0		0	0	0	
D27	0	0	0		0	0	0		0	0	0	
D28	0	0	0		0	0	0		0	0	0	

Table 3 Continued.

EFF033 w/ NMN												
	BR1				BR2				BR3			
	Death	Survive	Sens.	Tot. alive	Death	Survive	Sens.	Tot. alive	Death	Survive	Sens.	Tot. alive
D1	0	77	0	77	0	50	0	50	0	112	0	112
D2	0	77	0		0	50	0		0	112	0	
D3	0	77	0		0	50	0		0	112	0	
D4	0	77	0		0	50	0		0	112	0	
D5	0	77	4		0	50	36		0	112	0	
D6	0	77	0		0	50	0		0	112	8	
D7	0	77	0		0	50	0		0	112	0	
D8	0	77	0		4	46	0		3	109	0	
D9	0	77	0		3	43	0		8	101	0	
D10	2	75	0		2	41	0		10	91	0	
D11	2	73	0		5	36	0		0	91	0	
D12	6	67	0		0	36	1		11	80	0	
D13	8	59	0		5	31	3		16	64	0	
D14	18	41	4		16	15	0		6	58	0	
D15	25	16	3		3	12	0		0	58	0	
D16	15	1	2		8	4	0		13	45	0	
D17	1	0	0		0	4	0		8	37	0	
D18	0	0	0		2	2	0		14	23	0	
D19	0	0	0		0	2	0		8	15	0	
D20	0	0	0		0	2	0		13	2	0	
D21	0	0	0		2	0	0		1	1	0	
D22	0	0	0		0	0	0		0	1	0	
D23	0	0	0		0	0	0		0	1	0	
D24	0	0	0		0	0	0		0	1	0	
D25	0	0	0		0	0	0		1	0	0	
D26	0	0	0		0	0	0		0	0	0	
D27	0	0	0		0	0	0		0	0	0	
D28	0	0	0		0	0	0		0	0	0	

Table 3 Continued.

EFF030												
	BR1				BR2				BR3			
	Death	Survive	Sens.	Tot. alive	Death	Survive	Sens.	Tot. alive	Death	Survive	Sens.	Tot. alive
D1	0	78	0	78	0	85	0	85	0	78	0	78
D2	0	78	0		0	85	0		0	78	0	
D3	0	78	0		0	85	0		0	78	0	
D4	0	78	0		0	85	0		0	78	0	
D5	0	78	8		0	85	5		0	78	0	
D6	0	78	0		0	85	0		0	78	3	
D7	0	78	0		0	85	0		0	78	0	
D8	3	75	0		5	80	0		0	78	0	
D9	0	75	0		7	73	0		0	78	0	
D10	8	67	0		3	70	0		3	75	0	
D11	2	65	0		10	60	0		0	75	0	
D12	3	62	0		9	51	0		6	69	0	
D13	2	60	0		6	45	0		8	61	0	
D14	17	43	0		16	29	0		5	56	0	
D15	0	43	0		2	27	0		6	50	1	
D16	21	22	0		16	11	0		6	44	0	
D17	16	6	3		4	7	0		5	39	0	
D18	2	4	0		3	4	0		17	22	6	
D19	2	2	1		4	0	0		9	13	2	
D20	0	2	0		0	0	0		9	4	0	
D21	2	0	0		0	0	0		0	4	0	
D22	0	0	0		0	0	0		2	2	0	
D23	0	0	0		0	0	0		1	1	0	
D24	0	0	0		0	0	0		0	1	0	
D25	0	0	0		0	0	0		1	0	0	
D26	0	0	0		0	0	0		0	0	0	
D27	0	0	0		0	0	0		0	0	0	
D28	0	0	0		0	0	0		0	0	0	

Table 3 Continued.

EFF030 w/ NMN												
	BR1				BR2				BR3			
	Death	Survive	Sens.	Tot. alive	Death	Survive	Sens.	Tot. alive	Death	Survive	Sens.	Tot. alive
D1	0	80	0	80	0	77	0	77	0	65	0	65
D2	0	80	0		0	77	0		0	65	0	
D3	0	80	0		0	77	0		0	65	0	
D4	0	80	0		0	77	0		0	65	0	
D5	0	80	8		0	77	11		0	65	0	
D6	0	80	0		0	77	0		0	65	15	
D7	0	80	0		0	77	0		0	65	0	
D8	2	78	0		0	77	0		0	65	0	
D9	0	78	0		6	71	0		0	65	0	
D10	12	66	0		4	67	1		14	51	0	
D11	3	63	0		11	56	0		0	51	0	
D12	7	56	0		2	54	0		0	51	5	
D13	0	56	0		9	45	0		0	51	0	
D14	3	53	0		8	37	0		5	46	4	
D15	0	53	0		0	37	1		0	46	0	
D16	16	37	0		11	26	0		6	40	0	
D17	14	23	0		7	19	0		7	33	0	
D18	14	9	1		8	11	0		13	20	0	
D19	4	5	1		7	4	0		10	10	0	
D20	5	0	0		2	2	0		7	3	1	
D21	0	0	0		1	1	0		1	2	0	
D22	0	0	0		1	0	0		1	1	0	
D23	0	0	0		0	0	0		0	1	0	
D24	0	0	0		0	0	0		0	1	0	
D25	0	0	0		0	0	0		1	0	0	
D26	0	0	0		0	0	0		0	0	0	
D27	0	0	0		0	0	0		0	0	0	
D28	0	0	0		0	0	0		0	0	0	

Table 4 Calculated data from Lifespan assay. The data displayed from **Table 3** are pooled together and displayed in their respective column. Death is the total amount of worms that died at their age of adulthood. The survive column are the amount of worms that are still alive. The Sens. column is the amount of worms that died of non-ageing related causes. The Survival % column is the calculated survival index for each day of death.

N2					N2 w/ NMN				
Total					Total				
Death	Survive	Sens.	Tot. alive	Survival %	Death	Survive	Sens.	Tot. alive	Survival %
0	237	0	237	100	0	216	0	216	100
0	237	0		100	0	216	0		100
0	237	0		100	0	216	1		100
0	237	0		100	0	216	0		100
0	237	8		100	0	216	20		100
0	237	7		100	0	216	9		100
0	237	0		100	0	216	0		100
0	237	2		100	2	214	0		99.07407
10	227	0		95.78059	1	213	0		98.61111
14	213	0		89.87342	6	207	0		95.83333
24	189	0		79.74684	13	194	0		89.81481
26	163	0		68.77637	14	180	0		83.33333
33	130	0		54.85232	22	158	0		73.14815
16	114	5		48.10127	22	136	3		62.96296
20	94	7		39.66245	19	117	5		54.16667
14	80	4		33.75527	19	98	1		45.37037
41	39	1		16.4557	43	55	12		25.46296
10	29	0		12.23629	13	42	1		19.44444
6	23	0		9.704641	25	17	1		7.87037
6	17	0		7.172996	11	6	1		2.777778
9	8	0		3.375527	2	4	0		1.851852
2	6	0		2.531646	1	3	0		1.388889
0	6	0		2.531646	0	3	0		1.388889
1	5	0		2.109705	0	3	0		1.388889
4	1	0		0.421941	3	0	0		0
1	0	0		0	0	0	0		0
0	0	0		0	0	0	0		0
0	0	0		0	0	0	0		0

Table 4 Continued.

CK12					CK12 w/ NMN				
Total					Total				
Death	Survive	Sens.	Tot. alive	Survival %	Death	Survive	Sens.	Tot. alive	Survival %
0	242	0	242	100	0	234	0	234	100
0	242	0		100	0	234	0		100
0	242	0		100	0	234	0		100
0	242	0		100	0	234	0		100
0	242	14		100	0	234	17		100
7	235	7		97.10744	4	230	9		98.2906
16	219	0		90.49587	3	227	0		97.00855
14	205	0		84.71074	12	215	0		91.88034
32	173	0		71.4876	19	196	0		83.76068
13	160	0		66.1157	16	180	0		76.92308
26	134	0		55.3719	17	163	0		69.65812
19	115	3		47.52066	6	157	0		67.09402
22	93	0		38.42975	16	141	0		60.25641
9	84	3		34.71074	19	122	2		52.13675
24	60	1		24.79339	24	98	0		41.88034
7	53	0		21.90083	21	77	6		32.90598
18	35	0		14.46281	31	46	2		19.65812
10	25	0		10.33058	22	24	0		10.25641
1	24	0		9.917355	14	10	0		4.273504
4	20	0		8.264463	7	3	0		1.282051
13	7	0		2.892562	0	3	0		1.282051
2	5	0		2.066116	1	2	0		0.854701
3	2	0		0.826446	2	0	0		0
1	1	0		0.413223	0	0	0		0
1	0	0		0	0	0	0		0
0	0	0		0	0	0	0		0
0	0	0		0	0	0	0		0
0	0	0		0	0	0	0		0

Table 4 Continued.

EFF033					EFF033 w/ NMN				
Total					Total				
Death	Survive	Sens.	Tot. alive	Survival %	Death	Survive	Sens.	Tot. alive	Survival %
0	233	0	233	100	0	239	0	239	100
0	233	0		100	0	239	0		100
0	233	0		100	0	239	0		100
0	233	0		100	0	239	0		100
0	233	9		100	0	239	40		100
0	233	3		100	0	239	8		100
3	230	0		98.71245	0	239	0		100
6	224	0		96.13734	7	232	0		97.07113
17	207	0		88.8412	11	221	0		92.46862
4	203	0		87.12446	14	207	0		86.61088
13	190	5		81.54506	7	200	0		83.68201
19	171	8		73.39056	17	183	1		76.56904
35	136	0		58.3691	29	154	3		64.43515
34	102	0		43.77682	40	114	4		47.69874
25	77	7		33.04721	28	86	3		35.98326
21	56	0		24.03433	36	50	2		20.9205
19	37	0		15.87983	9	41	0		17.15481
14	23	0		9.871245	16	25	0		10.46025
7	16	5		6.866953	8	17	0		7.112971
7	9	0		3.862661	13	4	0		1.67364
3	6	0		2.575107	3	1	0		0.41841
4	2	0		0.858369	0	1	0		0.41841
1	1	0		0.429185	0	1	0		0.41841
0	1	0		0.429185	0	1	0		0.41841
1	0	0		0	1	0	0		0
0	0	0		0	0	0	0		0
0	0	0		0	0	0	0		0
0	0	0		0	0	0	0		0

Table 4 Continued.

EFF030					EFF030 w/ NMN				
Total					Total				
Death	Survive	Sens.	Tot. alive	Survival %	Death	Survive	Sens.	Tot. alive	Survival %
0	241	0	241	100	0	222	0	222	100
0	241	0		100	0	222	0		100
0	241	0		100	0	222	0		100
0	241	0		100	0	222	0		100
0	241	13		100	0	222	19		100
0	241	3		100	0	222	15		100
0	241	0		100	0	222	0		100
8	233	0		96.6805	2	220	0		99.0991
7	226	0		93.77593	6	214	0		96.3964
14	212	0		87.9668	30	184	1		82.88288
12	200	0		82.98755	14	170	0		76.57658
18	182	0		75.51867	9	161	5		72.52252
16	166	0		68.87967	9	152	0		68.46847
38	128	0		53.11203	16	136	4		61.26126
8	120	1		49.79253	0	136	1		61.26126
43	77	0		31.95021	33	103	0		46.3964
25	52	3		21.57676	28	75	0		33.78378
22	30	6		12.44813	35	40	1		18.01802
15	15	3		6.224066	21	19	1		8.558559
9	6	0		2.489627	14	5	1		2.252252
2	4	0		1.659751	2	3	0		1.351351
2	2	0		0.829876	2	1	0		0.45045
1	1	0		0.414938	0	1	0		0.45045
0	1	0		0.414938	0	1	0		0.45045
1	0	0		0	1	0	0		0
0	0	0		0	0	0	0		0
0	0	0		0	0	0	0		0
0	0	0		0	0	0	0		0

Table 5. Pumping raw data. A list of all the raw data that was used for the pumping assay. All coulmns are organized in different biological repeat for different days of pumping for each different strain.

BR 1								
Day 2								
	N2	N2 w/ NMN	CK12	CK12 /w NMN	EFF033	EFF033 w/ NMN	EFF030	EFF030 w/ NMN
1	185	175	169	117	168	169	144	157
2	170	195	166	166	186	181	145	184
3	176	185	174	166	182	187	144	172
4	179	169	154	150	166	192	155	158
5	171	144	155	155	165	173	152	164
6	170	183	125	117	154	158	179	158
7	173	182	162	161	166	156	175	158
8	179	178	154	173	157	167	160	174
9	172	140	166	152	149	160	171	138
10	172	182	166	175	161	172	173	132
11	176	180	170	150	176	154	163	127
12	170	170	170	166	145	156	173	148
13	172	174	169	166	127	165	130	146
14	174	175	172	175	166	173	147	138
15	194	185	170	164	190	183	156	118
Day 4								
1	131	156	132	116	143	142	143	136
2	155	145	125	125	160	144	141	147
3	160	125	118	111	158	127	137	133
4	158	140	122	124	144	147	141	157
5	165	92	131	123	165	142	141	152
6	98	94	145	123	131	144	143	136
7	150	133	131	136	145	135	130	149
8	141	133	137	102	145	137	152	149
9	134	150	122	124	118	177	150	145
10	156	141	160	98	146	168	141	144
11	98	92	126	100	142	148	127	146
12	102	129	134	126	142	149	144	148
13	140	133	161	106	143	131	141	140
14	136	140	106	140	142	152	129	147
15	143	147	144	131	146	135	146	138

Table A5. Continued.

Day 8

	N2	N2 w/ NMN	CK12	CK12 /w NMN	EFF033	EFF033 w/ NMN	EFF030	EFF030 w/ NMN
1	125	109	120	100	72	122	106	121
2	107	79	94	125	131	104	109	119
3	132	125	92	121	105	107	149	109
4	105	139	109	96	138	134	119	111
5	84	67	87	102	134	137	130	113
6	70	118	96	107	118	118	109	118
7	97	130	105	88	130	151	122	134
8	110	128	90	116	114	138	107	144
9	131	115	82	106	112	92	107	125
10	143	151	69	106	138	128	116	109
11	136	117	89	109	122	121	121	143
12	90	119	75	75	150	134	114	122
13	110	122	89	106	109	131	101	117
14	131	140	125	131	130	113	95	140
15	143	148	119	108	132	152	124	113

BR 2

Day 2

	N2	N2 w/ NMN	CK12	CK12 /w NMN	EFF033	EFF033 w/ NMN	EFF030	EFF030 w/ NMN
1	188	182	185	172	196	166	173	200
2	190	181	178	178	194	168	161	164
3	202	177	191	190	185	171	168	194
4	177	183	179	163	186	168	164	180
5	196	180	181	160	180	176	170	179
6	180	178	167	170	171	166	160	185
7	176	189	163	159	172	173	174	185
8	178	178	176	161	175	163	172	179
9	185	191	153	168	185	180	170	187
10	169	198	178	174	165	196	191	179
11	181	172	162	162	184	180	172	170
12	193	194	159	166	166	159	191	173
13	191	196	164	173	179	173	185	177
14	192	182	165	161	166	171	175	170
15	177	174	178	172	177	148	181	208

Table 5. Continued.

Day 4								
	N2	N2 w/ NMN	CK12	CK12 /w NMN	EFF033	EFF033 w/ NMN	EFF030	EFF030 w/ NMN
1	171	162	158	139	163	148	150	150
2	174	174	153	168	168	142	152	159
3	168	154	176	142	142	132	139	157
4	159	151	157	147	150	154	155	167
5	144	161	152	148	145	159	130	175
6	156	155	138	156	157	130	135	153
7	164	147	160	113	162	151	137	151
8	137	146	135	171	158	162	137	154
9	157	127	142	117	153	114	171	143
10	163	168	144	142	158	152	167	169
11	155	159	142	134	155	150	135	155
12	154	148	113	156	156	161	167	163
13	159	156	146	155	140	145	134	138
14	169	164	148	161	138	136	174	139
15	181	163	135	154	148	150	157	159
Day 8								
	N2	N2 w/ NMN	CK12	CK12 /w NMN	EFF033	EFF033 w/ NMN	EFF030	EFF030 w/ NMN
1	145	101	75	101	62	147	99	131
2	119	113	79	63	59	113	120	135
3	118	122	73	85	50	107	138	128
4	145	131	110	83	94	83	120	122
5	142	117	92	100	73	102	84	129
6	133	134	52	108	71	95	112	81
7	126	126	57	107	58	118	99	96
8	73	138	67	111	109	72	107	131
9	108	128	76	91	67	75	93	128
10	102	136	56	90	96	117	101	136
11	135	104	79	64	100	69	129	128
12	127	120	109	126	51	123	123	138
13	74	113	107	105	65	119	125	139
14	72	118	83	115	96	86	119	140
15	126	115	109	100	90	83	140	120

Table 5. Continued.

Day 10								
	N2	N2 w/ NMN	CK12	CK12 /w NMN	EFF033	EFF033 w/ NMN	EFF030	EFF030 w/ NMN
1	67	47	81	99	97	60	124	122
2	109	38	94	94	93	49	132	135
3	120	111	65	59	98	103	97	112
4	78	41	87	106	94	102	89	110
5	93	135		81	80	118	124	127
6	79	119	21	100	62	99	99	118
7	122	128		83	107	118	103	84
8	22	135		89	110		92	109
9		39		45	48		102	84
10		128		104			97	125
11	123	80	14	48	53	52	84	110
12	106	40	62	80	78	51	86	134
13	105	99		91	100		125	81
14	128	138		78	68		117	80
15	24	55		80	97		126	99

BR 3

Day 2

	N2	N2 w/ NMN	CK12	CK12 /w NMN	EFF033	EFF033 w/ NMN	EFF030	EFF030 w/ NMN
1	181	205	184	178	190	169	196	184
2	192	196	204	183	197	176	187	205
3	218	181	194	180	200	185	183	193
4	179	191	192	190	179	179	196	214
5	183	195	178	191	185	180	204	180
6	195	198	171	187	174	170	172	191
7	201	184	179	183	182	173	198	178
8	196	188	185	187	180	215	175	181
9	202	190	181	180	181	170	182	192
10	205	184	170	182	182	175	170	189
11	180	188	188	187	168	266	186	179
12	191	194	185	185	172	186	180	193
13	196	194	186	193	168	204	198	186
14	198	186	186	181	213	189	197	175
15	200	187	195	180	201	196	170	184
16						194		
17						196		
18						186		
19						177		
20						165		

Table 5 Continued.

Day 4

	N2	N2 w/ NMN	CK12	CK12 /w NMN	EFF033	EFF033 w/ NMN	EFF030	EFF030 w/ NMN
1	146	149	168	121	139	150	174	161
2	149	132	164	135	155	139	154	149
3	147	177	169	161	122	165	161	174
4	157	201	162	165	149	156	157	175
5	152	133	178	151	132	135	168	165
6	177	195	163	151	147	161	138	160
7	172	147	171	165	114	148	183	175
8	164	145	155	160	164	136	160	180
9	138	166	168	155	143	140	162	184
10	174	165	185	145	138	159	170	146
11	142	148	150	145	163	156	159	158
12	166	138	168	140	142	150	156	170
13	171	177	155	160	137	139	160	167
14	169	162	163	165	145	182	170	168
15	160	166	169	152	123	145	139	160
16						158		
17						142		
18						159		
19						172		
20						155		

Day 8

	N2	N2 w/ NMN	CK12	CK12 /w NMN	EFF033	EFF033 w/ NMN	EFF030	EFF030 w/ NMN
1	96	134	154	127	139	87	105	139
2	114	131	102	124	143	133	142	126
3	133	155	135	106	141	136	140	130
4	128	145	120	140	130	128	131	151
5	108	120	148	122	118	100	115	115
6	140	105	130	108	99	108	130	131
7	143	122	151	82	142	82	126	122
8	126	154	113	129	101	132	150	142
9	130	158	138	141	139	122	136	130
10	126	128	143	129	142	110	136	155
11	114	128	156	122	115	141	139	124
12	114	121	139	145	130	104	137	137
13	137	117	119	108	129	129	137	139
14	109	158	149	137	79	94	139	140
15	113	127	105	134	145	95	126	82
16						130		
17						111		
18						101		
19						121		
20						147		

Table 5 Continued.

Day 10								
	N2	N2 w/ NMN	CK12	CK12 /w NMN	EFF033	EFF033 w/ NMN	EFF030	EFF030 w/ NMN
1	91	77	20	85	121	91	111	127
2	70	111	23	35	102	133	97	120
3	30	110	55	111	91	123	122	119
4	54	118	95	42	110	97	87	
5	78	56	61		51	109	73	
6	57	56	73	56	125	66	111	70
7	64	106	18	60	113	103	102	115
8	89	143		31	133	71	111	117
9	96	128		77	58	96	88	134
10				91	39			
11	107	134	90	27	40	63	111	85
12	79	119	103	72	75	131	104	102
13	116	127	35	68	125		99	118
14	133	117	16				123	
15	110	141						
16						110		
17						34		
18						130		
19						90		
20						56		

Table 6 Calculated data of Pumping Assay.

Day 2					Day 4				
***p*-value Veh.**					***p*-value Veh.**				
	N2	**CK12**	**EFF033**	**EFF030**		**N2**	**CK12**	**EFF033**	**EFF030**
N2	-	<0.0001	0.0024	0.0001	**N2**	-	0.3135	0.0644	0.5125
CK12	****	-	0.4317	0.8322	**CK12**	ns	-	0.4873	0.6312
EFF033	**	ns	-	0.3546	**EFF033**	ns	ns	-	0.159
EFF030	***	ns	ns	-	**EFF030**	ns	ns	ns	-
	Veh.-NMN		**Mean**			**Veh.-NMN**		**Mean**	
	***p*-value**	**Significance**	**Veh.**	**NMN**		***p*-value**	**Significance**	**Veh.**	**NMN**
N2	0.4189	ns	185	183	N2	0.3741	ns	152.5	148.6
CK12	0.3011	ns	173	170	CK12	0.0239	*	148.5	139.1
EFF033	0.7154	ns	176	177	EFF033	0.4285	ns	146.1	148.2
EFF030	0.7494	ns	173	174	EFF030	0.0739	ns	150.2	155.4

Day 8					Day 10				
***p*-value Veh.**					***p*-value Veh.**				
	N2	**CK12**	**EFF033**	**EFF030**		**N2**	**CK12**	**EFF033**	**EFF030**
N2	-	0.0100	0.0878	0.4401	N2	-	0.0029	0.9340	0.0112
CK12	*	-	0.4680	0.0009	CK12	**	-	0.0017	<0.0001
EFF033	ns	ns	-	0.0163	EFF033	ns	**	-	0.0070
EFF030	ns	***	*	-	EFF030	*	****	**	-
	Veh.-NMN		**Mean**			**Veh.-NMN**		**Mean**	
	***p*-value**	**Significance**	**Veh.**	**NMN**		***p*-value**	**Significance**	**Veh.**	**NMN**
N2	0.0743	ns	117.6	125	N2	0.1898	ns	87.04	99.17
CK12	0.3169	ns	103.7	108.9	CK12	0.0416	*	56.28	73.78
EFF033	0.2705	ns	108.2	114	EFF033	0.7530	ns	87.7	90.2
EFF030	0.0895	ns	120.6	126.3	EFF030	0.3311	ns	104.9	109.5

Table 7 Thrashing/Swimming raw data.

BR1								
Day 4								
	N2	N2 w/ NMN	CK12	CK12 w/ NMN	EFF033	EFF033 w/ NMN	EFF030	EFF030 w/ NMN
1	97	78	80	88	34	75	56	57
2	79	85	96	86	89	84	53	97
3	89	84	94	75	86	79	50	60
4	92	76	91	84	78	84	64	70
5	91	88	104	117	54	82	64	81
6	92	71	99	92	94	57	81	78
7	94	78	98	93	93	98	64	64
8	94	75	90	62	64	61	61	62
9	96	71	74	95	91	91	56	70
10	97	78	91	75	96	94	67	56
Day 8								
	N2	N2 w/ NMN	CK12	CK12 w/ NMN	EFF033	EFF033 w/ NMN	EFF030	EFF030 w/ NMN
1	52	56	51	86	84	75	31	48
2	56	53	90	60	80	51	45	47
3	47	73	81	57	31	41	59	48
4	60	22	30	83	30	49	36	43
5	63	45	18	25	84	51	45	52
6	68	48	24	58	63	71	33	49
7	69	38	44	36	64	54	32	42
8	49	38	63	54	57	63	40	38
9	86	20	73	45	78	82	47	68
10	51		71		33	70	61	65
Day 10								
	N2	N2 w/ NMN	CK12	CK12 w/ NMN	EFF033	EFF033 w/ NMN	EFF030	EFF030 w/ NMN
1	80		37	38	67	52	28	39
2	53		55	67	52	51	17	73
3	24		39		29	63	48	52
4	69				54	55	30	29
5					8	54	27	34
6					81	29	47	41
7					11	56	55	
8					74	37	26	
9					15	37	34	
10					17	58		

Table 7 Continued.

BR2

Day 4

	N2	N2 w/ NMN	CK12	CK12 w/ NMN	EFF033	EFF033 w/ NMN	EFF030	EFF030 w/ NMN
1	108	90	102	78	99	99	74	74
2	92	112	96	53	96	85	110	50
3	94	75	91	98	77	71	87	58
4	93	91	77	90	92	100	88	76
5	120	83	94	88	80	93	102	86
6	112	95	99	119	73	51	92	58
7	98	88	84	100	85	88	90	72
8	76	90	95	85	90	50	97	81
9	117	107	79	81	101	88	53	66
10	108	131	131	90	91	85	110	91

Day 8

	N2	N2 w/ NMN	CK12	CK12 w/ NMN	EFF033	EFF033 w/ NMN	EFF030	EFF030 w/ NMN
1	43	68	35		83	65	22	70
2	107	76	17		46	82	64	58
3	58	55	43		59	62	66	55
4	36	58	18		66	43	91	48
5	59	72	28		49	59	74	49
6	44	45	28		99	62	36	35
7	80	92	33		54	75	64	38
8	57	73	47		62	84	70	45
9			12		53	83	52	45
10			17		56	47	59	47

Day 10

	N2	N2 w/ NMN	CK12	CK12 w/ NMN	EFF033	EFF033 w/ NMN	EFF030	EFF030 w/ NMN
1	61		21	37	72	67	54	41
2	47		20	29	84	40	59	58
3	20		19	30	50	36	46	42
4	44		24	17	41	51	51	57
5	50		24	30	62	42	55	40
6	87		24	18	39	33	48	87
7	17		26	26	38	68	45	59
8			27	30	61	42	45	37
9				24	77	74	51	64
10					51	41	38	40

Table 7 Continued.

BR3

Day 4

	N2	N2 w/ NMN	CK12	CK12 w/ NMN	EFF033	EFF033 w/ NMN	EFF030	EFF030 w/ NMN
1	85	87	63	55	112	99	89	99
2	105	68	63	87	96	91	59	68
3	121	110	78	51	96	94	38	74
4	86	71	80	71	98	100	82	93
5	90	125	61	76	99	97	70	97
6	100	60	68	65	98	86	84	93
7	106	102	86	78	91	101	83	92
8	117	117	86	102	104	77	73	93
9	102	93	87	99	98	103	77	98
10	113	107	61	73	100	97	87	97

Day 8

	N2	N2 w/ NMN	CK12	CK12 w/ NMN	EFF033	EFF033 w/ NMN	EFF030	EFF030 w/ NMN
1	45	74	41	25	72	73	35	56
2	58	65	35	34	81	79	34	46
3	66	48	40	23	38	80	42	53
4	46	62	30	30	87	88	41	47
5	62	72	30	29	72	53	62	48
6	59	61	55	46	82	72	49	70
7	63	51	35	33	87	113	55	41
8	76	75	30	36	53	72	49	65
9	45	62		32	92	70	61	53
10	60	36		74	68	40	57	59

Day 10

	N2	N2 w/ NMN	CK12	CK12 w/ NMN	EFF033	EFF033 w/ NMN	EFF030	EFF030 w/ NMN
1				15	69	77	53	42
2				18	28	79	42	41
3				22	26	41	38	57
4				30	92	56	43	62
5				18	31	70	44	52
6				22	87	76	47	52
7				17	48	67	52	43
8				21	79	73	40	41
9					58	73	42	55
10					47	85	46	49

Table 7 Continued.

BR 4

	Day 8				Day 10			
	N2	N2 w/ NMN	CK12	CK12 w/ NMN	N2	N2 w/ NMN	CK12	CK12 w/ NMN
1	55	37	92	78	40	68	68	57
2	69	56	49	84	30	24	57	56
3		58		72	24	22	52	47
4				68	22	28	74	45
5				73	36	41	55	101
6				73	35	55	26	34
7				70	22	37	34	25
8				83	29	46	25	43
9				67	37	40	110	44
10				81	34	35	32	35
11				72	45	44	15	37
					53	43	61	
					38	30	15	
					29	78	88	
					56	33	55	
					45	35	24	
					32	64	32	
					26	54	25	
					34	35	25	
						24		

Extra

Day 10

	N2 w/ NMN	EFF030	EFF030 w/ NMN
1	35	24	69
2	51		43
3	48		51
4	37		45
5	26		
6	30		
7	23		
8	34		
9	20		
10	83		

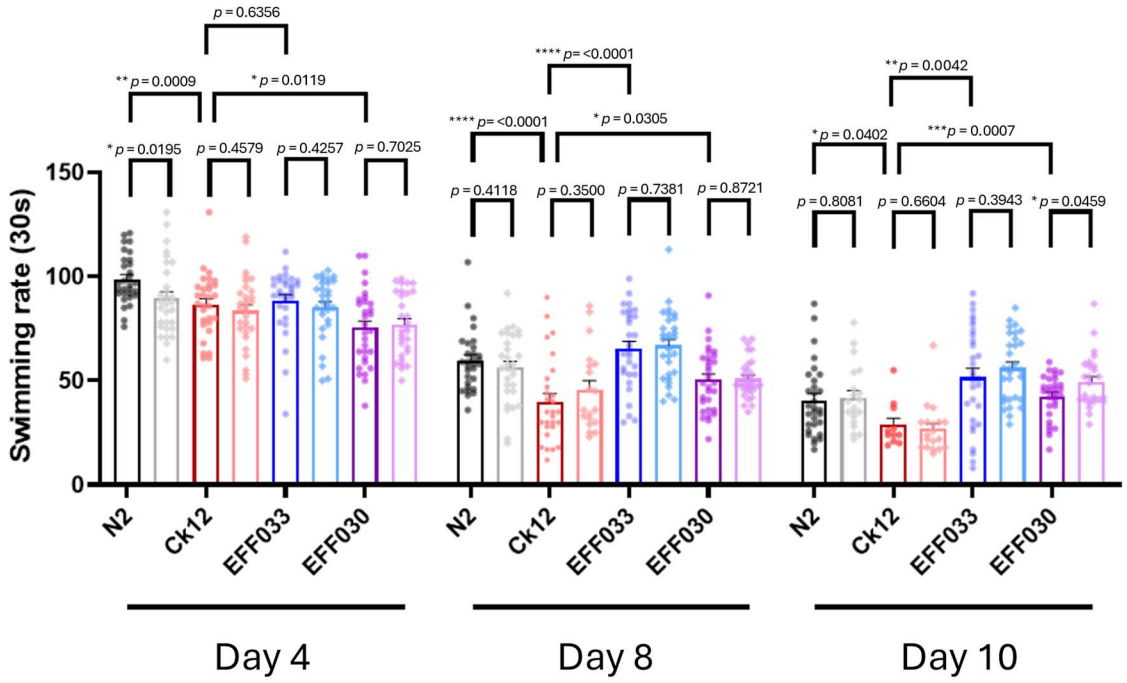

Fig. 11 Swimming/Thrashing assay without the CK12 BR4 data. A column graph showing the swimming/thrashing rate of *C.* elegans. The thrashing rate was measured on day 4, 8, and 10 of adulthood. The thrashing rate was measured at 30 seconds, and 10 worms was measured for each condition on each strain. there are in total 2 conditions for each strain, where the strains measured are N2, CK12, EFF033, and EFF030. The two conditions are one vehicle group, and one group with added 2 mM NMN. Both conditions were added 2 mM of FuDR. This graph shows 3 biological repeats pooled together and analyzed in total. The p-value was calculated in Prism using an unpaired t-test between each condition in each individual strain with a confidence interval of 95%. An unpaired t-test was also conducted between N2-CK12, CK12-EFF030, and CK12-EFF033. * p = <0.05, **p = <0.005, *** p = <0.0005, **** p = <0.0001.

Table 8 Memory assay data.

BR 1										
	Naïve				IA					
	T	IA	S	Tot.	T	IA	S	Tot.	Naïve %	IA %
N2	26	86	11	123	39	29	26	94	48.78049	-10.6383
EFF033	14	68	9	91	14	54	17	85	59.34066	47.05882
CK12	3	14	11	28	23	22	33	78	39.28571	-1.28205
EFF030	11	88	10	109	25	41	31	97	70.6422	16.49485
N2 w/ NMN	28	108	11	147	41	82	22	145	54.42177	28.27586
EFF033 w/ NMN	14	73	11	98	13	31	10	54	60.20408	33.33333
CK12 w/ NMN	4	55	41	100	24	22	51	97	51	-2.06186
EFF030 w/ NMN	8	94	14	116	48	48	53	149	74.13793	0

Table 9 Memory assay data (not in use).

BR 0										
	Naïve				IA					
	T	IA	S	Tot.	T	IA	S	Tot.	Naïve %	IA %
N2	22	261	27	310	16	77	4	97	77.09677	62.8866
EFF033	4	99	5	108	4	45	4	53	87.96296	77.35849
CK12	10	212	19	241	17	62	67	146	83.81743	30.82192
EFF030	3	93	7	103	3	71	14	88	87.37864	77.27273
N2 w/ NMN	13	417	15	445	14	270	8	292	90.78652	87.67123
EFF033 w/ NMN	5	89	7	101	2	27	2	31	83.16832	80.64516
CK12 w/ NMN	9	141	15	165	17	107	74	198	80	45.45455
EFF030 w/ NMN	1	70	3	74	4	96	10	110	93.24324	83.63636

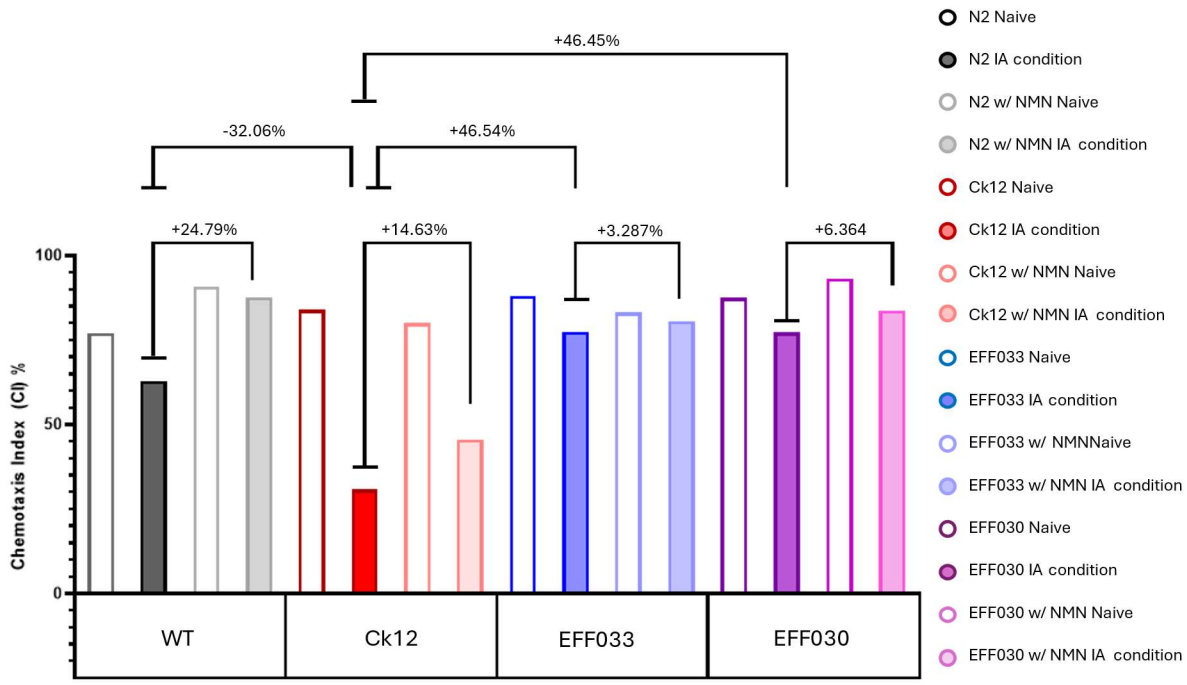

Fig. 12 Memory assay of the first biological repeat. A column graph showing the short-term memory assay of *C. elegans*. The worms were either conditioned in an empty NGM plate (Naïve) or in a NGM plate with pure IA on top of the lid (IA) for 90 minutes. In total there are 8 groups: N2, CK12, EFF033, EFF030, where there were 2 conditions (Veh., 2mM NMN). After the 90 min conditioning, the worms were then transferred to their assigned memory assay plate where they would be left in room temperature (20-25°C) for 2 hours. This graph shows only one biological repeat. The percentage value is calculated as the difference between the different IA groups, as the IA group is the one that is being tested for memory.

Norges miljø- og biovitenskapelige universitet
Noregs miljø- og biovitskapelege universitet
Norwegian University of Life Sciences

Postboks 5003
NO-1432 Ås
Norway